Publication No. FHWA-RD-03-053
September 2002 (Revised October 2003)

U.S. Department
of Transportation

Federal Highway Administration

User's Manual for FESWMS FST2DH

Two-dimensional Depth-averaged Flow and Sediment Transport Model

Release 3

Federal Highway Administration
Office of Research, Development, and Technology
Turner-Fairbank Highway Research Center
6300 Georgetown Pike
McLean, Virginia 22101

This page has been left blank intentionally.

Technical Report Documentation Page

1. Report No. FHWA-RD-03-053	2. Government Accession No.	3. Recipient's Catalog No.
4. Title and Subtitle User's Manual for FESWMS FST2DH Two-dimensional Depth-averaged Flow and Sediment Transport Model Release 3		5. Report Date September 2002 (Revised October 2003) 6. Performing Organization Code
7. Author(s) David C. Froehlich		8. Performing Organization Report No.
9. Performing Organization Name and Address University of Kentucky Research Foundation 211 Kinkead Hall University of Kentucky Lexington, Kentucky 40506-0057		10. Work Unit No. (TRAIS) 11. Contract or Grant No. DTFH61-91-C-00093
12. Sponsoring Agency Name and Address Federal Highway Administration Office of Research, Development, and Technology Turner-Fairbank Highway Research Center 6300 Georgetown Pike McLean, Virginia 22101		13. Type of Report and Period Covered 14. Sponsoring Agency Code

15. Supplementary Notes

FHWA Project Manager: Larry A. Arneson; UKRF Research Administrator: Mark Pittman

16. The Depth-averaged Flow and Sediment Transport Model (*FST2DH*) is a computer program that simulates movement of water and sediment in rivers, estuaries, and coastal waters. *FST2DH* applies the finite element method to solve steady-state and time-dependent systems of equations that describe two-dimensional depth-averaged surface-water flow and sediment transport. You can use *FST2DH* to simulate flow in surface-water bodies where vertical velocities and accelerations are small in comparison to those in horizontal directions. Special emphasis has been placed on modeling highway river crossings where complex hydraulic conditions exist because conventional analyses based on one-dimensional flow calculations often cannot provide the needed level of solution detail at these sites.

Release 3 of *FST2DH* expands the capabilities of previous releases by adding or improving numerical simulation of the following phenomena: sediment transport, armoring of channel beds, turbulence-induced shear stresses, combined current and wave shear stresses, tropical cyclone windfields and barometric pressure fields, coastal storm surge hydrographs, wetting and drying of elements, pressure flow under bridge decks, flow resistance from bridge piers, local scour at bridge piers, bridge pier riprap sizing, flow over roadway embankments, flow through culverts, flow through gate structures, flow through drop-inlet spillways, and combined one-dimensional/two-dimensional flow and sediment transport.

The purpose of this document is to enable users to apply *FST2DH* in sensible and effective ways. The manual provides theoretical backgrounds of formulas, algorithms, and numerical methods used to solve equations that describe water motion and sediment transport. It presents input data formats, describes various output files that *FST2DH* can generate, and suggests how to interpret results of simulations. It does not describe programming details beyond formatting of input data and the organization of output data files.

17. Key Words	18. Distribution Statement
Bridge hydraulics, depth-averaged flow, open-channel flow, sediment transport, finite element analysis, scour, storm surge, tropical cyclone, bridge piers, scour, erosion, armoring, riprap	This document is available to the public through the National Technical Information Service, Springfield, VA 22161 Tel: (703) 487-4650

19. Security Classif, (of this report)	20. Security Classif. (of this page)	21. No. of Pages	22. Price
Unclassified	Unclassified	209	

Form DOT F 1700.7 (8-72) Reproduction of completed page authorized

Table of Contents

List of Tables

List of Figures

List of Symbols

Symbol	Definition
a	bed storativity coefficient formula parameter
a_i	vector of unknown nodal values at the ith iteration
Δa_i	change of the solution vector a_i at the ith iteration
A	cross section flow area; dimensionless coefficient in Ackers-White sediment transport rate formula
A'	coefficient in Ackers-White sediment transport rate formula
A_c	cross-section area of a culvert; cross section area of a drop inlet spillway conduit
A_e	area of an element
A_o	cross section area of a drop inlet spillway orifice
A_p	below-water area of a pier projected normal to approaching streamflow
$A_w = uw/2\pi$	orbital amplitude of wave motion at the bed
b	bridge pier width; bed storativity coefficient formula parameter
$\tilde{b}$	bridge pier width projected normal to approach flow
B_{cl}	channel link width
c_f	bottom shear stress coefficient
c_β	momentum correction coefficient model coefficient
$c_s,\ c_{s1},\ c_{s2}$	wind stress model coefficients
$c_{\mu 1}, c_{\mu 21}$	kinematic eddy viscosity model coefficients
c'	culvert inflow flow (submerged) equation coefficient
C	Chézy discharge coefficient; dimensionless coefficient in Ackers-White sediment transport rate formula
C_c	culvert discharge coefficient; drop inlet spillway conduit discharge coefficient
C_d	pier drag coefficient
C_{es}	bed mass flux rate coefficient
C_i	unknown parameter at node i
C_o	drop inlet spillway orifice discharge coefficient
C_s	weir segment submergence coefficient
$C_{si} = q_{si}/q$	discharge-weighted sediment concentration for the ith sediment particle size class
$C_{si}^* = q_{si}^*/q_{si}$	discharge-weighted equilibrium sediment concentration for the ith sediment particle size class
C_w	weir segment discharge coefficient; drop inlet spillway weir discharge coefficient
d_s	local scour depth below mean ambient bed elevation
d_{sc}	clear-water contraction scour depth
d_{sl}	local pier scour depth
D_c	inside diameter of a pipe culvert or the maximum inside height of a pipe-arch culvert
D_A	reference particle diameter used in Ackers-White-Day sediment transport rate formula
D_{gr}	dimensionless grain diameter
D_n	sediment particle diameter for which n% of the mixture is finer by weight, for example D_{84}, D_{90}
D_s	tropical cyclone time parameter, $D_s = R_{max}/V_f$
D_{50}	median sediment particle diameter.

Symbol	Definition
e_*	dimensionless diffusivity
f	known function; Darcy-Weisbach friction factor
f_w	wave friction factor
f_{ws}	wave friction factor for rough turbulent flow
F_{gr}	grain mobility number used in Ackers-White sediment transport rate formula
Fr	Froude number
Fr_a	Froude number of bridge pier approach flow
g	gravitational acceleration = 9.81 m/s^2 (32.2 ft/sec^2)
H	water depth
H_{cl}	channel link water depth
H_{sc}	clear-water contraction scour flow depth
H_w	height of water wave
H_{ws}	significant wave height
$[J]$	Jacobian matrix
$\|J\|$	determinant of a Jacobian matrix
$k = 2\pi/L$	wave number or water waves
k_e	culvert entrance loss coefficient; drop inlet spillway entrance loss coefficient
k_o	drop inlet spillway conduit outlet loss coefficient
K'	culvert inflow flow (unsubmerged) equation coefficient
K_1, K_2, K_3	local pier scour equation correction coefficients for pier shape, flow alignment, and bed condition, respectively
K_i	coefficient in Laursen sediment transport rate formula
ℓ	bridge pier length
$\mathcal{L}$	differential operator
L_c	length of a culvert
L_w	length of a weir segment; total length of drop inlet spillway weir crest
m	exponent in Ackers-White sediment transport rate formula
m_b	bed shear-stress adjustment factor to account for slope
m_c	ceiling shear-stress adjustment factor to account for slope
M	culvert inlet flow (unsubmerged) equation coefficient; coefficient in Yang sediment transport rate formula
M_i	linear interpolation function associated with node *i*
n	Manning roughness coefficient; exponent in Ackers-White sediment transport rate formula
n_c	Manning roughness coefficient of a culvert barrel
n_{cl}	Manning roughness coefficient of a channel link
n_{cover}	Manning roughness coefficient of protective soil cover
n_{deck}	Manning roughness coefficient of underside of bridge deck
n_{soil}	Manning roughness coefficient of bare soil
N	coefficient in Yang sediment transport rate formula
N_i	quadratic interpolation function associated with node *i*
N^*_i	coordinate interpolation function associated with node *i*
p_a	atmospheric pressure
p_i	fraction of particle size class *i* in the active layer
P	pressure head
$q_1 = HU$	unit flow rate in the *x* direction
$q_2 = HV$	unit flow rate in the *y* direction
q_s	volumetric sediment transport rate in the streamwise direction

Symbol	Definition
q_s^*	volumetric equilibrium sediment transport rate in the streamwise direction
q_{sx}, q_{sy}	volumetric discharge-weighted sediment transport rates in the x and y directions, respectively
q_{xi}, q_{yi}	unit flow rates in the x and y directions, respectively, at node i
Q_i	source/sink (inflow/withdrawal) at a node point
Q_c	culvert flow rate
Q_i^o	flow rate across an open boundary resulting from node i
Q_i^c	flow rate across a closed boundary resulting from at node i.
Q_s	volumetric sediment transport rate
Q_w	flow over a weir segment
Q_{xi}	flow rate through a cross section assigned to node i
r_i	update vector used in a quasi-Newton solution
R	solution domain; residual load vector
R_c	hydraulic radius of a culvert flowing full; hydraulic radius of a drop inlet spillway conduit flowing full
R_H	continuity equation residual
$R_w = u_w A_w/\nu$	wave Reynolds number
S_{cl}	channel link bed slope
S_e	element boundary; energy gradient
$S_s = \rho_s/\rho$	specific gravity of sediment particles
T	period of water wave
Δt	time step or length of time between successive solution time levels
t	time
u	exact value of a dependent variable; point velocity in the x direction
$\tilde{u}$	approximation of a dependent variable
U	depth-averaged velocity in the x direction
U_n	depth-averaged velocity normal to a boundary
U_s	depth-averaged velocity tangent to a boundary
u_w	wave orbital velocity amplitude at bed
u_*	total bed shear velocity or friction velocity
u_{*s}	grain-friction velocity
v	point velocity in the y direction
V	depth-averaged velocity in the y direction
V_a	depth-averaged velocity of bridge pier approach flow
V_f	tropical cyclone forward speed
w	point velocity in the z direction
w_i	numerical integration weighting factor at the ith integration point
w_s	terminal fall velocity (settling velocity) of a sediment particle in water
W	wind speed
W_i	weighting function corresponding to node i
W_{min}	minimum wind speed used to compute surface wind stress coefficient
x	Cartesian coordinate (a horizontal direction)
y	Cartesian coordinate (a horizontal direction)
y_a	local pier scour equation approach flow depth
z	Cartesian coordinate (the vertical direction)
z_b	bed elevation
z_c	crest elevation of a weir segment; ceiling elevation
z_e	energy head elevation
z_{inv}	culvert invert elevation

Symbol	Definition
z_w	water-surface elevation
z_0	total bed roughness height
z_{0s}	grain roughness height for hydrodynamically rough flows
z_{0f}	bed-form roughness height due to ripples
z_{0t}	sediment transport roughness height
α	coefficient used to compute time derivatives
β	isotropic momentum correction coefficient
β_{uv}	directional component of the momentum correction coefficient
β_o	momentum correction coefficient model constant
δ_i	update vector used in a quasi-Newton solution
Δ_{rc}	height of ripples generated by currents
Δ_{rw}	height of ripples generated by waves
$\tilde{\Gamma}$	kinematic eddy diffusivity
ϵ	residual
ζ	bed storativity depth
η	natural coordinate
η_b	storativity depth factor
η_s	porosity of bed sediment
η_x	direction cosine between the outward normal to a network boundary and the *x*-coordinate direction
η_y	direction cosine between the outward normal to a network boundary and the *y*-coordinate direction
θ	time-integration factor
κ	von Karman's constant
λ_b	bed storativity coefficient.
λ_{rc}	wavelength of ripples generated by currents
λ_{rw}	wavelength of ripples generated by waves
$\tilde{\nu}$	isotropic depth-averaged kinematic eddy viscosity
$\tilde{\nu}_{xy}$	directional component of depth-averaged kinematic eddy viscosity
$\tilde{\nu}_o$	kinematic eddy viscosity model constant
ξ	natural coordinate
ρ	mass density of water
ρ_a	mass density of air
ρ_s	mass density of sediment
σ_t	turbulent Prandtl or Schmidt number
$\tau_b = \rho u_*^2$	total bed shear-stress due to current alone
τ_{bx}, τ_{by}	bed shear-stresses in the *x* and *y* direction, respectively
$\tilde{\tau}_{bx}, \tilde{\tau}_{by}$	bed shear-stresses in the *x* and *y* direction, respectively, modified to account for added resistance from bridge piers
τ_c	critical bed shear-stress
τ_{cp}	critical shear stress of protective soil cover
τ_{cs}	critical shear stress of soil
τ_{cx}, τ_{cy}	ceiling shear stresses in the *x* and *y* directions, respectively
τ_{sx}, τ_{sy}	surface shear stresses caused by wind in the *x* and *y* directions, respectively
τ_m	mean bed shear-stress during a wave cycle under combined wind and currents
τ_{xy}	directional component of lateral shear stress caused by turbulence
τ_w	amplitude of oscillatory bed shear-stress due to waves
τ_{ws}	grain shear-stress

Symbol	Definition
τ_{ws*}	dimensionless grain shear-stress
τ_{wall}	wall shear-stress
ϕ	angle of latitude; bridge pier shape factor
ϕ_n	Manning equation units factor (ϕ_n = 1.0 for SI units, 1.486 for U.S. Customary units)
Ψ	wave mobility number
ω	angular velocity
ω_r	iterative solution over/under-relaxation parameter
Ω	Coriolis parameter
∂	partial differential symbol

This page has been left blank intentionally.

1. Introduction

The Depth-averaged Flow and Sediment Transport Model (*FST2DH*) is a computer program that simulates movement of water and noncohesive sediment in rivers, estuaries, and coastal waters. *FST2DH* applies the finite element method to solve steady-state or time-dependent systems of equations that describe two-dimensional depth-averaged surface-water flow and transport of noncohesive sediment by surface waters. You can use *FST2DH* to simulate flows in surface-water bodies where vertical velocities and accelerations are small in comparison to those in horizontal directions. Special emphasis has been placed on modeling highway river crossings where complex hydraulic conditions exist, because conventional analyses based on one-dimensional flow calculations often cannot provide the needed level of solution detail at these sites (see Figure 1-1). *FST2DH* is part of the Federal Highway Administration's Finite Element Surface-water Modeling System (*FESWMS*).

Figure 1-1. A highway bridge that creates complex hydraulic conditions by constricting floodplain flows at high stages.

Applications of *FST2DH*

Water levels and flow distributions at confluences of large rivers, in river bends, around islands, at highway river crossings with more than one bridge opening, into and out of river diversion channels at dams and powerplants, in river estuaries, in coastal marshes, in tidal lagoons and tidal inlets, and in bays and harbors can be calculated using *FST2DH*. Effects and features simulated by *FST2DH* include the following items:

- Bottom shear stress or bed friction
- Wind shear stress
- Coriolis force
- Turbulence-induced shear stresses
- Combined current and wave shear stresses
- Barometric pressure gradients
- Tropical cyclone windfields and barometric pressure fields
- Coastal storm surge hydrographs
- Wetting and drying of elements
- Pressure flow under bridge decks
- Flow resistance from bridge piers
- Flow over roadway embankments
- Flow through culverts with or without flap-gates
- Flow through gate structures
- Flow through drop-inlet spillways
- Live-bed and clearwater contraction scour at bridges
- Local scour at bridge piers
- Transport of eight noncohesive sediment particle size classes
- Erosion and deposition of transported sediment
- Armoring of channel beds
- Wave effects on nearshore sediment transport
- Bridge pier riprap sizing
- Supercritical flow and hydraulic jumps
- Combined one-dimensional/two-dimensional flow and sediment transport
- Pressure flow in one-dimensional closed conduits.

FST2DH can simulate both steady and unsteady (that is, time-dependent) surface-water flows. However, because of the need for initial conditions, and because of difficulties modeling large areas that periodically are flooded and then drain, the range of flow conditions that can be modeled with reasonable ease is limited. For example, long reaches of rivers where water-surface elevations have comparatively large changes between the upstream and downstream ends require that a series of simulations be carried out as boundary conditions are incremented in stages from some initial values for which trivial solutions are easily obtained to the final desired values. Additionally, flooding and subsequent drainage of large areas such as broad floodplains or marshland generally requires that small time steps be used, which leads to long solution times. Other computer models based on different numerical solution techniques may be better suited to these types of applications.

Purpose of the User's Manual

The purpose of this document is to help you apply *FST2DH* in sensible and effective ways. The manual provides theoretical backgrounds of formulas, algorithms, and numerical methods used to solve equations that describe water motion and sediment transport. It presents input data formats, describes various output files that *FST2DH* can generate, and suggests how to interpret results of simulations. It does not include programming details beyond formatting of input data and the organization of output data files.

Background Knowledge

We have designed *FST2DH* carefully with emphasis on logical and straightforward modeling approaches and data needs. However, by itself this user's manual will not provide you all the knowledge needed to apply the model effectively or to decide whether simulation results are reasonable. You need to comprehend thoroughly pertinent physical principles of surface-water flow and sediment transport before using *FST2DH*. You also need to have a basic understanding of the numerical methods used to solve the resulting systems of partial differential equations. This manual will not provide all the background knowledge needed to carry out skillful and effective mathematical modeling of depth-averaged surface-water flow and sediment transport

Licensing and Disclaimer

FESWMS FST2DH is a contribution of the Federal Highway Administration and is not subject to copyright. Although every effort has been made to ensure the accuracy and correctness of the program and information, the Federal Highway Administration makes no warranties, either expressed or implied, with respect to the software and documentation, including but not limited to the implied warranties of suitability and fitness for a particular purpose. *FESWMS FST2DH* may be freely distributed.

Contents Overview

An overview of the finite element method is presented in Chapter 2 of this manual. Users can gain a fundamental idea of the mathematics and numerical procedures used to solve the governing partial differential equations describing surface-water flow and sediment transport. The main point to remember is that solution regions are divided into assemblies of connected subregions called elements that are in the shape of triangles and quadrilaterals. An assemblage of elements forms a network or mesh. Position and

geometry of the elements in a mesh are defined by node points at the element vertices, midside points, and, for nine-node quadrilaterals, at their centers. Solution variables are defined at the nodes, and continuous approximations of quantities are made within elements using interpolation functions and the node point values. The partial differential equations describing water motion and transport of sediment are approximated by algebraic expressions using nodal quantities as unknown values for which solutions are to be found. The system of algebraic equations formed in this way is then solved simultaneously for values at the nodes using an efficient equation solver based on the frontal method.

Equations that govern two-dimensional, depth-averaged surface-water flow and one-dimensional, cross-section-averaged surface water flow that are solved by *FST2DH* are presented in Chapter 3. Auxiliary expressions used to calculate flow at weir structures, culverts, drop-inlet spillways, and gate structures are also described.

Sediment transport by two-dimensional depth-averaged flow and by one-dimensional cross-section-averaged flow is addressed in Chapter 4. For most conditions, sediment transport is inherently a time-dependent phenomenon, and unsteady flows will need to be considered. Calculation of streambed erosion at bridges is also discussed in this chapter.

Steps generally taken when applying *FST2DH* to investigate surface-water flow and sediment transport are presented in Chapter 5. Possible data needed to construct a mesh and to assign boundary conditions are summarized. Network design, which is a critical stage of any useful simulation, is discussed, and several useful ideas and rules for constructing reliable meshes are presented.

Results of a few simple numerical experiments are presented in Chapter 6 to show the effects of various element properties and other parameters on solutions. Knowledge of the possible effects of variations in roughness coefficients and kinematic eddy viscosities is useful when trying to match solutions to measured flow properties. Other items that can have significant effects on solutions include conditions applied at closed boundaries (that is, slip, semi-slip, and no-slip conditions), and the effects of shear stresses along vertical walls that form closed boundaries. Wind can also have a significant influence on solutions. Flow calculations carried out using small experimental channels show some effects of these factors.

Operation of *FST2DH* is described in Chapter 7, including the many different input and output data files that might be used. *FST2DH* runs as a console application that does not require graphics output written to the screen. It looks about the same whether run on a personal computer, a workstation, or a terminal connected to a mainframe computer. Output files containing many different items produced by a solution can be generated and displayed graphically using various computer programs. Several computational aspects of *FST2DH* are also described in this section.

The references section in Chapter 8 is followed by two appendices. Appendix A contains detailed descriptions of all input data file formats and output data files. Data items used by *FST2DH* to control solutions, define finite element meshes, assign initial and boundary conditions, and apply element properties are explained thoroughly. Appendix B contains a detailed description of the tropical storm model used to calculate windfield and pressure distributions caused by tropical cyclones.

This page has been left blank intentionally.

2. Overview of the Finite Element Method and Equation Solution

The finite element method is a numerical procedure for solving differential equations encountered in problems of physics and engineering. Continuous quantities are approximated by sets of variables at discrete points that form networks or meshes. Because the finite element method can be adapted to problems of great complexity and unusual geometry, it is an extremely powerful tool in the solution of problems in heat transfer, fluid mechanics, and mechanical systems. Furthermore, availability of fast and inexpensive computers allows problems that are intractable using analytic or mechanical methods to be solved straightforwardly by the finite element method. A large amount of literature on the subject has already emerged. Lee and Froehlich (1986) provide an extensive, although not up-to-date, review of literature on finite element solutions of the equations of two-dimensional depth-averaged surface-water flow.

FST2DH uses the Galerkin finite element method to solve the governing system of differential equations. Solutions begin by dividing the physical region of interest into subregions, which are called elements. Two-dimensional elements can be either triangular or quadrilateral in shape, and are defined by node points placed along their boundaries and interiors. Lists of nodes connected to elements are easily recorded for identification and use. Dependent variables are approximated within elements using values defined at element node points along with sets of interpolation functions (also called shape, basis, or trial functions). Mixed interpolation is used in *FST2DH* to help stabilize the numerical solution (that is, quadratic functions are used to interpolate unit flow rates based on solution values at all the nodes of an element, and linear functions are used to interpolate water depths based on solution values at only vertex nodes.)

The method of weighted residuals is applied to the governing differential equations to form a set of equations for each element. Approximations of the dependent variables are then substituted into the governing equations, which generally are not satisfied exactly, to form residuals. The residuals are made to vanish, in an average sense, when they are multiplied by weighting functions and integrated with respect to the solution domain. Weighting functions are chosen to be the same as the interpolation functions. By requiring summations of weighted residuals to equal zero, the finite element equations take on integral forms. Coefficients of the equations are integrated numerically, and all of the element (local) equations are assembled to obtain the complete (global) system of equations. The global set of algebraic equations is solved simultaneously in *FST2DH* using Gaussian elimination.

Method of Weighted Residuals

The method of weighted residuals is a mathematical technique for approximating solutions to partial differential equations. Although the technique provides a means of forming the element equations, it is not directly related to the finite element method. Applying the method of weighted residuals involves two basic steps. The first step is to adopt a general functional behavior of the dependent variables so that the governing differential equations and boundary condition equations can be satisfied approximately. Substituting initial values of the dependent variables into the governing equations usually yields errors, which are called residuals. Solutions are obtained by requiring residuals to vanish, in an average sense, within the solution regions. The second step of the method is to solve the residual equations for parameters of the functional representations of the dependent variables.

To be more specific, the differential equation for a problem containing one dependent variable is written as

$$\mathcal{L}u - f = 0 \tag{2-1}$$

where $\mathcal{L}$ = differential operator, u = dependent variable, and f = known function. The dependent variable is represented by $\tilde{u}$, which is defined by some unknown parameters, C_i, and a set of functions, N_i, as follows:

$$u \approx \tilde{u} = \sum_{i=1}^{m} N_i C_i \tag{2-2}$$

When $\tilde{u}$ is substituted for u in the problem, it is unlikely the equation will be satisfied exactly. In fact, a trial solution is given by

$$\mathcal{L}\tilde{u} - f = \varepsilon \ , \tag{2-3}$$

where ε = residual or error of the approximate solution. The method of weighted residuals is used to solve for the m unknown parameters, C_i, so that the error, ε, is as small as possible within the solution region. One way of reducing ε is to form a weighted average of the error and then equate the average to zero after it is integrated with respect to the entire solution region. The weighted average is computed as

$$\int_R W_i \, \varepsilon \, dR = 0; \text{ for } i=1,2,...,m \tag{2-4}$$

where R = solution domain, and W_i = linearly independent weighting functions. After the weighting functions have been specified, a set of m simultaneous equations remain to be solved for the unknown parameters C_i. The second step in applying the method of weighted residuals is to solve for C_i to obtain an approximate representation of the unknown dependent variable u.

Choice of weighting functions used to form the residual expressions is flexible. Often the weighting functions are chosen to be the same as the interpolation functions used to approximate u (that is, $W_i = N_i$, for I = 1, 2,..., m). This finite element approximation to the differential equation is known as Galerkin's method and is given by

$$\int_R N_i (\mathcal{L}\tilde{u} - f) \, dR = 0; \text{ for } i=1,2,...,m \tag{2-5}$$

After the interpolation functions N_i are specified, the equations can be evaluated explicitly, and the solution found in a routine way.

Elements and Interpolation Functions

The basic idea of the finite element method is to divide a solution region into subregions, called elements. Within each element, values of continuous quantities are approximated by sets of piecewise smooth functions using values of those quantities at finite numbers of points. The piecewise smooth functions are known as interpolation or shape functions, and are analogous to the functions N_i described in the previous section. Locations at which continuous quantities are defined are called node points, and values of quantities at node points are analogous to the undetermined parameters C_i.

Approximations of continuous quantities within elements are written as

$$\tilde{u}^{(e)} = \sum_{i=1}^{n} N_i^{(e)} C_i^{(e)} \tag{2-6}$$

where $N_i^{(e)}$ = interpolation functions specified for an element, and $u_i^{(e)}$ = unknown values of u at the n node points in the element. This equation applies to a single point in the solution region, or to any collection of points, such as those comprising an element. Weighted residuals are then found as sums of integrals for each element as follows:

$$\int_{R^{(e)}} N_i^{(e)} (\mathcal{L}\tilde{u}^{(e)} - f^{(e)})\, dR^{(e)} = 0; \text{ for } i=1,2,...,m \tag{2-7}$$

where $R^{(e)}$ = element domain, and $f^{(e)}$ = defined element function.

Sets of integrals expressions are written for each element in the assemblage or network. Element (local) expressions are assembled to form the complete set of system (global) equations in which values of quantities at node points are the unknowns. Behavior of a solution within an entire assemblage of elements is described by the element interpolation functions and the node point values, after they have been found.

Before element equations can be assembled, the particular types of elements that will be used to model a region, and the associated interpolation functions, need to be specified; that is, the functions N_i need to be chosen. Interpolation functions also need to satisfy certain criteria so that convergence of numerical solutions to exact solutions of the governing differential equations can be achieved. The functions depend on the shapes of elements and the orders of approximation desired. Because the fundamental premise of the finite element method is that a region of arbitrary shape can be accurately described by an assemblage of elements, most finite element networks consist of elements that are geometrically simple. The most commonly used two-dimensional elements are triangles and quadrilaterals. Although it is conceivable that many types of functions could be used as interpolation functions, most finite element solutions use polynomials because of their simplicity.

If polynomial interpolation functions are used, linear variation of quantities within elements can be described by values provided at the corners (vertices) of triangular or quadrilateral elements. For quadratic variation of quantities, additional values need to be defined along the sides, and possibly in the interiors, of elements. *FST2DH* uses three types of two-dimensional elements as shown in Figure 2-1: (1) Six-node triangles, (2) eight-node "serendipity" quadrilaterals, and (3) nine-node "Lagrangian" quadrilaterals. Both types of quadrilateral elements use identical linear interpolation functions, but their quadratic functions differ because of the presence of additional nodes at the centers of nine-node quadrilateral elements.

Complex geometric features using elements that have curved sides rather than straight sides, or a combination of curved and straight sides, can be modeled by transforming elements through coordinate mappings from simple "parent" elements, defined in natural coordinates, to the desired curved shapes, defined in global Cartesian coordinates. Coordinate mappings for triangular and quadrilateral elements are illustrated in Figure 2-2. Transformation from straight to curved sides is accomplished by expressing the global coordinates (x, y) in terms of the natural coordinates (ξ, η) using interpolation functions in just the same way solution variables are interpolated within elements. Global coordinates are then computed as follows:

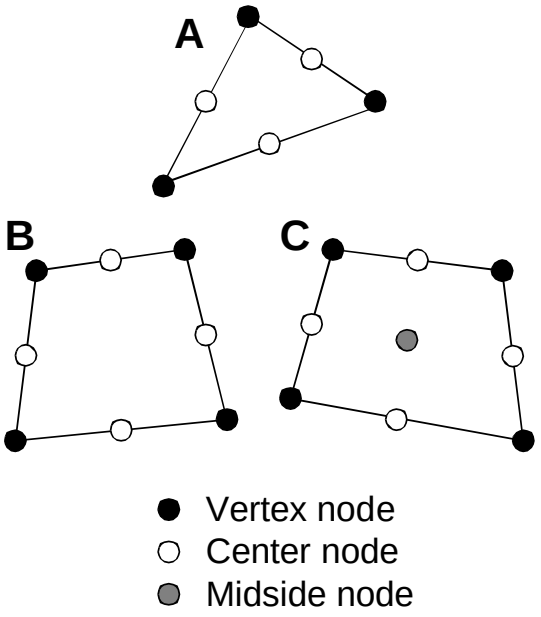

Figure 2-1. Types of two-dimensional elements used by *FST2DH* include (A) six-node triangles, (B) eight-node quadrilaterals, and (C) nine-node quadrilaterals.

$$x = \sum_{i=1}^{n} N_i^{*(e)} x_i^{(e)} \qquad y = \sum_{i=1}^{n} N_i^{*(e)} y_i^{(e)} \tag{2-8}$$

where the coordinate interpolation function $N_i^{*(e)}$ is defined in terms of the natural element coordinates ξ and η. *FST2DH* uses quadratic interpolation functions to transform natural coordinates to global coordinates.

Natural coordinates (ξ and η) depend on element shapes (that is, triangular or quadrilateral). Natural coordinate systems and interpolation functions for parent elements of triangular and quadrilateral global elements are shown in Figures 2-3 to 2-5. Both linear and quadratic interpolation functions are given for each element shape because mixed

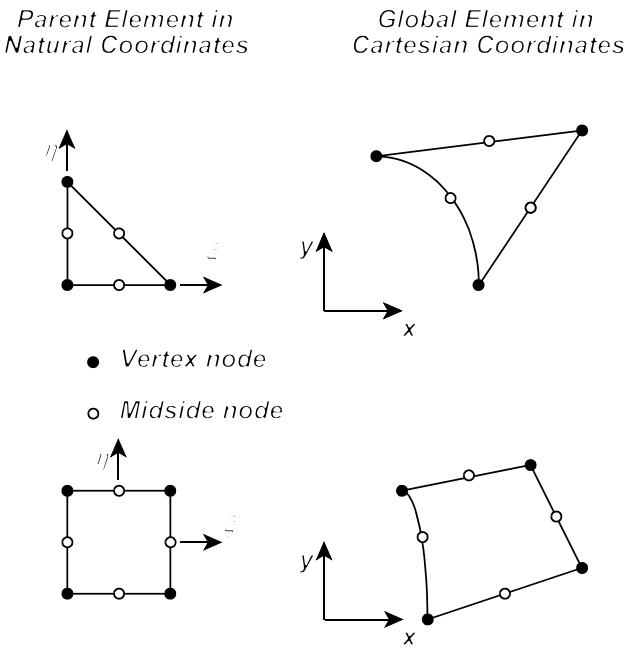

Figure 2-2. Mapping of triangular and quadrilateral parent elements defined in natural coordinates to global elements in Cartesian coordinates.

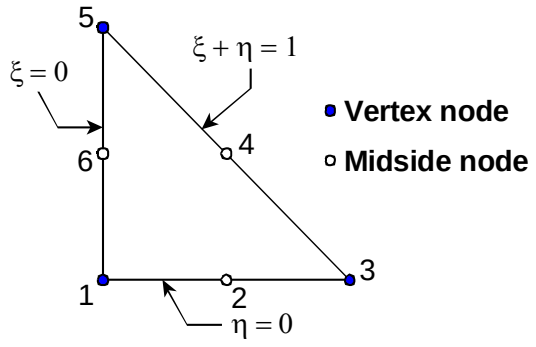

Linear Interpolation Functions

Vertex nodes:

$M_1 = 1 - \xi - \eta$

$M_3 = \xi$

$M_5 = \eta$

Quadratic Interpolation Functions

Vertex nodes:

$N_1 = (1 - \xi - \eta)(1 - 2\xi - 2\eta)$

$N_3 = \xi(2\xi - 1)$

$N_5 = \eta(2\eta - 1)$

Midside nodes:

$N_2 = 4\xi(1 - \xi - \eta)$

$N_4 = 4\xi\eta$

$N_6 = 4\eta(1 - \xi - \eta)$

Figure 2-3. Natural coordinate system and interpolation functions for a triangular parent element.

interpolation is used to solve the governing differential equations (that is, linear functions are used to interpolate depth, and quadratic functions are used to interpolate depth-averaged velocities). When finite element equations contain derivatives of dependent variables with respect to global coordinates *x* and *y*, interpolation function derivatives with respect to *x* and *y* also need to be defined because, for example,

$$\frac{\partial u}{\partial x} = \frac{\partial}{\partial x}\left(\sum_{i=1}^{n} N_i^{*(e)} u_i^{(e)}\right) = \sum_{i=1}^{n} \frac{\partial N_i^*}{\partial x} u_i^{(e)} \tag{2-9}$$

Since the interpolation functions are calculated using natural coordinates, derivatives with respect to natural coordinates need to be transformed to derivatives with respect to global coordinates. By the general rules of partial differentiation,

$$\frac{\partial N_i}{\partial x} = \frac{\partial N_i}{\partial \xi}\frac{\partial \xi}{\partial x} + \frac{\partial N_i}{\partial \eta}\frac{\partial \eta}{\partial x} \tag{2-10}$$

and

$$\frac{\partial N_i}{\partial y} = \frac{\partial N_i}{\partial \xi}\frac{\partial \xi}{\partial y} + \frac{\partial N_i}{\partial \eta}\frac{\partial \eta}{\partial y} \tag{2-11}$$

where the superscript (e) has been dropped for convenience. However, ξ and η usually cannot be expressed explicitly by the coordinates *x* and *y*. By first considering N_i a function of *x* and y, derivatives of N_i with respect to ξ and η can be written in matrix form as

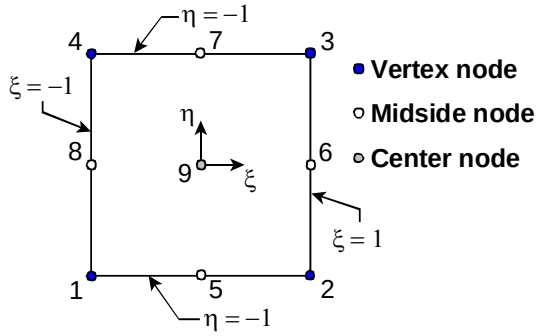

Linear Interpolation Functions

Vertex nodes

$M_1 = ¼ (1 - \xi)(1 - \eta)$

$M_2 = ¼ (1 + \xi)(1 - \eta)$

$M_3 = ¼ (1 + \xi)(1 + \eta)$

$M_3 = ¼ (1 - \xi)(1 + \eta)$

Quadratic Interpolation Functions

Vertex nodes

$N_1 = ¼ \xi\eta(1 - \xi)(1 - \eta)$

$N_2 = - ¼ \xi\eta(1 + \xi)(1 - \eta)$

$N_3 = ¼ \xi\eta(1 + \xi)(1 + \eta)$

$N_4 = - ¼ \xi\eta(1 - \xi)(1 + \eta)$

Midside nodes

$N_5 = - ½ \eta(1 - \xi^2)(1 - \eta)$

$N_5 = ½ \xi(1 + \xi)(1 - \eta^2)$

$N_7 = ½ \eta(1 - \xi^2)(1 + \eta)$

$N_8 = - ½ \xi(1 - \xi)(1 - \eta^2)$

Center node

$N_9 = (1 - \xi^2)(1 - \eta^2)$

Figure 2-4. Natural coordinate system and interpolation functions for a "Lagrangian" quadrilateral parent element.

$$\begin{Bmatrix} \frac{\partial N_i}{\partial \xi} \\ \frac{\partial N_i}{\partial \eta} \end{Bmatrix} = \begin{bmatrix} \frac{\partial x}{\partial \xi} & \frac{\partial y}{\partial \xi} \\ \frac{\partial x}{\partial \eta} & \frac{\partial y}{\partial \eta} \end{bmatrix} \begin{Bmatrix} \frac{\partial N_i}{\partial x} \\ \frac{\partial N_i}{\partial y} \end{Bmatrix} \tag{2-12}$$

where

$$[J] = \begin{bmatrix} \frac{\partial x}{\partial \xi} & \frac{\partial y}{\partial \xi} \\ \frac{\partial x}{\partial \eta} & \frac{\partial y}{\partial \eta} \end{bmatrix} \tag{2-13}$$

is known as the Jacobian matrix. The Jacobian matrix can be evaluated explicitly by the derivatives of the interpolation function with respect to natural coordinates, and the global node point coordinates, as

$$[J] = \begin{bmatrix} \sum_{i=1}^{n} \frac{\partial N_i^*}{\partial \xi} x_i & \sum_{i=1}^{n} \frac{\partial N_i^*}{\partial \xi} y_i \\ \sum_{i=1}^{n} \frac{\partial N_i^*}{\partial \eta} x_i & \sum_{i=1}^{n} \frac{\partial N_i^*}{\partial \eta} y_i \end{bmatrix} \tag{2-14}$$

where N_i^* = interpolation functions that define coordinate transformations. Global derivatives are then given by

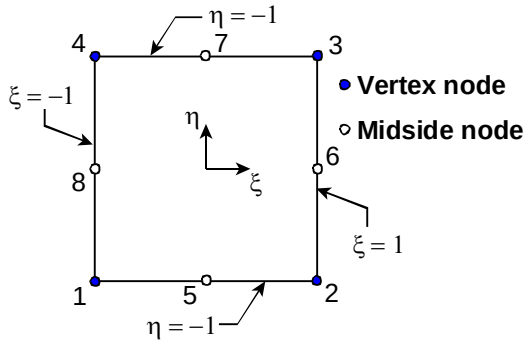

Linear Interpolation Functions

Vertex nodes:

$$M_1 = \tfrac{1}{4}(1 - \xi)(1 - \eta)$$

$$M_2 = \tfrac{1}{4}(1 + \xi)(1 - \eta)$$

$$M_3 = \tfrac{1}{4}(1 + \xi)(1 + \eta)$$

Quadratic Interpolation Functions

Vertex nodes:

$$N_1 = -\tfrac{1}{4}(1 - \xi)(1 - \eta)(1 + \xi + \eta)$$

$$N_2 = -\tfrac{1}{4}(1 + \xi)(1 - \eta)(1 - \xi + \eta)$$

$$N_3 = -\tfrac{1}{4}(1 + \xi)(1 + \eta)(1 - \xi - \eta)$$

$$N_4 = -\tfrac{1}{4}(1 - \xi)(1 + \eta)(1 + \xi - \eta)$$

Midside nodes:

$$N_5 = \tfrac{1}{2}(1 - \xi^2)(1 - \eta)$$

$$N_5 = \tfrac{1}{2}(1 + \xi)(1 - \eta^2)$$

$$N_7 = \tfrac{1}{2}(1 - \xi^2)(1 + \eta)$$

$$N_8 = \tfrac{1}{2}(1 - \xi)(1 - \eta^2)$$

Figure 2-5. Natural coordinate system and interpolation functions for a "seredipipity" quadrilateral parent element.

$$\begin{Bmatrix} \frac{\partial N_i}{\partial x} \\ \frac{\partial N_i}{\partial y} \end{Bmatrix} = [J]^{-1} \begin{Bmatrix} \frac{\partial N_i}{\partial \xi} \\ \frac{\partial N_i}{\partial \eta} \end{Bmatrix} \tag{2-15}$$

Expanding gives

$$\frac{\partial N_i}{\partial x} = |J|^{-1}\left(\frac{\partial y}{\partial \eta}\frac{\partial N_i}{\partial \xi} - \frac{\partial y}{\partial \xi}\frac{\partial N_i}{\partial \eta} \right) \tag{2-16}$$

and

$$\frac{\partial N_i}{\partial y} = |J|^{-1}\left(\frac{\partial x}{\partial \xi}\frac{\partial N_i}{\partial \eta} - \frac{\partial x}{\partial \eta}\frac{\partial N_i}{\partial \xi\eta} \right) \tag{2-17}$$

where

$$|J| = \frac{\partial x}{\partial \xi}\frac{\partial y}{\partial \eta} - \frac{\partial x}{\partial \eta}\frac{\partial y}{\partial \xi} \tag{2-18}$$

is the determinant of [*J*]. Operations in equations 2-15 through 2-17 depend on existence of [*J*] everywhere in elements. In addition, coordinate mappings are one-to-one only if $|J|$ does not vanish within elements. Poorly constructed elements having overlapping sides will exhibit this undesirable trait.

Curved-side elements are defined in *FST2DH* by prescribing the coordinates of midside nodes. Ordinarily, coordinates of a midside node are not specified at all. The midside node is placed halfway between the two adjacent vertex nodes automatically. However, coordinates are not calculated if they have already been specified. Therefore,

curved element sides can easily be formed when needed by entering appropriate coordinates for a midside node. Where element sides are not curved, coordinates of the midside nodes do not need to be specified.

Horizontal areas of elements also need to be expressed using the natural coordinates ξ and η. Sokolnikoff and Redheffer (1966, page 355) show that incremental element areas can be computed as

$$dx\,dy = |J|\,d\xi\,d\eta \tag{2-19}$$

Using this relation, functions can be integrated numerically with respect to the areas of two-dimensional triangular or quadrilateral elements that have straight or curved sides.

Numerical Integration

Numerical integration is used to evaluate the integrals that appear in the finite element equations. To integrate numerically, the function being integrated is evaluated at specific locations within an element, the values are then multiplied by weighting factors, and then summed. The summation process for a two-dimensional element is

$$\int_{A_e} f(\xi,\eta)\,d\xi\,d\eta \approx A_e \sum_{i=1}^{k} w_i f(\xi_i,\eta_i) \tag{2-20}$$

where A_e = element area, f = integrated function, k = number of numerical integration points, w_i = weighting factor that applies to the ith integration point, and ξ and η = natural coordinates of the ith integration point. The natural coordinates, ξ_i and η_i, are invariant with respect to the shape of the element in the global coordinate system.

Numerical integration schemes need to be accurate enough to assure convergence of finite element solutions. Strang and Fix (1973) find that convergence will be guaranteed if integration schemes compute exactly element areas. Formulas providing at least third-order accuracy are needed to integrate curve-sided elements exactly. However, while exact integration of element areas might guarantee convergence as the sizes of elements approach zero, integration formulas that have greater accuracy might be needed to integrate some terms in governing equations accurately. For this reason, numerical integration formulas that provide at least sixth-order accuracy are used in *FST2DH*. Locations of numerical integration points and the associated weighting factors are shown in Figure 2-6.

Equation Solution

Many methods can be used to solve the system of nonlinear algebraic equations that results from a finite element discretization of the governing partial-differential equations. However, solution methods that work well for one problem might not work at all for another problem. Solving the nonlinear equation system is the most costly aspect of the finite element solution carried out in *FST2DH*. Computational efficiency dictates that symmetric equation systems are formed and solved if possible. However, the coefficient matrix that is formed is nonsymmetric because of nonlinear inertia and bottom friction terms that appear in the governing equations.

Finite element solutions of the governing equations produce sets of global discretized equations in the form

$$K(a) = f \tag{2-21}$$

where K = matrix of assembled element coefficients; a = vector of unknown nodal values; and f =global load vector. The simultaneous nonlinear system of equations is solved using

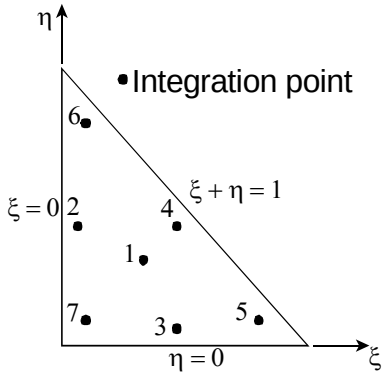

Point number	Coordinates		Integration weight, w
	ξ	η	
1	⅓	⅓	0.225
2	α_1	β_1	γ_1
3	β_1	α_1	γ_1
4	β_1	β_1	γ_1
5	α_2	β_2	γ_2
6	β_2	α_2	γ_2
7	β_2	β_2	γ_2

where α_1 = 0.05971587, β_1 = 0.47014206, α_2 = 0.79742698, β_2 = 0.10128651, γ_1 = 0.13239415, and γ_2 = 0.12593918.

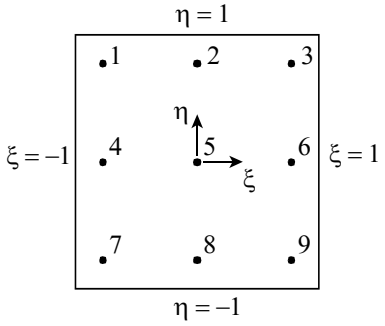

Point number	Coordinates		Integration weight, w
	ξ	η	
1	- α	α	γ_1
2	0	α	γ_2
3	α	α	γ_1
4	-α	0	γ_2
5	0	0	0.19753086
6	α	0	γ_2
7	-α	-α	γ_1
8	0	-α	γ_2
9	α	-α	γ_1

where α = 0.77459667, γ_1= 0.07716049, γ_2= 0.12345679

Figure 2-6. Numerical integration point coordinates and weighting factors for triangular and quadrilateral parent elements.

a strategy that combines full-Newton iteration, quasi-Newton iteration, and a frontal solution scheme.

Solution Strategy

Full-Newton iteration is written as

$$a_{i+1} = a_i - J(a_i)^{-1} R(a_i) \tag{2-22}$$

where a_{i+1} = newly computed solution vector; a = known solution vector at the ith iteration; $J(a_i)$ = Jacobian (tangent) matrix computed from a_i; and $R(a_i) = K(a_i)a_i - f$ = residual load vector. In practice, the iteration is carried out as

$$J(a_i)\Delta a_i = -R(a_i) \tag{2-23}$$

where Δa_i = incremental solution value. An updated solution is computed as

$$a_{i+1} = a_i + \omega_r \Delta a_i \tag{2-24}$$

where ω_r = relaxation factor that is allowed to range from 0 to 1 (the default value is 1). A solution usually converges rapidly when the initial estimate is close to the true solution.

During a full-Newton solution the Jacobian matrix is decomposed into lower and upper triangular matrices. These factorized matrices can be updated in a relatively simple manner rather than being recalculated completely at each iteration. Broyden's update procedure in inverse form (Engleman et al. 1981) is used to update the factored Jacobian matrix. This quasi-Newton method can reduce significantly the computation time needed to obtain a solution. Given an initial solution estimate, a_0, the LU factorization of its Jacobian, J_0 , and the initial search direction, Δa_0, the quasi-Newton algorithm proceeds as follows:

For i = 1 to I

1. Form $\delta_i = \Delta a_{i-1}$
2. Compute $\Delta a_i = -J_0^{-1} R(a_i)$
3. For j = 1 to I-1
   Compute $\Delta a_i = \Delta a_i - \rho_j(\delta_j + r_j)\delta_i' \Delta a_i$
   Next j
4. Form $r_i = \Delta a_i - \delta_i$ and $\rho_i = 1/(\delta_i' r_j)$
5. Compute $\Delta a_i = \Delta a_i - \rho_i(\delta_i + r_i)\delta_i' \Delta a_i$

Next I

where δ'_i = transpose of the vector δ_i.

At each iteration a single linear system is solved for which the triangular factors of the coefficient matrix are already known, plus the vector operations that are needed to update the matrix. Two updating vectors (ρ and r) are created at each iteration and are kept and used again in subsequent iterations, up to a limit imposed by the user. When the upper limit is reached, the updating vectors are shifted one position downward (thereby losing the first pair) and computations continue. If the limiting number of updates is set to zero, the coefficient matrix is not updated and modified-Newton iteration results.

A choice of solution strategies is provided in *FST2DH*. A solution might combine both full-Newton and quasi-Newton iterations in an attempt to achieve the fastest solution possible. Usually, several or more full-Newton iterations are used when starting cold (that is, when initial velocities are set to zero and a constant water-surface elevation is assigned), or after making substantial changes to boundary conditions or the geometry of a finite element network. Initial iterations can be followed by one or more quasi-Newton iterations, or by a combination of full-Newton and quasi-Newton iterations.

The optimal number of update vectors to use in a quasi-Newton iteration will vary from solution to solution. Beyond a limit, the updating procedure becomes uneconomical. Maintaining more than about five sets of update vectors in memory has been found to result in wasted computational effort. The number of update vectors used in *FST2DH* is limited to a maximum of five.

Frontal Solution Scheme

The frontal solution technique is a direct solution scheme that is closely related to the finite element method. Designed to minimize core-storage requirements as well as the number of arithmetic operations needed to solve a system of linear algebraic equations, the main idea of the frontal method is to assemble and eliminate element equations at the same time. As soon as an equation is formed completely from the contributions of all relevant elements, it is reduced and eliminated from the “active” coefficient matrix. An equation that has been eliminated from the active coefficient matrix is written to a buffer contained in core memory. When the buffer is full, it is written to an auxiliary storage device. A

coefficient matrix usually is never formed in its entirety. An active matrix contains at any given instant only those equations that have been partly assembled or are complete but not yet eliminated.

The number of unknowns in a wavefront at any given step in a solution is called the frontwidth and generally will change continually during a solution. The maximum frontwidth reached during a solution determines the required maximum size of an active coefficient matrix. When element assembly is complete, the upper triangular matrix of the LU decomposition will have been formed and will be ready for back substitution.

A modified version of the frontal solution scheme presented by Hood (1976 and 1977) is used in *FST2DH*. Modifications were made to eliminate unnecessary computations and to save both the upper and lower triangular matrix decompositions if a quasi-Newton solution is to be carried out. Also, eliminated equations are stored in a buffer (the size of which depends on available computer storage and storage-device limitations), which is written to storage when it is full or nearly full. Data transfer time decreases as the size of the equation buffer is increased.

When solving equation systems by Gaussian elimination, the element along the diagonal of the coefficient matrix by which other elements are divided is called the pivot element. The equation solution procedure can be numerically unstable unless pivoting (exchanging rows and columns as appropriate) is used to make sure that large pivot elements are used. Partial pivoting is the interchanging of rows only, and full pivoting is the interchanging of both rows and columns in order to place a particularly "good" element in the diagonal position prior to a particular operation. Both of these pivoting strategies can be used in *FST2DH,* along with a simple diagonal-pivoting scheme in which equations that are complete and ready for elimination are scanned, and the equation that has the largest diagonal element is eliminated next. Partial pivoting is used by default.

Element Resequencing

The frontal technique assembles and reduces the equations on an element-by-element basis. As soon as the coefficients of a particular equation are assembled, the completed equation can be eliminated and stored out-of-core. During a frontal solution, the entire global coefficient matrix is never formed completely in core. At any given instant, equations contained in core are those that are either not complete (partially assembled) or those that have just been completed but have not yet been eliminated.

The degrees-of-freedom that correspond to the equations contained in core are called the wavefront, or simply the front, because the line of node points at which the degrees-of-freedom are located moves through the network in the form of a wave as elements are processed in order. The number of degrees-of-freedom in the front is called the frontwidth. The frontwidth will vary in size during equation solution and the maximum frontwidth will determine how much core memory is needed. The sum of frontwidths-squared as each equation is eliminated is proportional to the number of arithmetic operations carried out during the solution. The sequence in which the elements are assembled determines the maximum frontwidth and the sum of frontwidths-squared. Therefore, the assembly sequence also defines the core memory and computational effort needed to solve a system of equations. An element assembly sequence that keeps the maximum frontwidth and the sum of frontwidths-squared to a minimum also will keep core memory requirements and equation solution time to a minimum.

For small networks, a manual determination of an optimal element assembly sequence is possible, but for large networks the task quickly becomes tedious and uneconomical to perform by hand. Two methods are available in *FST2DH* to develop an efficient element assembly sequence automatically: (1) the *minimum frontgrowth method,*

and (2) the *level structure method*. Because it is usually impractical to investigate all the combinations of element sequences, the minimum frontgrowth method and the level structure method provide good, but not necessarily the best, assembly sequences.

The two element resequencing methods are based on different strategies, but both methods need an initial list of elements (at least one) to begin a resequencing. From a starting element list, assembly sequences are determined for the remaining elements in a network. For both methods, several different starting element lists probably need to be tried to find a good element assembly sequence. An initial starting list that usually will provide a good assembly sequence consists of all or just some of the elements that form the most narrow edge of a network.

Minimum frontgrowth method

The minimum frontgrowth method maintains the smallest possible frontwidth at all times. An initial wavefront is determined from the starting element list and is defined in terms of nodes rather than degrees-of-freedom. The nodes that form the wavefront form a boundary between elements that have been assembled and elements that have not been assembled. A list of unassembled elements that border the front is called the adjacent element list. The element in the adjacent element list that provides the smallest frontwidth upon its assembly is chosen to be the next element assembled. If more than one element provides the same minimum frontwidth, various tie-breaking strategies are used to choose between them. After an element is assembled, the wavefront is modified and the adjacent element list is updated. This process continues until all elements have been resequenced.

Sometimes an element in an adjacent element list is passed over for assembly a great number of times, resulting in excessively large frontwidths. To avoid this occurrence, the length-of-stay of an element in an adjacent element list is limited. An appropriate value for the maximum length-of-stay needs to be determined by trial-and-error, but a value equal to about twice the expected maximum frontwidth (in terms of nodes) will be a good first try. The maximum frontwidth can be estimated as the number of nodes in a line that extends across the widest part of a network when the network is aligned lengthwise.

Level structure method

The level structure method uses a simple layer-by-layer resequencing strategy and is much faster than the minimum-frontgrowth method, especially for large networks. From a starting element list, a wavefront and a list of elements adjacent to the wavefront are determined. Then, the first element in the adjacent element list is assembled and the unassembled elements adjacent to it are added to the adjacent element list. The adjacent element list is updated and the process is repeated until all elements have been assembled.

3. Hydrodynamics

Equations describing the flow of water in floodplains, estuaries, and other surface-water bodies are based on the classical concepts of conservation of mass and momentum. For many practical surface-water flow applications, knowledge of the full three-dimensional flow structure is not needed. Often it is sufficient to know about depth-averaged flow quantities acting in two perpendicular horizontal directions only, or about cross-section-averaged flow quantities acting in the longitudinal channel direction only. Equations that describe depth-averaged two-dimensional flow, cross-section-averaged one-dimensional flow, as well as special cases of one-dimensional flow through culverts and small bridges, one-dimensional flow over weirs and highway embankments, flow through gate structures, and flow through drop-inlet spillways are presented in this chapter. Initial and boundary conditions needed to solve the set of governing water flow equations are described as well.

Two-dimensional Depth-averaged Flow Equations

Depth-averaged velocity components in the horizontal x and y coordinate directions, respectively, are defined as follows:

$$U = \frac{1}{H}\int_{z_b}^{z_w} u \, dz \qquad V = \frac{1}{H}\int_{z_b}^{z_w} v \, dz \tag{3-1}$$

where H = water depth, z = vertical direction, z_b = bed elevation, $z_w = z_b + H$ = water-surface elevation, u = horizontal velocity in the x direction at a point along the vertical coordinate, and v = horizontal velocity in the y direction at a point along the vertical coordinate. The coordinate system and variables are illustrated in Figure 3-1, and depth-averaged velocity is shown in Figure 3-2.

Equations describing depth-averaged surface-water flow are found by integrating the three-dimensional mass and momentum transport equations with respect to the vertical coordinate from the bed to the water surface, considering vertical velocities and accelerations to be negligible. The vertically-integrated mass transport equation or continuity equation is

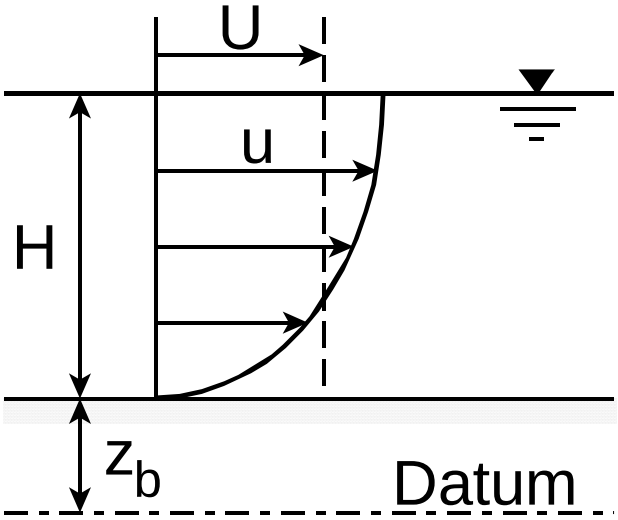

Figure 3-1. Depth-averaged velocities are mean horizontal velocities in the *x* and *y* directions.

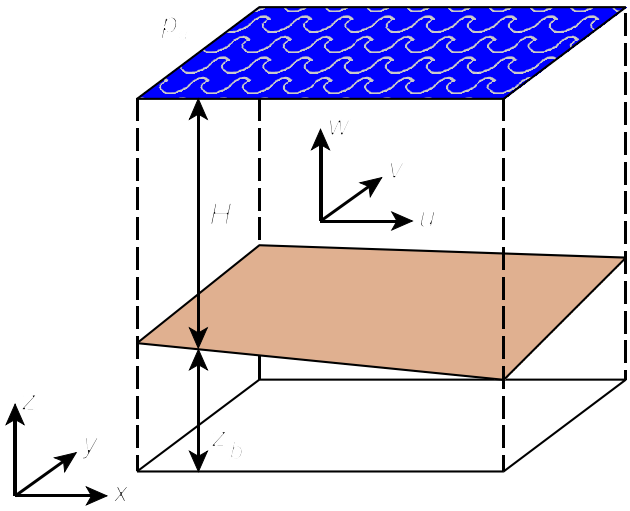

Figure 3-2. Three-dimensional coordinate system and variables.

$$\frac{\partial z_w}{\partial t} + \frac{\partial q_1}{\partial x} + \frac{\partial q_2}{\partial y} = q_m \tag{3-2}$$

where $q_1 = UH$ = unit flow rate in the x direction, $q_2 = VH$ = unit flow rate in the y direction, q_m = mass inflow rate (positive) or outflow rate (negative) per unit area, and water mass density ρ is considered constant throughout the modeled region. Equations describing momentum transport in the x and y directions, respectively, are as follows:

$$\frac{\partial q_1}{\partial t} + \frac{\partial}{\partial x}\left(\beta \frac{q_1^2}{H} + \frac{1}{2} g H^2\right) + \frac{\partial}{\partial y}\left(\beta \frac{q_1 q_2}{H}\right) + gH\frac{\partial z_b}{\partial x} + \frac{H}{\rho}\frac{\partial p_a}{\partial x} - \Omega q_2 + \frac{1}{\rho}\left[\tau_{bx} - \tau_{sx} - \frac{\partial (H\tau_{xx})}{\partial x} - \frac{\partial (H\tau_{xy})}{\partial y}\right] = 0 \tag{3-3}$$

and

$$\frac{\partial q_2}{\partial t} + \frac{\partial}{\partial x}\left(\beta \frac{q_1 q_2}{H}\right) + \frac{\partial}{\partial y}\left(\beta \frac{q_1^2}{H} + \frac{1}{2} g H^2\right) + gH\frac{\partial z_b}{\partial y} + \frac{H}{\rho}\frac{\partial p_a}{\partial y} + \Omega q_1 + \frac{1}{\rho}\left[\tau_{by} - \tau_{sy} - \frac{\partial (H\tau_{yx})}{\partial x} - \frac{\partial (H\tau_{yy})}{\partial y}\right] = 0 \tag{3-4}$$

where β = isotropic momentum flux correction coefficient that accounts for the variation of velocity in the vertical direction, g = gravitational acceleration, ρ = water mass density, p_a = atmospheric pressure at the water surface, Ω = Coriolis parameter, τ_{bx} and τ_{by} = bed shear stresses acting in the x and y directions, respectively, τ_{sx} and τ_{sy} = surface shear stresses acting in the x and y directions, respectively, and τ_{xx}, τ_{xy}, τ_{yx}, and τ_{yy} = shear stresses caused by turbulence where, for example, τ_{xy} is the shear stress acting in the x direction on a plane that is perpendicular to the y direction.

Momentum Flux Correction Coefficient

Vertical velocity profiles can be approximated by the logarithmic function

$$u = \frac{u_*}{\kappa} \log_e \left(\frac{z - z_b}{k} \right) \tag{3-5}$$

where $u_* = \sqrt{c_f}\, U$ = bed shear velocity or bed friction velocity, c_f = bed shear-stress coefficient, κ = von Karman's constant, and k = roughness height. When vertical velocities follow the logarithmic profile, the momentum flux correction coefficient is given by

$$\beta = 1 + \frac{c_f}{\kappa^2} \tag{3-6}$$

Momentum flux correction coefficients in *FST2DH* are calculated as

$$\beta = \beta_o + c_\beta c_f \tag{3-7}$$

where β_o and c_β are specified coefficients. Comparing the two expressions for β gives $\beta_o = 1$ and $c_\beta = 1/\kappa^2$. For most open-channel flows, the coefficient $\kappa \approx 0.4$, which gives $c_\beta = 6.25$. Constant momentum flux correction factors can be specified by setting β_o to the desired value, and setting c_β to zero. Default values in *FST2DH* are $\beta_o = 1$ and $c_\beta = 0$. Using these default values means that the effects of vertical variations in velocity on solutions are considered negligible.

Coriolis Parameter

Effect of the Earth's rotation on water movement is taken into account by terms in the momentum equations that contain the Coriolis parameter $\Omega = 2\omega \sin \phi$, where ω = angular velocity of the rotating Earth (7.27×10^{-5} radians per second), and ϕ = angle of latitude. The sign of ϕ is positive in the northern hemisphere and negative in the southern hemisphere. A constant value of the Coriolis parameter is used in *FST2DH* (that is, the variation of Ω within the area covered by a finite element network is considered negligible). For most shallow flows where the horizontal extent to depth ratio is large (for example, flows in nearly all rivers and flood plains), the Coriolis effect will be small and can be safely ignored.

Bed Shear Stresses

Directional components of bed shear stress are computed as follows:

$$\tau_{bx} = \rho c_f m_b \frac{q_1 \sqrt{q_1^2 + q_2^2}}{H^2} \qquad \tau_{by} = \rho c_f m_b \frac{q_2 \sqrt{q_1^2 + q_2^2}}{H^2} \tag{3-8}$$

where c_f = dimensionless bed-friction coefficient, and

$$m_b = \sqrt{1 + \left(\frac{\partial z_b}{\partial x} \right)^2 + \left(\frac{\partial z_b}{\partial y} \right)^2} \tag{3-9}$$

is a factor that accounts for increased shear stress caused by a sloping bed. Bed friction coefficients c_f are given by

$$c_f = \frac{g n^2}{\phi_n^2 H^{1/3}} = \frac{g}{C^2} \tag{3-10}$$

where n = Manning's roughness coefficient, ϕ_n = 1.486 for U.S. Customary units, or 1.0

for SI units, and C = Chézy discharge coefficient. Both Manning and Chézy coefficients can be described by linear functions of water depth in *FST2DH*. Variations in flow resistance with water depth might occur when short vegetation is submerged and possibly bent by the flow, or where tree branches come into contact with flow at high stages.

Appropriate flow resistance coefficients for natural and constructed channels, and for floodplains, can be estimated using references such as Chow (1959), Barnes (1967), and Arcement and Schneider (1984). However, coefficients in these references have been determined on the basis of one-dimensional flow approximations, and implicitly account for the effects of turbulence and deviation from a uniform velocity in a cross section. Because the depth-averaged flow equations directly account for horizontal variations of velocity and the effect of turbulence, values of c_f computed using coefficients based on a one-dimensional flow might be larger than necessary. Little information is available to help select coefficients for two-dimensional depth-averaged flow computations. For the time being, flow resistance coefficients can be estimated on the basis of available references and experience.

Wind Shear Stresses

Directional components of surface shear stress caused by wind are calculated as follows:

$$\tau_{sx} = c_s \rho_a W^2 \cos\psi \qquad \tau_{sy} = c_s \rho_a W^2 \sin\psi \tag{3-11}$$

where c_s = dimensionless surface stress coefficient; ρ_a = mass density of air; W = characteristic wind velocity near the water surface; and ψ = angle between the wind direction and the positive x-axis. Surface stress coefficients have been found to depend on wind speeds and are calculated in *FST2DH* by the general relation

$$c_s = \begin{cases} c_{s1} \times 10^{-3}; \ if \ W \le W_{min} \\ [c_{s1} + c_{s2}(W - W_{min})] \times 10^{-3}; \ if \ W > W_{min} \end{cases} \tag{3-12}$$

where c_{s1}, c_{s2}, and W_{min} are coefficients.

For wind speed in meters per second, measured 10 meters above the water surface, Garratt (1977) finds that c_{s1} = 1.0, c_{s2} = .067, and W_{min} = 4 m/s. Wang and Connor (1975) compare several relations for c_s and conclude that c_{s1} = 1.1, c_{s2} = 0.0536, and W_{min} = 0 m/s. Hicks (1972) suggests the coefficients c_{s1} = 1.0, c_{s2} = 0.05, and W_{min} = 5.0 m/s. However, factors other than wind velocity can influence the value of the surface stress coefficient c_s. For example, Hicks et al. (1974) show that as water becomes shallow (less than 2.5 m deep) long period waves are not able to develop fully. As a result, water surfaces will be smoother and the value of c_s remains close to 0.001 for all wind speeds. Default values of wind shear stress coefficients in *FST2DH* are as follows: c_{s1} = 1.0, c_{s2} = 0.0, and W_{min} = 0.0 m/s.

Lateral Shear Stresses Caused by Turbulence

Depth-averaged lateral shear stresses caused by turbulence are computed using Boussinesq's eddy viscosity concept whereby the turbulent stresses, like viscous stresses, are considered proportional to gradients of the depth-averaged velocities. These stresses are computed as follows:

$$\tau_{xx} = \rho\nu_t\left(\frac{\partial U}{\partial x}+\frac{\partial U}{\partial x}\right),\quad \tau_{xy}=\tau_{yx}=\rho\nu_t\left(\frac{\partial U}{\partial y}+\frac{\partial V}{\partial x}\right),\quad \tau_{yy}=\rho\nu_t\left(\frac{\partial V}{\partial y}+\frac{\partial V}{\partial y}\right) \qquad (3\text{-}13)$$

where ν_t = depth-averaged kinematic eddy viscosity or turbulent exchange coefficient, which is considered isotropic.

Eddy viscosity is related to eddy diffusivity for heat or mass transfer Γ_t as

$$\Gamma_t = \frac{\nu_t}{\sigma_t} \qquad (3\text{-}14)$$

where σ_t = an empirical constant called the Prandtl number (for diffusion of heat) or Schmidt number (for diffusion of mass). Many experiments on spreading of dye in open channels (Fischer et al., 1979) show dimensionless diffusivity, $e_* = \Gamma_t / u_* H$, to be between 0.1 and 0.2 in straight uniform open channels, and that channel curves and sidewall irregularities increase e_*. Values of e_* in natural streams hardly ever are less than 0.4. Heat and mass transfer experiments show the turbulent Prandtl/Schmidt number to vary from 0.5 in free shear flows to 0.9 in flow regions near walls (Rodi 1982, page 587). Considering turbulent exchange of mass and momentum to be similar (that is, $\sigma_t = 1.0$), eddy viscosity in natural open channels can be related to the bed shear velocity and depth by

$$\nu_t = (0.6 \pm 0.3) u_* H \qquad (3\text{-}15)$$

where larger values are likely to occur if channels have sharp curves or rapid changes in geometry.

Relating eddy viscosity to the scales of motion being resolved by a mesh and the local deformation field, Smagorinsky (1963) proposes the following formula:

$$\nu_t = \alpha \Delta x \Delta y \sqrt{\left(\frac{\partial U}{\partial x}\right)^2+\left(\frac{\partial V}{\partial y}\right)^2+\frac{1}{2}\left(\frac{\partial U}{\partial y}+\frac{\partial V}{\partial x}\right)^2} \qquad (3\text{-}16)$$

where α = dimensionless coefficient, and Δx, Δy = horizontal dimensions of rectangular computational cells. Numerical experiments show that $0.01 \le \alpha \le 0.5$, and that $\alpha \approx 0.10$ provides kinematic eddy viscosities that are consistent with measured values.

Kinematic eddy viscosities are calculated in *FST2DH* as follows:

$$\nu_t = \nu_{t0} + c_{\mu 1} u_* H + c_{\mu 2} |J| \sqrt{\left(\frac{\partial U}{\partial x}\right)^2+\left(\frac{\partial V}{\partial y}\right)^2+\frac{1}{2}\left(\frac{\partial U}{\partial y}+\frac{\partial V}{\partial x}\right)^2} \qquad (3\text{-}17)$$

where ν_{t0} = base kinematic eddy viscosity, $c_{\mu 1}$, $c_{\mu 2}$ = dimensionless coefficients, $|J|$ = determinant of the jacobian matrix of element coordinate transformations, which provides pointwise measures of element area. Comparing expressions for ν_t shows that $c_{\mu 1} \approx 0.6 \pm 0.3$ in natural channels when $\nu_{t0} = 0$ and $c_{\mu 2} = 0$; and that $c_{\mu 2} \approx 0.10$ when $\nu_{t0} = 0$ and $c_{\mu 1} = 0$. Constant eddy viscosities are assigned by specifying $c_{\mu 1} = c_{\mu 2} = 0$ and $\nu_{t0} > 0$. Base eddy viscosities ν_{t0} = 10 ft^2/sec or 1 m^2/s for medium to large rivers are within reason.

Element Wetting and Drying

Node points become dry when calculated water-surface elevations are lower than their bed elevations. Elements that contain at least one dry node are turned off at the start of an iteration and are not included in calculations. All elements that are turned off are checked at the start of an iteration to see if they can be turned back on as previously dry nodes become wet (that is, as the water surface rises above the bed), and boundary conditions are modified. Adjustment of boundaries in this way allows a finite element network to be constructed without too much concern for the limits of inundation. However, solution stability can be affected adversely by elements switching on and off, especially if the elements in transition are comparatively large, and if only small portions of those elements are actually dry.

By introducing the concept of *element storativity*, partially dry elements can be retained in calculations when solving the governing equations. *Bed storativity coefficients*, λ_b, are ratios of changes in stored water per unit element area with respect to changes in water elevation, and are calculated as follows:

$$\lambda_b = \begin{cases} 1;\ if\ z_w \geq z_b + \zeta \\ a + (1-a)\left(\dfrac{z_w - z_b + b}{\zeta + b}\right);\ if\ z_b + \zeta > z_w > z_b - b \\ a;\ if\ z_b - b \geq z_w > z_b - \eta_b\zeta \\ 0;\ z_w \leq z_b - \eta_b\zeta \end{cases} \tag{3-18}$$

where ζ = storativity depth, a = minimum element storativity, η_b = storativity depth factor, and

$$b = \zeta\left[\frac{1-(1+2\eta_b)a}{1-a}\right] \tag{3-19}$$

is the depth below z_b at which $\lambda_b = a$. Element storativity $\lambda_b = a$ for z_b - b $\geq z_w \geq z_b - \eta_b\zeta$. The coefficient λ_b represents the ability of elements to store water when water depth is less than ζ, and is shown in Figure 3-3 as a function of z_w and ζ,

Element storativity is implemented in computations by replacing water depth $H = z_w - z_b$ with an effective water depth H_{eff}, which is given by

$$H_{eff} = \int_{z_b - \eta_b\zeta}^{z_w} \lambda_b\, dz \tag{3-20}$$

The expression for the bed storativity coefficient λ_b assures that $H_{eff} = H$ when $z_w \geq z_b + \zeta$. Storativity depth ζ depends on ground surface variability within an element as shown in Figure 3-4, and may reasonably range from 0.5 ft (0.15 m) to 3 ft (1 m). Storativity depths vanish for elements having perfectly planar surfaces. However, non-zero storativity depths might be assigned even for perfectly planar elements to keep them from being turned off when only small sections of them are dry. Therefore, use of element storativity is beneficial because of both physical and computational reasons. Numerical experiments show that assigning $a = 0.01$ and $\eta_b = 3$ provides a good means of controlling element transition from wet to dry states.

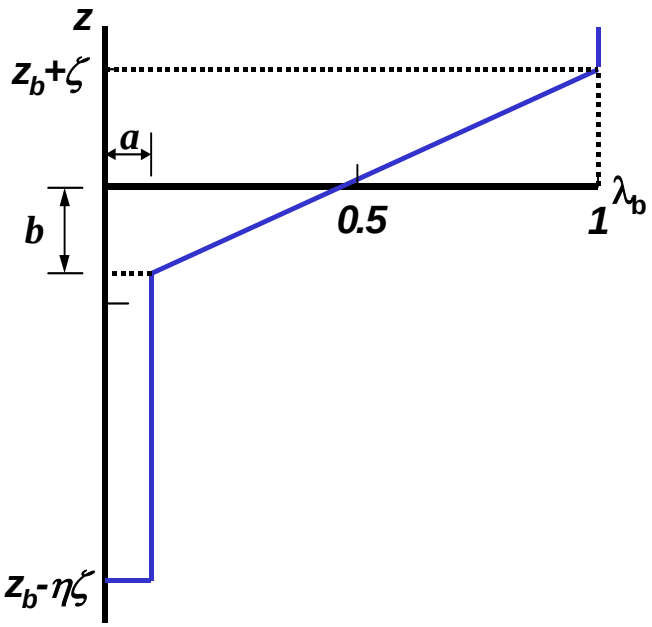

Figure 3-4. Element storativity coefficient λ_b as a function of water surface elevation z_w storativity depth ζ, minimum storativity *a*, and storativity depth factor η_b.

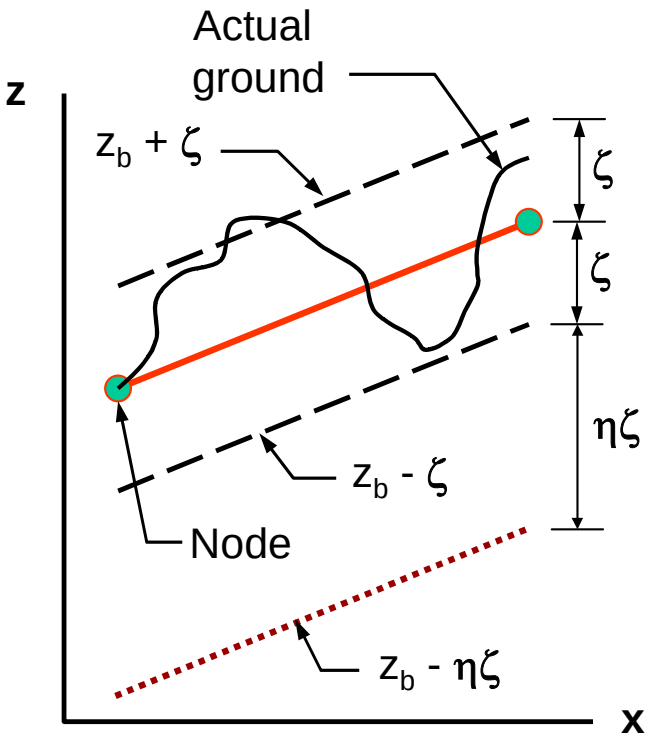

Figure 3-3. Variation of bed elevation within an element showing storativity depth ζ.

Bridge/Culvert Flow

Flow through bridges and culverts can be simulated as either one-dimensional or two-dimensional flow. Bridge flow probably needs to be modeled with two-dimensional elements if the width of the bridge or culvert is large in comparison to the width of the channel or floodplain on which it is located (Figure 3-5).

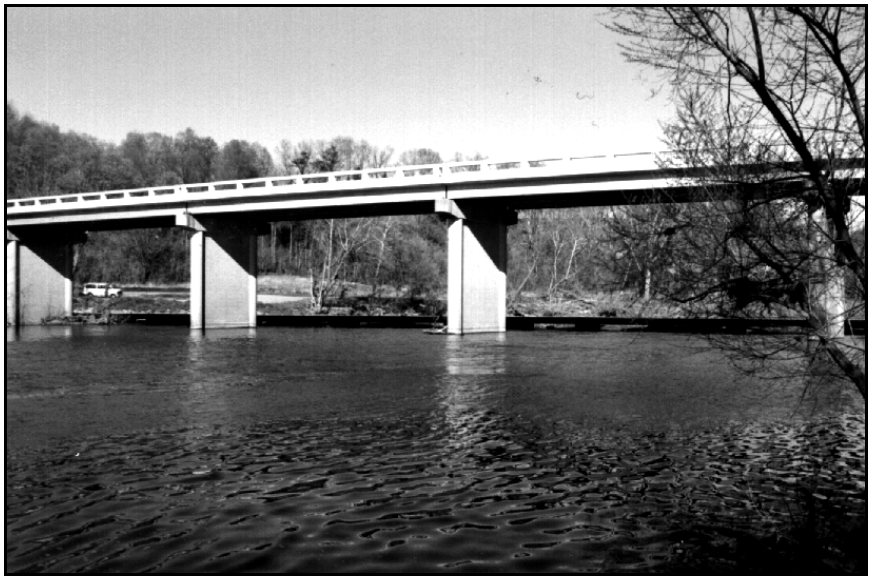

Figure 3-5. View of a bridge where two-dimensional flow might be modeled because of the comparatively large width of the opening.

Two-Dimensional Representation

Two-dimensional flow through a bridge or culvert is modeled exactly as ordinary free-surface flow when the water surface is not in contact with the top of the bridge or culvert opening (unconfined flow). When the water surface is in contact with the top or *ceiling* of the opening pressure flow conditions exist. Depth-averaged flow equations are modified at node points where pressure flow occurs, and pressure head rather than depth is computed. Usually piers will not be modeled directly in a network because their widths are small in comparison to bridge spans (see Figure 3-5) and because their base areas are significantly smaller than the areas of elements used to discretize bridge openings. However, the effect of piers or piles on flow can be taken into account by increasing bed friction coefficients within elements that contain them. This adjustment is carried out automatically in *FST2DH.*

Depth-averaged Pressure Flow

Depth-averaged pressure flow through a bridge or culvert is modeled by specifying a *ceiling elevation* at node points within the opening. When the water surface is in contact with the ceiling, pressure flow exists and the governing depth-averaged flow equations are modified. For small bed slopes the momentum equations become

$$\frac{\partial q_1}{\partial t} + \frac{\partial}{\partial x}\left(\beta\frac{q_1^2}{H} + gHP - \frac{1}{2}gH^2\right) + \frac{\partial}{\partial y}\left(\beta\frac{q_1 q_2}{H}\right) + gP\frac{\partial z_b}{\partial x} - g(P-H)\frac{\partial z_c}{\partial x} - \Omega q_2 + \frac{1}{\rho}\left[\tau_{bx} + \tau_{cx} - \frac{\partial(H\tau_{xx})}{\partial x} - \frac{\partial(H\tau_{xx})}{\partial x}\right] = 0 \quad (3\text{-}21)$$

for flow in the x direction, and

$$\frac{\partial q_1}{\partial t} + \frac{\partial}{\partial x}\left(\beta\frac{q_1 q_2}{H}\right) + \frac{\partial}{\partial y}\left(\beta\frac{q_1^2}{H} + gHP - \frac{1}{2}gH^2\right) + gP\frac{\partial z_b}{\partial y} - g(P-H)\frac{\partial z_c}{\partial y} + \Omega q_2 + \frac{1}{\rho}\left[\tau_{by} + \tau_{cy} - \frac{\partial(H\tau_{yx})}{\partial x} - \frac{\partial(H\tau_{yy})}{\partial y}\right] = 0 \quad (3\text{-}22)$$

for flow in the *y* direction, where P = pressure head, z_c = ceiling elevation, τ_{cx} and τ_{cy} = directional components of shear stress at the ceiling, and $H = z_c - z_b$. The continuity equation becomes

$$\frac{\partial q_1}{\partial x} + \frac{\partial q_2}{\partial y} - q_m = 0 \quad (3\text{-}23)$$

because water depth can no longer change with time. Dependent variables in the confined flow case are q_1, q_2, and P. Increased frictional resistance created by contact between water and the ceiling is described by the surface shear stress terms which are computed as follows:

$$\tau_{cx} = \rho c_f m_c \frac{q_1\sqrt{q_1^2 + q_2^2}}{H^2} \qquad \tau_{cy} = \rho c_f m_c \frac{q_2\sqrt{q_1^2 + q_2^2}}{H^2} \quad (3\text{-}24)$$

where

$$m_c = \sqrt{1 + \left(\frac{\partial z_c}{\partial x}\right)^2 + \left(\frac{\partial z_c}{\partial y}\right)^2} \quad (3\text{-}25)$$

is a factor that accounts for increased resistance caused by a sloped ceiling, and c_f is the same dimensionless friction coefficient used to model the bed shear stress. When pressure flow occurs, surface stresses caused by wind are not considered.

Bridge Pier Drag Force

Total drag force exerted on a bridge pier by the flow is given by

$$F_d = \frac{1}{2}C_d\rho V^2 A_p \quad (3\text{-}26)$$

where C_d = pier drag coefficient (dimensionless), and A_p = below-water cross-sectional area of the pier projected normal to the direction of the approaching streamflow. Added resistance caused by the pier is taken into account by distributing the drag force evenly across the element containing the pier as shown in Figure 3-6. Directional components of the bed shear stress within the element are modified by adding the additional "pier shear stresses" as follows:

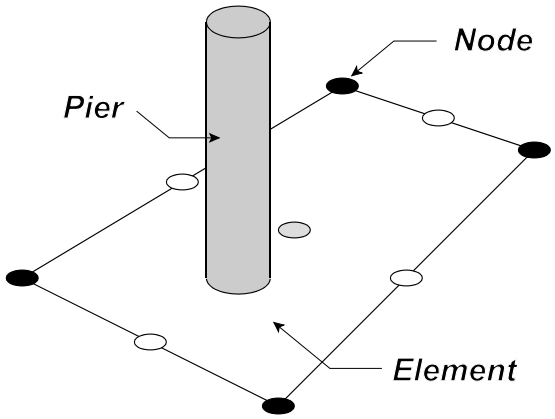

Figure 3-6. Effects of bridge piers can be approximated by distributing the hydrodynamic drag caused by the piers evenly across the elements that contain them.

$$\tilde{\tau}_{bx} = \tau_{bx} + \frac{1}{2} C_d \rho \frac{q_1 \sqrt{q_1^2 + q_2^2}}{H^2} \left(\frac{A_p}{A_e} \right)$$

$$\tilde{\tau}_{by} = \tau_{by} + \frac{1}{2} C_d \rho \frac{q_2 \sqrt{q_1^2 + q_2^2}}{H^2} \left(\frac{A_p}{A_e} \right) \qquad (3\text{-}27)$$

where A_e = area of the element in which the pier is located. Bed shear stress within an element is increased accordingly for each pier whose center is contained within the element. Although the bed shear stress adjustment takes into account added flow resistance created by bridge piers, the effect of piers on flow within bridge openings is only approximated.

One-dimensional Representation

Culverts are short closed conduits that convey water under roadways, railroads, canals, or some other type of flow obstruction (Figure 3-7). If the width of a bridge or culvert is small in comparison to the floodplain width, and if a detailed description of flow in the vicinity of the structure is not needed, the bridge or culvert might be modeled accurately by a one-dimensional flow approximation. One-dimensional flow through a small bridge or a culvert is calculated using an equation developed for flow through culverts.

Figure 3-7. Bridges and culverts can be modeled well by one-dimensional flow approximations when their widths are small in comparison to the channel and floodplain.

Rates of flow through culverts depend primarily on *headwater* depths (that is, depths of water above inverts at their

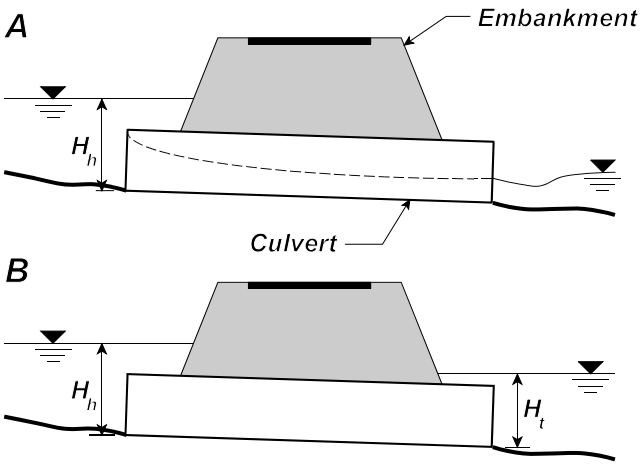

Figure 3-8. Flow through culverts under (A) inlet control and (B) outlet control.

upstream ends). Other factors that affect culvert flow rates are tailwater elevations (that is, the water-surface elevations at the downstream ends), and physical properties of the culverts including cross-sectional area, cross-sectional shape, inlet geometry, length, longitudinal slope, and roughness. If flow capacities of culverts are small, headwater depths may become large enough to send flow over embankments or cause flood damage to surrounding properties.

Culvert flow is classified as being controlled primarily by characteristics of either the inlet or the outlet of the culvert (Figure 3-8). Hydraulic capacity is calculated differently for the two types of control. The controlling condition is considered the one that yields the smallest flow rate for specified headwater and tailwater depths.

Inlet Control Flow

Under *inlet control*, culverts have shallow, high-speed supercritical flow immediately downstream from their inlets. Hydraulic jumps may form within their barrels depending on tailwater depths. Culverts will never flow full throughout their lengths when inlet conditions control, behaving like orifices when their inlets are submerged, or like weirs when they are not. Flow rates under these conditions depend primarily on headwater depths and inlet characteristics, with culvert barrel slope affecting submerged flows slightly. Headwater depth ratios for unsubmerged (weir flow) and submerged (orifice flow) inlet control discharge are calculated using the FHWA procedure (Norman et al., 1985) as follows:

$$\frac{H_w}{D_c} = \begin{cases} K'\left[\dfrac{Q}{A_c\sqrt{gD_c}}\right]^M; \textit{ for unsubmerged flow} \\ c'\left[\dfrac{Q}{A_c\sqrt{gD_c}}\right]^2 + Y + mS_o; \textit{ for submerged flow} \end{cases} \tag{3-28}$$

where H_w = headwater depth above inlet control section invert; D_c = interior height of culvert barrel; Q = barrel flow rate; A_c = full cross section area of culvert barrel; g = gravitational acceleration; S_o = culvert barrel slope; K', M, c', Y = coefficients that depend on culvert material, barrel cross section shape, and inlet characteristics; and m = 0.7 for mitered inlets, and -0.5 for all other inlets. Note that the inlet control formulas have been made dimensionless by inclusion of gravitational acceleration in the formulas given by Normann et al. (1985). Consequently, the coefficients K and c given in Normann et al. (1985) differ from the coefficients K' and c' as follows: $K = K'g^{M/2}$ and $c = c'g$. Coefficients K', M, c', and Y for various culvert barrel material and inlet combinations are summarized in Table 3-1.

Table 3-1. Summary of culvert inlet flow formula coefficients.

Barrel material	Barrel shape	Inlet description	Coefficients[b]			
			K'	M	c'	Y
Concrete	Circular	Headwall; square edge	0.3153	2.0000	1.2804	0.6700
Concrete	Circular	Headwall; gooved edge	0.2509	2.0000	0.9394	0.7400
Concrete	Circular	Projecting; grooved edge	0.1448	2.0000	1.0198	0.6900
Cor. metal	Circular	Headwall	0.2509	2.0000	1.2192	0.6900
Cor. metal	Circular	Mitered to slope	0.2112	1.3300	1.4895	0.7500
Cor. metal	Circular	Projecting	0.4593	1.5000	1.7790	0.5400
Concrete	Circular	Beveled ring; 45 deg bevels	0.1379	2.5000	0.9651	0.7400
Concrete	Circular	Beveled ring; 33.7 deg bevels	0.1379	2.5000	0.7817	0.8300
Concrete	Rectangular	Wingwalls; 30 to 75 deg flares; square edge	0.1475	1.0000	1.2385	0.8100
Concrete	Rectangular	Wingwalls; 90 and 15 deg flares; square edge	0.2242	0.7500	1.2868	0.8000
Concrete	Rectangular	Wingwalls; 0 deg flares; square edge	0.2242	0.7500	1.3608	0.8200
Concrete	Rectangular	Wingwalls; 45 deg flare; beveled edge	1.6230	0.6670	0.9941	0.8000
Concrete	Rectangular	Wingwalls; 18 to 33.7 deg flare; beveled edge	1.5466	0.6670	0.8010	0.8300
Concrete	Rectangular	Headwall; 3/4 in chamfers	1.6389	0.6670	1.2064	0.7900
Concrete	Rectangular	Headwall; 45 deg bevels	1.5752	0.6670	1.0101	0.8200
Concrete	Rectangular	Headwall; 33.7 deg bevels	1.5466	0.6670	0.8107	0.8650
Concrete	Rectangular	Headwall; 45 deg skew; 3/4 in chamfers	1.6611	0.6670	1.2932	0.7300
Concrete	Rectangular	Headwall; 30 deg skew; 3/4 in chamfers	1.6961	0.6670	1.3672	0.7050
Concrete	Rectangular	Headwall; 15 deg skew; 3/4 in chamfers	1.7343	0.6670	1.4493	0.6800
Concrete	Rectangular	Headwall; 10-45 deg skew; 45 deg bevels	1.5848	0.6670	1.0520	0.7500
Concrete	Rectangular	Wingwalls; non-offset 45˚ flares; 3/4 in chamfers	1.5816	0.6670	1.0906	0.8030
Concrete	Rectangular	Wingwalls; non-offset 18.4˚ flares; 3/4 in chamfers	1.5689	0.6670	1.1613	0.8060
Concrete	Rectangular	Wingwalls; non-offset 18.4˚ flares; 30˚ skewed barrel	1.5752	0.6670	1.2418	0.7100
Concrete	Rectangular	Wingwalls; offset 45˚ flares; beveled top edge	1.5816	0.6670	0.9715	0.8350
Concrete	Rectangular	Wingwalls; offset 33.7˚ flares; beveled top edge	1.5752	0.6670	0.8107	0.8810
Concrete	Rectangular	Wingwalls; offset 18.4˚ flares; top edge bevel	1.5689	0.6670	0.7303	0.8870
Cor. metal	Rectangular	Headwall	0.2670	2.0000	1.2192	0.6900
Cor. metal	Rectangular	Projecting; thick wall	0.3023	1.7500	1.3479	0.6400
Cor. metal	Rectangular	Projecting; thin wall	0.4593	1.5000	1.5956	0.5700
Concrete	Horizontal ellipse	Headwall; square edge	0.3217	2.0000	1.2804	0.6700
Concrete	Horizontal ellipse	Headwall; grooved edge	0.1379	2.5000	0.9394	0.7400
Concrete	Horizontal ellipse	Projecting; gooved edge	0.1448	2.0000	1.0198	0.6900
Concrete	Horizontal ellipse	Headwall; square edge	0.3217	2.0000	1.2804	0.6700
Concrete	Horizontal ellipse	Headwall; grooved edge	0.1379	2.5000	0.9394	0.7400
Concrete	Horizontal ellipse	Projecting; gooved edge	0.3056	2.0000	1.0198	0.6900
Cor. metal	Pipe arch (18" corner)	Headwall	0.2670	2.0000	1.5956	0.5700
Cor. metal	Pipe arch (18" corner)	Mitered to slope	0.1702	1.0000	1.4895	0.7500
Cor. metal	Pipe arch (18" corner)	Projecting	0.4593	1.5000	1.5956	0.5300
Structural plate	Pipe arch (18" corner)	Projecting	0.3998	1.5000	1.5667	0.5500
Structural plate	Pipe arch (18" corner)	Headwall; square edge	0.2799	2.0000	1.1613	0.6600
Structural plate	Pipe arch (18" corner)	Headwall; beveled edge	0.0965	2.0000	0.8493	0.7500
Structural plate	Pipe arch (31" corner)	Projecting	0.3998	1.5000	1.5667	0.5500
Structural plate	Pipe arch (31" corner)	Headwall; square edge	0.2799	2.0000	1.1613	0.6600
Structural plate	Pipe arch (31" corner)	Headwall; beveled edge	0.0965	2.0000	0.8493	0.7500
Cor. metal	Arch	Headwall	0.2670	2.0000	1.2192	0.6900
Cor. metal	Arch	Mitered to slope	0.9651	2.0000	1.4895	0.7500
Cor. metal	Arch	Projecting	0.4593	1.5000	1.5956	0.5700
Concrete	Circular	Tapered throat	1.3991	0.5550	0.6305	0.8900
Cor. metal	Circular	Tapered throat	1.5760	0.6400	0.9297	0.9000
Concrete	Rectangular	Tapered throat	1.5116	0.6670	0.5758	0.9700

[a]From Norman et al. (1985, Table 9, pages 147-148)
[b]Coefficients K' and c' have been made non-dimensional and, therefore, differ from the coefficients K and c given by Norman et al. (1985).

Table 3-2. Entrance loss coefficients for various culvert types and entrance conditions.

Type of culvert	Entrance description	Entrance loss coefficient[a], K_e
Concrete pipe	Projecting from fill, grooved end	0.2
	Projecting from fill, square-cut end	0.5
	Headwall or headwall with wingwalls (concrete or cement sandbags)	
	Grooved pipe end	0.2
	Square-cut pipe end	0.5
	Rounded pipe end	0.1
	Mitered end that conforms to embankment slope	0.7
	Manufactured end section of metal or concrete that conforms to embankment slope	
	Without grate	0.5
	With grate	0.7
Corrugated metal pipe or pipe-arch	Projecting from embankment (no headwall)	0.9
	Headwall with or without wingwalls (concrete or cement sandbags)	0.5
	Mitered end that conforms to embankment slope	0.7
	Manufactured end section of metal or concrete that conforms to embankment slope	
	Without grate	0.5
	With grate	0.7
Reinforced concrete box	Headwall parallel to embankment (no wingwalls)	
	Square-edged on three sides	0.5
	Rounded on three sides to radius of 1/12 of barrel dimension	0.2
	Wingwalls at 30° to 75° to barrel	
	Square-edged at crown	0.4
	Crown edge rounded to radius of 1/12 of barrel dimension	0.2
	Wingwalls at 10° to 30° to barrel	
	Square-edged at crown	0.5
	Wingwalls parallel to embankment	
	Square-edged at crown	0.7

[a]Summarized from entrance loss coefficients given by Norman et al. (1985) and "Roadway and traffic design standards" (1998, Index No. 249 "Pipe end treatment application guide").

Table 3-3. Culvert Manning roughness coefficients for various culvert barrel materials and barrel conditions.

Culvert barrel material	Entrance description	Manning roughness coefficient, n_c
Concrete	Good joints, smooth walls	0.012
	Projecting from fill, square-cut end	0.015
	Poor joints, rough walls	0.017
Corrugated metal or structural plate corrugated metal	2-2/3 inch × ½ inch corrugations	0.025
	6 inch × 1 inch corrugations	0.024
	5 inch × 1 inch corrugations	0.026
	3 inch × 1 inch corrugations	0.028
	6 inch × 2 inch corrugations	0.034
	9 inch × 2-½ inch corrugations	0.035

Outlet Control Flow

Under *outlet control*, culverts either flow full for their entire lengths, or flow in subcritical states without being completely filled. Outlet control flow is calculated based on a straightforward energy balance between the upstream and downstream ends of a culvert as follows:

$$\frac{H_w}{D_c} = \frac{H_o}{D_c} + \frac{Q^2}{2gA_c^2 D_c}\left(1 + K_e + \frac{2gn_c^2 L}{\phi_n R_c^{4/3}}\right) - S_o\frac{L_c}{D_c} \tag{3-29}$$

where $H_o = \max\{T_w, (d_c + D_c)/2\}$, T_w = tailwater depth above the barrel invert, d_c = critical depth at the outlet, K_e = entrance energy loss coefficient, L_c = barrel length, n_c = Manning roughness coefficient of the culvert barrel, and ϕ_n = units conversion factor (1.0 for SI units, 1.486 for US customary units.) The energy balance considers channel velocities both upstream and downstream from the culvert barrel to be small in comparison to the barrel velocity. The outlet energy loss coefficient is taken as unity. Entrance loss coefficients K_e are summarized in Table 3-2 for various inlet configurations, and Manning roughness coefficients for different barrel materials are summarized in Table 3-3.

Based on (3-28) and (3-29), culvert flow rates are found as follows:

$$Q_c = N_b C_c A_c \sqrt{2gH_c} \tag{3-30}$$

where N_b = number of identical barrels, C_c = discharge coefficient that depends on the flow control (inlet or outlet) and culvert characteristics,

$$H_c = \begin{cases} z_s^h - z_{inv}; \text{ for inlet control} \\ z_s^h - z_s^t; \text{ for outlet control} \end{cases} \tag{3-31}$$

is culvert head, z_w^h = water-surface elevation at the upstream end of a culvert (that is, the headwater elevation), z_w^t = water-surface elevation at the downstream end of the culvert (that is, tailwater elevation); and z_{inv} = invert elevation at the culvert entrance. For inlet control flow,

$$C_c = Min\left\{\sqrt{\frac{1 - \frac{D_c}{H_h}(Y + mS_o)}{2c'}}, \frac{1}{\sqrt{2}K'^{\frac{1}{M}}}\left(\frac{H_h}{D_c}\right)^{\frac{1}{M}-\frac{1}{2}}\right\} \tag{3-32}$$

where $H_h = z_w - z_{inv}$ is headwater depth. The first inlet control discharge coefficient is used when the culvert entrance is submerged and functions like an orifice; the second coefficient applies when the entrance is not submerged and acts as a weir. Discharge coefficients for outlet control flow are calculated as follows:

$$C_c = \frac{1}{\sqrt{1 + K_e + \frac{2gn_c^2 L_c}{\phi_n^2 R_c^{4/3}}}} \tag{3-33}$$

Weir Flow and Roadway Overtopping

Depth-averaged flow equations are derived by considering velocity in the vertical direction to be negligible. However, flow over weirs, or weir-like structures such as roadway embankments (Figure 3-9), can have significant vertical motion and might not be simulated accurately using depth-averaged flow approximations. Weir flow likely will be modeled more accurately using an empirical equation to calculate discharge over a horizontal weir segment.

Flow over a weir segment, Q_w, is calculated as

$$Q_w = K_w \left(z_w^h - z_{wc} \right)^{1.5} \tag{3-34}$$

where K_w = weir coefficient; z_w^h = water-surface elevation at the upstream or headwater node; and z_{wc} = crest elevation of the weir segment. Weir coefficients, K_w, are given by

$$K_w = C_s C_w \sqrt{g} L_w \tag{3-35}$$

where C_s = weir submergence factor used to adjust K_w when flow over a weir segment is affected by tailwater; C_w = dimensionless discharge coefficient for free (that is, not submerged) weir flow (usually about 0.54); and L_w = length of the weir segment. Submergence coefficients, C_s, are calculated as

$$C_s = \left(1 - Y_t^{a_{sub}} \right)^{b_{sub}} \tag{3-36}$$

where

$$Y_t = \left(\frac{z_w^t - z_{wc}}{z_w^h - z_{wc}} \right) \tag{3-37}$$

is the submergence ratio, z_w^t = water-surface elevation at the downstream or tailwater node, and a_{sub}, b_{sub} = dimensionless submergence factor coefficients. Unless specified, default values of weir segment coefficients C_w, a_{sub}, and b_{sub} will be used based on the assigned weir segment type as summarized in Table 3-4.

Figure 3-9. Weir flow over roadway embankments is modeled using an empirical formula that connects finite element networks on the upstream and downstream sides of the embankments.

Table 3-4 Submergence function default coefficients[a]

Weir segment description	C_w	a_{sub}	b_{sub}
Undefined	0.544	16.4	0.432
Paved roadway	0.544	16.4	0.432
Gravel roadway	0.544	15.4	0.608
Single railroad track	0.577	7.25	0.5
Double railroad track	0.52	7.25	0.5
Sharp-crested weir	0.544	1.5	0.385
Broad-crested weir	0.544	7.25	0.5

[a]Weir coefficients are based on formulas and charts presented by King and Brater (1963, page 5-19) and Hulsing (1976, page 27).

Gate Structures

Gate structures are movable barriers that can be used to control the flow of water through or over a dam or embankment. Two general types of gates are considered here: (1) underflow gates, and (2) overflow gates. Underflow or submerged gates act as orifices and include vertical lift gates and radial gates. Overflow or crest gates act as weirs and include sector gates, flap gates, and roller gates.

Discharge through underflow gates is calculated as (Novak et al. 1996, pages 232-233)

$$Q = C_{gu} w_{gu} h_{gu} \sqrt{2g(z_w^u - z_{gu})} \tag{3-38}$$

where

$$C_{gu} = \frac{C_{gc}}{\sqrt{1 + C_{gc} \dfrac{h_{gu}}{z_w^u - z_{gu}}}} \tag{3-39}$$

is a discharge coefficient,

$$c_{gc} = 1 - 0.75 \frac{\theta}{90} + 0.36 \left(\frac{\theta}{90} \right)^2 \tag{3-40}$$

is a contraction coefficient, w_{gu} = underflow gate width, h_{gu} = underflow gate height, z_w^u = upstream water-surface elevation, z_{gu} = underflow gate bottom elevation, and θ = angle of gate inclination.

The underflow gate formulas apply to gates having planar and cylindrically shaped skin plates with free flow conditions and a downstream horizontal apron. Outflow edges of the gates are inclined at angle θ to the flow ($\theta < 90°$ and varies according to the gate position).

Overflow gate discharge is calculated as

$$Q = C_{go} \sqrt{g} w_{go} \left(z_w^u - z_{go} \right)^{3/2} \tag{3-41}$$

where C_{go} = overflow gate discharge coefficient (dimensionless), w_{go} = overflow gate

width, and z_{go} = overflow gate crest elevation. Only unsubmerged flow conditions are considered.

Gate structures are modeled in the same way as culverts and weir segments. Each gate structure is described by either one or two nodes, a set of coefficients, and physical parameters. Two nodes are needed, one at the upstream side and one at the downstream side, if the areas on both the upstream and downstream sides of the weir are included in the finite element mesh, otherwise only the upstream node is needed.

Drop Inlet Spillways

Drop inlet spillways are overfall structures in which water drops through a vertical riser connected to a discharge conduit ("Design and construction" 1996), and are often used in reservoirs to convey flow past a dam as shown in Figure 3-10. Water flows over the horizontal crest of the riser (the weir), drops through a vertical or sloping shaft (the transition), and then flows to the downstream exit through a horizontal or nearly horizontal closed channel or tunnel (the conduit). Three possible flow conditions can exist in a drop inlet spillway depending on the relative discharge capacities of the weir, the transition, and the conduit. The controlling hydraulic feature is the one that limits the flow through the structure. As the hydraulic head at the spillway increases, control shifts from weir flow over the crest to orifice flow through the transition and then to full pipe flow in the conduit.

Flow through a drop inlet spillway is modeled by specifying two node points, one at the entrance and one at the exit, and a set of parameters that describe the structure. If flow leaves the finite element network through the inlet and does not return to the network only the entrance node point is specified. Water-surface elevations and velocities at the entrance and exit nodes are used to compute the flow rates over the weir, through the transition, and through the conduit. The smallest computed flow rate is the one that is selected for the spillway.

Weir Flow

Weir flow over a drop inlet crest is computed as follows:

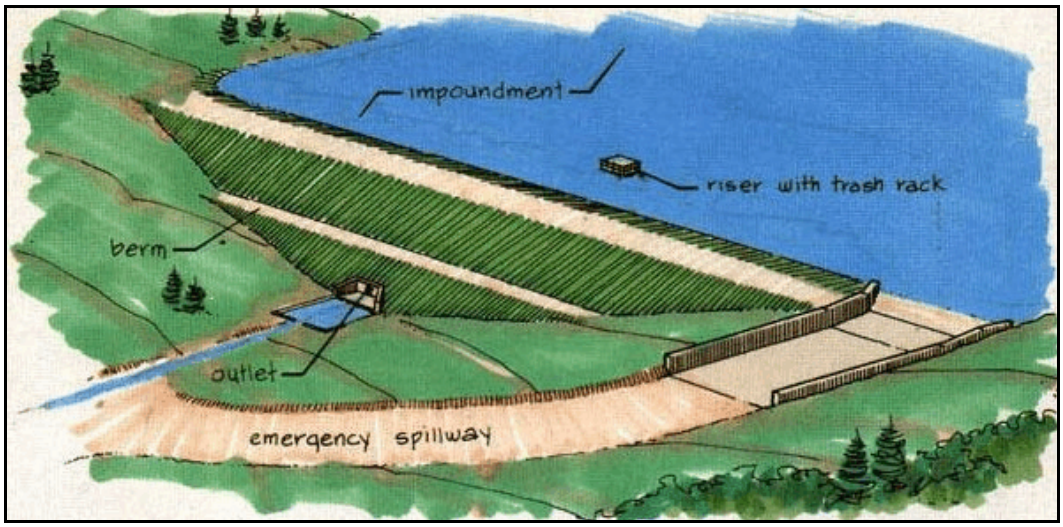

Figure 3-10. Drop inlet spillways are overfall structures in which water drops through a vertical riser connected to a discharge conduit .

$$Q = C_{dw}\sqrt{g}L_{dw}\left(z_s^h - z_{dw}\right)^{1.5} \tag{3-42}$$

where C_{dw} = dimensionless weir discharge coefficient, L_{dw} = total weir crest length of the drop inlet, z_w^h = water-surface elevation at the entrance node point, and z_{dw} = weir crest elevation of the drop inlet. Dimensionless weir discharge coefficients for semicircular shaped drop inlet crests are usually about 0.67.

Orifice Flow

Discharge through the vertical shaft of a riser is given by an orifice flow formula as

$$Q = C_{do}A_{do}\sqrt{2g(z_s^h - z_{do})} \tag{3-43}$$

where C_{do} = dimensionless orifice flow discharge coefficient, z_{do} = orifice elevation, and A_{do} = cross sectional area of the orifice.

Conduit Flow

Flow through the outlet conduit of a drop-inlet spillway is calculated by considering the conduit to flow completely full its entire length using the following formula:

$$Q = C_{dc}A_{dc}\sqrt{2g\left(z_s^h - z_{de}^t\right)} \tag{3-44}$$

where

$$C_{dc} = \frac{1}{\sqrt{K_{de} + \dfrac{2gn_{dc}^2L_{dc}}{\lambda^2R_{dc}^{4/3}} + K_{do}}} \tag{3-45}$$

is a dimensionless conduit flow discharge coefficient, K_{de} = entrance loss coefficient (usually about 0.2), n_{dc} = drop-inlet conduit Manning roughness coefficient, L_{dc} = drop-inlet conduit length, R_{dc} = hydraulic radius of the conduit, K_{do} = outlet loss coefficient (usually 1.0), A_{dc} = cross-sectional area of the conduit, and z_{de}^t = conduit exit tailwater elevation.

Channel Links

Channel links represent short sections of comparatively flat ground across which water movement can be approximated as uniform flow using Manning's formula as follows:

$$Q = \frac{\phi_n}{n_{cl}}B_{cl}H_{cl}^{5/3}S_{cl}^{1/2} \tag{3-46}$$

where n_{cl} = Manning roughness coefficient, B_{cl} = constant width of the channel link, H_{cl} = average water depth calculated based on water-surface elevations at the two ends of the link, and S_{cl} = constant bed slope of the link.

Modeled in the same way as culverts and weir segments, each channel link is described by either one or two nodes, a set of coefficients, and physical parameters. Two nodes are needed, one at either end of, if the areas on both the upstream and downstream

sides of the link are included in the finite element mesh, otherwise only the upstream node is needed.

Cross-section-averaged Flow Equations

Sometimes areas in which two-dimensional depth-averaged flow is modeled are connected by long channels of comparatively small width. Many two-dimensional elements might be needed to model these channels which would increase computation time significantly. As an option, areas modeled using two-dimensional elements can be connected by "one-dimensional" channels in which cross-section averaged flow is simulated (Figure 3-11) if two-dimensional descriptions of flow in these channels are not needed. Flow in both open channels and closed conduits can be considered.

Open-channel Flow

Cross-section averaged continuity and momentum equations describing one-dimensional flow in open channels are as follows:

$$B\frac{\partial z_w}{\partial t} + \frac{\partial Q}{\partial x} - q_\ell = 0 \tag{3-47}$$

and

$$\frac{\partial Q}{\partial t} + \frac{\partial(\beta Q^2/A)}{\partial x} + gA\left(\frac{\partial z_w}{\partial x} + S_f\right) - B\frac{\tau_s}{\rho} - \beta q_\ell v_x = 0 \tag{3-48}$$

where B = cross-section flow area topwidth, z_w = water-surface elevation (considered constant across the section), t = time, Q = volumetric water flow rate through the cross section, x = longitudinal channel direction (positive in a downstream direction), q_ℓ = lateral inflow rate of water, β = momentum flux correction factor, A = cross section flow area, g = gravitational acceleration, S_f = friction slope derived from Manning's resistance equation, τ_s = wind shear stress in the positive longitudinal channel direction, ρ = water mass density, and v_x = longitudinal velocity of lateral inflow. Bridge, culverts, and weir

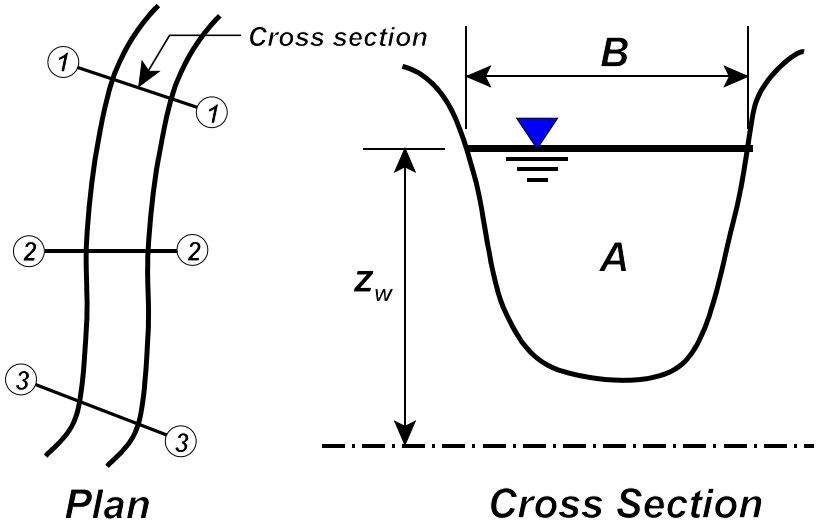

Figure 3-11. Cross-section averaged flow provides the average water surface elevation across a section along with the total flow rate through the wetted area of the section.

structures are not included in channels modeled by one-dimensional cross-section averaged flow.

Cross section approximations are defined by exactly eight ground points as shown in Figure 3-12. The third and sixth points represent channel banks, the four and fifth points are consider to be limits of the "active bed", within which sediment can be transported. Three roughness coefficients are assigned to each section, one representing the left overbank region (from points one to three), one representing the main channel (from point three to point six), and one representing the right overbank region (from point six to point eight).

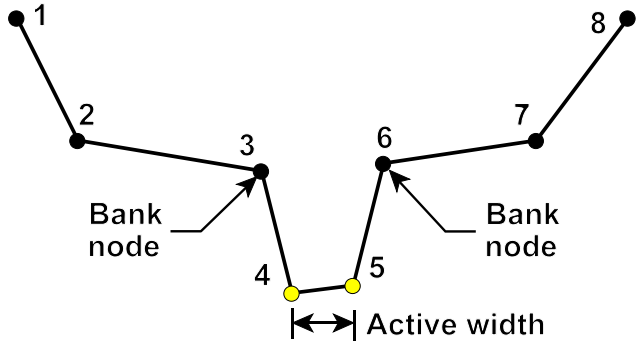

Figure 3-12. Approximate representation of cross sections used to simulate one-dimensional flow in open channels. Exactly eight ground points are specified for each section.

Closed-conduit Flow

Cross sections representing closed conduits within which water can flow under pressure (that is, the water surface will be in contact with the covering) include descriptions of the top surface or ceiling as shown in Figure 3-13. Ceiling elevations are specified for each of the eight points that define the section. Vertical sidewalls are assumed to exist at the first and last points when the ground elevations are less than the ceiling elevations.

Increased frictional resistance caused by the covering surface is taken into account when water is in contact with the ceiling. Additionally, when pressure flow occurs (that is, when water is in contact with the ceiling across the entire section), a minimum flow area topwidth B_{min} is assigned to the section (that is, $B = B_{min}$) following the logic of Cunge et al. (1980, pages 366-368). Since B_{min} is small (on the order of 0.03 ft or 0.01 m) the volume of water contained in the narrow vertical slot it represents is negligible in comparison to the channel volume, so the continuity equation is still satisfied. Consequently, the free surface level calculated when pressure flow occurs represents the piezometric level.

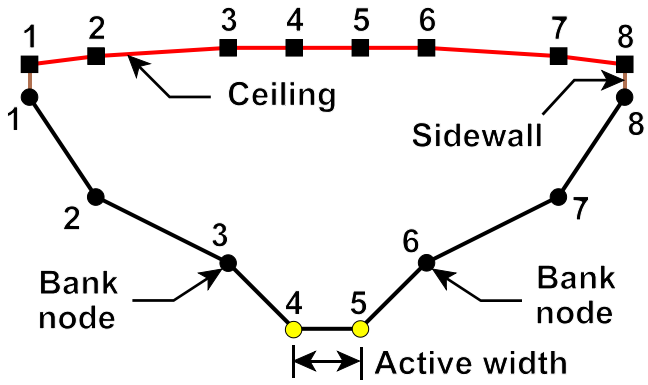

Figure 3-13. Closed conduit cross sections include elevations of the top surface or ceiling.

Initial and Boundary Conditions

From a mathematical viewpoint, the governing depth-averaged flow equations form a mixed initial value/boundary value problem. Both initial conditions and boundary conditions need to be specified that make the problem well-posed (that is, stable). A well-posed problem is one in which increasingly smaller changes to boundary conditions produce increasingly smaller changes in the solution at points not located on the boundary. When an incorrect number of boundary conditions or boundary conditions of the wrong type are specified, small changes to the boundary conditions might result in large solution changes in the interior of the modeled region. Systems of equations that exhibit this kind of unstable behavior are said to be ill-posed.

Initial Conditions

Water depth H, and unit flow rates in the x and y directions, q_1 and q_2, need to be specified as initial conditions of the problem throughout the entire solution region for both steady and time-dependent flows.

Hot starts

When results from a previous simulation are available they may be used as initial conditions for a subsequent run even if the boundary conditions have changed from those of the previous simulation or the network has been modified slightly. Using results from a previous run as initial conditions is referred to as a *hot start*. However, solutions might not converge if changes in boundary conditions are large or if networks are modified significantly.

Cold starts

When models have just been constructed and previous solutions are not available, initial conditions are unknown and *cold starts* are made. During cold starts, the same water-surface elevation is assigned to every node point in the finite element network, from which the bed elevation is subtracted to obtain water depth, and unit flow rates are set to zero everywhere, that is

$$\left.\begin{aligned} H &= z_w^* - z_b \\ q_1 &= q_2 = 0 \end{aligned}\right\} \quad \begin{array}{c} \textit{Initial conditions at all node points} \\ \textit{for a cold start} \end{array} \tag{3-49}$$

Boundary Conditions

Certain values called boundary conditions need to be specified around the entire boundary of a network for the duration of a simulation. Boundary condition data consist of either the normal mass flux (normal flow) or the normal force (normal stress), in addition to either the tangential mass flux (tangential flow) or the tangential force (shear stress) at all points on the boundary of a network. Needed boundary information depends on boundary type and flow conditions. Physically, two types of boundaries are encountered in surface-water flow problems as shown in Figure 3-14: (1) a *closed* or zero-flux boundary; and (2) an *open* boundary.

Closed boundary

Closed boundaries defines a geometric feature such as natural shorelines, highway embankments, jetties, or seawalls. Generally, no flow passes through closed boundaries, that is, the normal flow rate $q_n = 0$ everywhere along a closed boundary. Additionally,

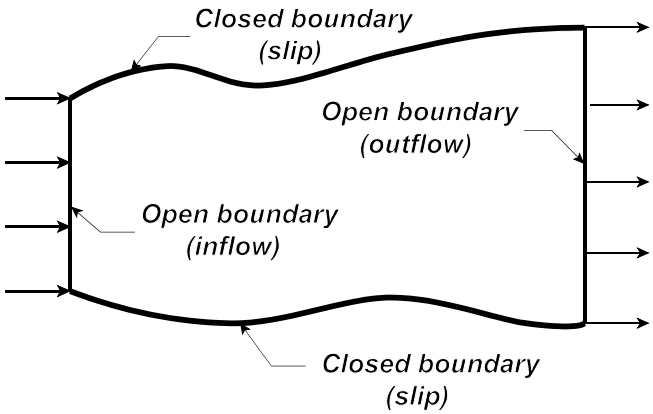

Figure 3-14. Network boundaries are either "open" or "closed." Water can flow only parallel to closed boundaries, but can pass through open boundaries.

either tangential unit flow rates, the tangential shear stresses, or relations between tangential unit flow rates and tangential shear stresses need to be specified on closed boundaries by applying one of the following three types of conditions: (1) a *slip* condition, (2) a *no-slip* condition, or (3) a *semi-slip* condition.

Slip condition. A slip condition allows flow in a direction that is tangent to the boundary at a node point and imposes zero tangential shear stress at the boundary. The tangential direction at a boundary node is determined by requiring that the net flow across the closed boundary resulting from velocities at the node be zero. Slip conditions are usually applied when the closed boundary represents an imaginary vertical wall where flow depths are shallow and lateral shear stresses are negligible.

No-slip condition. A no-slip condition is specified at a closed boundary node by setting the velocities equal to zero; therefore, the requirement of zero net flow across the boundary will be satisfied automatically. No-slip conditions are usually applied when velocities along a boundary are known to be very small and a network of closely-spaced node points is constructed to resolve any large velocity gradients that might exist near the boundary.

Semi-slip condition. A semi-slip condition is imposed on a closed boundary by allowing flow in a direction that is tangent to the boundary just as for a slip condition, and by prescribing a non-zero tangential shear stress caused by friction generated by flow against a vertical wall. Vertical wall friction τ_w is computed as

$$\tau_w = c_f \rho U_w^2 \tag{3-50}$$

where c_f = friction coefficient (dimensionless) used to calculate bed shear stresses within an element, and U_w = velocity tangent to the wall (that is, at the boundary node where a vertical wall is considered to exist). Semi-slip conditions are usually applied when the closed boundary represents an actual physical boundary such as a wall that is vertical or nearly vertical. Increased frictional resistance caused by the wall will then be considered.

Open boundary

An open boundary, which is exactly what the name implies, defines an area along the boundary of a finite element network where flow is allowed to enter (an inflow boundary) or leave (an outflow boundary). The values that need to be specified at an open boundary depend on the type of boundary (inflow or outflow) and the type of flow

(subcritical or supercritical). Boundary flow is *subcritical* if $U^2 + V^2 \leq gH$, or *supercritical* if $U^2 + V^2 \geq gH$.

Inflow boundary. If flow at an inflow boundary node is subcritical, then one of the following combinations needs to be specified in addition to tangential shear stress: (1) velocities normal and tangent to the boundary, (2) unit flow normal and tangent to the boundary, or (3) water-surface elevation and the flow direction. If the flow at an inflow boundary node is supercritical, unit flow normal to the boundary, unit flow tangent to the boundary, and water-surface elevation need to be specified at the node. Tangential shear stresses acting on an open boundary are automatically set to zero if unit flow tangent to the boundary is not specified. Velocity rather than unit flow can be specified at an open boundary node. However, the ability to prescribe velocity directly at a node point seems to offer no practical advantages.

Usually unit flow in both the *x* and *y* directions will be specified at inflow boundary nodes, and water-surface elevation (from which depth is determined by subtracting the ground elevation) is specified at outflow boundary nodes of a channel/flood plain model. Total flow at a cross section composed of nodes lying on the network boundary can also be specified. Assigning open boundary inflows using this feature of *FST2DH* greatly simplifies the specification of unit flows at upstream boundaries of channel/flood plain models (outflows can be specified as well). Water-surface elevations along a cross section composed of boundary nodes can also be specified. Water-surface elevations might be constant across the section, or slope from one side of the cross section to the other.

Outflow boundary. Tangential shear stresses are automatically set to zero at all outflow boundary nodes. Therefore, only water-surface elevation needs to be specified at an outflow boundary node if the flow is subcritical If the flow is subcritical no values need to be specified. However, the fact that a node is a supercritical outflow boundary node still needs to be made known.

Weakly-reflecting boundary. Assigning boundary conditions at the upstream limits of tributary streams to estuaries or bays in which flow is controlled primarily by tides (see Figure 3-15) presents a problem if the tributary boundary is influenced by the tidal variations. During and immediately after flood tide the water surface will usually be rising at the tributary boundary, while during and immediately after ebb tide the water

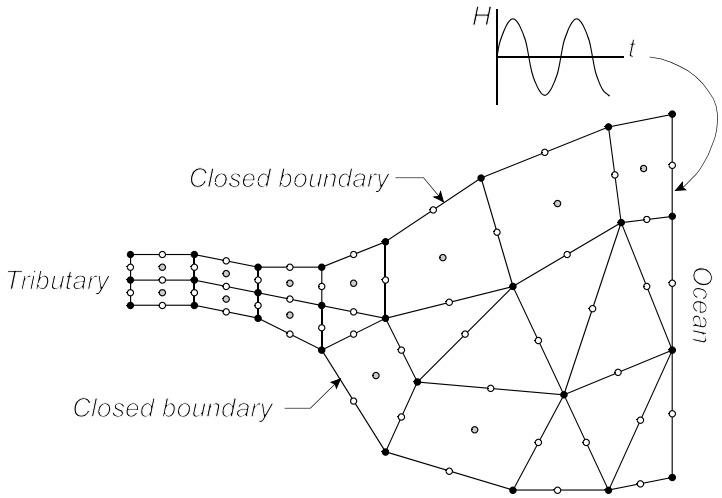

Figure 3-15. "Weakly-reflecting" boundary conditions can be applied at tributaries to bays or estuaries where unsteady tidal elevations are applied along the open ocean boundary.

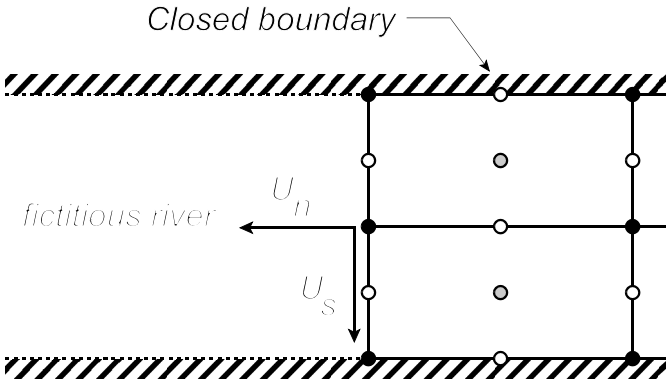

Figure 3-16. Weakly-reflecting boundary conditions are formed by considering a fictitious river having constant dimensions, but without frictional resistance, to extend far upstream from the boundary.

surface will usually be falling. Inflows and outflows at the tributary boundary are also affected by the tidal variation in water-surface elevation. All of these responses are part of the solution of the governing equations and cannot be specified in advance. One way of addressing this problem is to extend the boundary of the tributary upstream to a location that is not influenced by tidal variations at the mouth of the estuary or bay. However, tidal effects can extend long distances inland from coastal waters, requiring a large network extension.

Another way of handling the problem is to not to move the tributary boundary and apply a condition that allows a tidal wave to pass through the boundary without being reflected, or at least only *weakly reflected*. The mathematical statement for this boundary condition is found from the characteristic solution of the depth-averaged flow equations by imagining a fictitious river having constant dimensions, but without frictional resistance, to extend far upstream from the boundary as shown in Figure 3-16. At a weakly-reflecting boundary use is made of an invariant condition that stipulates

$$-U_n + 2\sqrt{gH} = -U_{n\infty} + 2\sqrt{gH_\infty} \qquad (3\text{-}51)$$

where U_n = normal outward velocity at the open boundary, $U_{n\infty}$ = normal outward velocity in the fictitious river at an upstream location not affected by tides, and H_∞ = depth in the fictitious river far upstream. Some reflection of outgoing waves will occur at the boundary because the frictionless condition in the fictitious river causes a roughness change at the boundary. Weakly-reflecting boundary conditions are best applied where incoming and outgoing waves enter and leave networks in directions that are approximately normal to the boundaries.

Boundary Condition Summary

Types and combinations of boundary conditions that can be specified are summarized in Table 3-5. In general, conditions specified along the boundary of a network cannot depend on what occurs inside the network. In other words, boundary conditions need to be known in advance. Usually common sense along with an understanding of the physical processes that are being modeled will allow appropriate boundary conditions to be selected.

If boundary conditions are not known exactly then they need to be estimated as closely as possible. Boundaries can be extended further away from areas where accurate solutions are needed to reduce the likelihood of inexact boundary conditions having an

Table 3-5. Possible boundary specifications[a] for various two-dimensional depth-averaged flow conditions and boundary types.

Type of boundary	Flow condition	
	Subcritical	Supercritical
Closed, $U_n = 0$	$U_n = U_n^*$ (usually $U_n^* = 0$)	
Inflow, $U_n < 0$	$U_n = U_n^*$ and $U_s = U_s^*$, or $q_n = q_n^*$ and $q_s = q_s^*$, or $H = H^*$ and $U_s = U_s^*$, or $H = H^*$ and $q_s = q_s^*$ (usually $U_s = q_s = 0$).	$U_n = U_n^*$, $U_s = U_s^*$, and $H = H^*$, or $q_n = q_n^*$, $q_s = q_s^*$, and $H = H^*$ (usually $U_s = q_s = 0$).
Outflow, $U_n > 0$	$H = H^*$	nothing
Weakly-reflecting	$-U_n + 2\sqrt{gH} = -U_{n\infty} + 2\sqrt{gH_\infty}$	

[a] U_n = outward normal velocity, U_s = tangential velocity, $q_n = UH$ = outward normal unit flow rate, $q_s = UH$ = tangential unit flow rate, $U_{n\infty}$ = outward normal velocity in a fictitious river far upstream from the boundary, H_∞ = depth in a fictitious river far upstream from the boundary.

adverse effect on the solution. Also, if the wrong type of boundary condition is specified, or if insufficient boundary conditions are specified, an accurate solution might still be obtained where needed. For example, the open boundary of a network that represents an estuary will be an inflow boundary during flood tide and an outflow boundary during ebb tide. Strict compliance with mathematical stipulation of boundary conditions means that two items need to be specified on this open boundary during flood tide, and only one item during ebb tide. Normally, all that is known and all that will be specified, even during flood tide, is water-surface elevation based on tide gage records or estimated tidal elevations at the ocean entrance. However, lack of one boundary condition during flood tide at an open boundary subject to tidal variations has not seemed to damage simulations, especially if areas of interest lie far from the open boundary. Nonetheless, care needs to taken in apply the proper number and type of boundary conditions.

Boundary condition application in *FST2DH* can be simplified by specifying values along *cross sections* that form part of the network boundary. Cross sections usually represent channel/flood plain transects where either total flow, water-surface elevation, or the invariant quantity at a weakly-reflecting boundary can be specified. Total flow is distributed between the cross sections that comprise the boundary based on a one-dimensional flow approximation using the concept of cross-section conveyance.

Application of boundary conditions in *FST2DH* can be simplified by specifying values along *cross sections* that form part of the network boundary. Cross sections usually represent channel/flood plain transects where either total flow, water-surface elevation, or the invariant quantity at a weakly-reflecting boundary can be specified. Total flow is distributed between the cross sections that comprise the boundary based on a one-dimensional flow approximation using the concept of cross-section conveyance.

Storm Surge and Tropical Cyclones

Storm or tidal surge is an abnormal elevation in sea level along a coast caused by strong onshore winds in combination with low atmospheric pressure. Storm surges typically have periods from 12 to 24 hours, and can produce changes in sea level of several meters. Surges are particularly destructive to low-lying coastal areas if the peak of the storm is coincident with a high astronomical tide. When wind stresses dissipate, sea levels can exhibit damped oscillations called seiches that may last for several days. Maximum water depths and velocities in estuaries and tidal inlets in the United States are likely to occur during storm surges.

The most destructive storm surges are caused by strong cyclonic tropical storms or hurricanes, which produce winds with speeds of 75 mi/h (120 km/h) or more. A mature tropical cyclone is characterized by a circular pattern of storm clouds and torrential rains, accompanied by winds that may reach speeds of 100 to 180 mi/h (160 to 300 km/h) within a radius of 6 to 60 mi (10 to 100 km) from the storm center or core. Winds diminish rapidly with increasing distance from the core. At a radius of 300 mi (500 km), wind speed is usually less than 18 mi/h (30 km/h). Tropical cyclones move with the large-scale wind currents in which they are embedded, with average speeds of about 16 mi/h (25 km/h). Although some storms may travel at twice the typical speed, others can remain stalled in the same location for several days.

Simulating tropical storms and the resulting surges in detail is a complex and time-consuming effort. Therefore, storm surge elevations on ocean boundaries can be calculated using a simple approach suggested by Edge et al. (1998) in which a surge stage hydrograph is synthesized from tropical storm windfield parameters and a known peak stage as

$$S_t(t) = S_p\left(1 - e^{|D_s/t|}\right) \tag{3-52}$$

where $D_s = R_{max}/V_f$ is storm duration, R_{max} = radius of maximum storm winds, V_f = forward speed of the storm, t = time since start of the storm, and S_p = peak storm surge height for a selected annual exceedance probability. Combining surge stage with astronomical tide elevations gives the total storm surge stage

$$S_{tot}(t) = S_t(t) + H_t(t) \tag{3-53}$$

where H_t = astronomical tide stage. Radius of maximum winds R_{max} and forward speed V_f can be obtained from Ho et al. (1987), where probability distributions of tropical storm parameters can be found. Edge et al. (1998) find that 50 percent probability (that is, mean values) of R_{max} and V_f produce storm durations D_s that are similar to durations obtained from analyses of historical storm surge hydrographs. Mean estimates are the most likely values to occur for a given surge height of any recurrence interval. The 100-year storm surge hydrograph, for example is developed using the 100-year peak surge height S_p and 50 percent values of R_{max} and V_f.

Peak heights of 50-, 100-, and 500-year storm surges can be obtained for 346 locations along the Atlantic and Gulf coasts of the United States from a database prepared by Scheffner et al. (1994). The storm surge database was formed through simulation of a series of 134 historical hurricanes spanning a period of 104 years, and is therefore not linked to a specific design storm or return period. All storm surges were simulated without tides, and are relative to mean sea level. Therefore, peak stages need to be combined with various phases of astronomical tides to find the needed hydraulic conditions at bridges.

Wind is the primary driving force in cyclonic storms, transferring momentum from the atmosphere to water by shear stress at the water surface. Surface wind shear stress τ_w and atmospheric pressure p_a act across large distances, creating complex forces that can

persist for days after a storm has passed. Empirical expressions for horizontal pressure profiles and resulting windfields associated with hurricanes have been developed from measured pressure distributions. The tropical storm model used by the Federal Emergency Management Agency (FEMA) in their Coastal Surge Model ("Coastal flooding" 1988), which is an extension of the National Weather Service (NWS) windfield model described by Ho et al. (1987), is used in *FST2DH* to calculate appropriate wind shear stresses corresponding to applied storm surge hydrographs. The model of tropical cyclone winds requires the following parameters to describe a storm: (1) location of the storm center, (2) radius of maximum winds, (3) forward storm speed, (4) storm track angle, (5) atmospheric pressure at the storm's center, and (6) ambient atmospheric pressure outside the storm. A good source for these data is *NOAA Technical Report NWS-38* (Ho et al. 1987). A detailed description of the tropical storm model used in *FST2DH* is presented in Appendix B.

Initial location of a tropical cyclone can be specified directly, or calculated based on specification of landfall coordinates, and by considering forward speed and track angle to remain constant. Additionally, a simple empirical model for predicting the decay of tropical cyclone winds after landfall (Kaplan and DeMaria 1995) can be applied as an option.

This page has been left blank intentionally.

4. Sediment Transport and Bridge Scour

Sediment is a fragmental material, ranging in size from clay particles to boulders, that originates from mechanical and chemical breakdown of rocks that comprise the earth's crust. When water is the principal means of transportation, the fragmental material is called fluvial sediment. Fluvial sediment moves by being suspended in water (suspended load) and by sliding or rolling along a streambed (bedload). Some sediment particles are interchangeably transported in both ways. Transport of sediment in river channels is simulated as an option in *FST2DH*. Equations governing sediment motion for both two-dimensional depth-averaged flow and one-dimensional cross-section averaged flow are described in this chapter. Additionally, local scour at bridge piers can be calculated by *FST2DH* as part of a solution. Formulas used to estimate local scour are also described.

Depth-averaged Sediment Transport Equations

Changes in bed levels from erosion or deposition of sediment by two-dimensional depth-averaged flows are given by the sediment continuity equation

$$(1-\eta_s)\frac{\partial z_b}{\partial t}+\frac{\partial q_{s1}}{\partial x}+\frac{\partial q_{s2}}{\partial y}=0 \tag{4-1}$$

where η_s= porosity of bed material, and q_{s1}, q_{s2} = discharge-weighted volumetric total sediment transport rates (that is, bedload and suspended load combined) in the x and y directions. Sediment is considered to move in the same direction as water (that is, the streamwise direction denoted by s), consequently, sediment continuity can be described by

$$(1-\eta_s)\frac{\partial z_b}{\partial t}+\frac{\partial q_s}{\partial s}=0 \tag{4-2}$$

where $q_s=\sqrt{q_{s1}+q_{s2}}$ = volumetric sediment transport rate in the streamwise direction. Transport rates of mixtures of particles of different sizes are calculated as

$$q_s=\sum_i q_{si} \tag{4-3}$$

where q_{si} = volumetric transport rate of a single sediment size class characterized by particles of diameter D_i. Bed elevation changes are then given by

$$(1-\eta_s)\frac{\partial z_b}{\partial t}+\sum_i\frac{\partial q_{si}}{\partial s}=0 \tag{4-4}$$

Discharge-weighted sediment concentration for the ith particle size class $C_{si}=q_{si}/q$, expressed in volume per unit volume, is described by the following transport equation:

$$\frac{\partial(C_{si}H)}{\partial t}+\frac{\partial(C_{si}q_1)}{\partial x}+\frac{\partial(C_{si}q_2)}{\partial y}=C_{es}(C_{si}^*-C_{si}) \tag{4-5}$$

where $C_{si}^*=q_{si}^*/q$ = equilibrium discharge-weighted sediment concentration, q_{si}^* = equilibrium volumetric sediment transport rate, and C_{es} = bed mass flux rate coefficient calculated as

$$C_{es} = \begin{cases} K_{es} w_{si}; \text{ for } C_{si}^{*} > C_{si} \text{ (erosion)} \\ w_{si}; \text{ for } C_{si}^{*} < C_{si} \text{ (deposition)} \end{cases} \quad (4\text{-}6)$$

where K_{es} = sediment erosion rate coefficient, and w_s = terminal fall velocity or settling velocity of a sediment particle in still water. Appropriate values of K_{es} depend on sediment and flow properties and are not yet well-defined, although some guidance is available. For example, for sediment particles transported in suspension, Armanini and Di Silvio (1988) calculate K_{es} as follows:

$$K_{es} = \frac{1}{\frac{T_a}{H} + \left(1 - \frac{T_a}{H}\right) \exp\left[-1.5 \frac{w_{si}}{u_*} \left(\frac{T_a}{H}\right)^{-1/6}\right]} \quad (4\text{-}7)$$

where T_a = thickness of the surface or active layer. Sediment erosion rate coefficient need to be specified in *FST2DH*. As an option, K_{es} can be calculated automatically by (4-7). However, K_{es} = 1.0 is assigned by default.

Sediment fall velocities are found from the graphical relations given in "Some fundamentals of particle size analysis" (1957) for a particle shape factor of 0.7 using tabulated values developed by Stevens and Yang (1989). The relations apply to particle diameters up to 10 mm, and water temperatures less than 40° C.

Bed sediments can be divided into as many as eight particle size classes by *FST2DH*. One transport equation is needed to account for each size class. Streamline balancing diffusion terms (Zienkiewicz and Taylor 1991, page 456) are added to the transport equation to negate artificial diffusion created by numerical approximations of spatial derivatives.

Bed Composition Accounting

The conceptual model of streambed erosion and deposition used in *FST2DH* is based on the ideas of Bennett and Nordin (1977). Beds are divided into two or three layers depending on whether net erosion or net deposition has occurred previously (Figure 4-1). The upper bed layer is called the active layer and is always present. Thickness of the active layer is constant. Sediment is added to the active layer from above when deposition

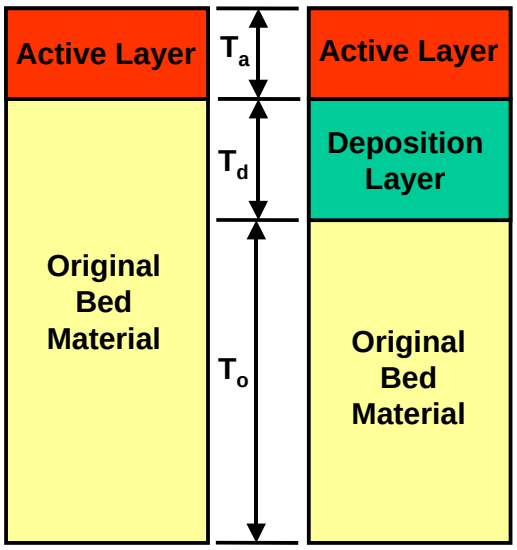

Figure 4-1. Schematic of bed composition accounting concept. The active layer thickness is specified. Material eroding from the active layer is replaced by an equal volume from the deposition layer, if present, or from the original bed material. An equal volume of material deposited on the surface is removed from the active layer and added to the deposition layer.

occurs, and composition of the active layer is immediately recalculated. An equal amount of sediment is then subtracted from the active layer and added to the deposition layer below. Thickness of the deposition layer is unlimited. When sediment is eroded from the active layer an equal volume of material is subtracted from the deposition layer if it exists, or the original bed material layer otherwise, and added to the active layer. Each of the bed layers is considered homogeneous and to have the same porosity as the original bed material. However, composition of the active and deposition layers depends on the cumulative effects of scour and deposition over time.

Material within the active layer is available immediately for transport by streamflows. Bed armoring is simulated by the process of selective entrainment of surface particles, and by limiting erosion of sediment size classes during a single time step to the amounts contained in the active layer. Conceptually, the active layer represents the thickness of the channel bed that can be worked or sorted through by the action of flowing water during a single time step to provide the material eroded. Thickness of the active layer, therefore, is related to the height of sedimentary ripples and dunes that form on the bed, their speed of movement, and the computational time step. Active layer thickness equals one-half the height of bed forms when the time step is large enough to allow translation distances that exceed bed form lengths. Because time steps will often be small in comparison to translation times of bedforms for many flow problems, specification of a nominal active layer thickness based on average bed material grain size will usually be appropriate. Active layer thickness of two times the median bed material particle diameter may be justified, with a minimum thickness of 0.05 ft (0.015 m).

Equilibrium Total Load Transport Formulae

Total load transport formulae presented by Engelund and Hansen (1967), Ackers and White (1973), White and Day (1983), Yang (1973, 1984), Laursen (1958), and Meyer-Peter and Mueller (1948) are used to model movement of cohesionless sediments. Each of these formulas provides discharge-weighted sediment concentrations that apply strictly to equilibrium conditions (that is, conditions in which all acting influences are canceled by others, resulting in a stable river bed that is unchanging.) Some formulas do not explicitly account for beds composed of more than one size class. For these relations, equilibrium total sediment concentrations of a particular particle size class are found by multiplying the estimate given by the selected transport formula times the fraction of the size class contained in the active layer as follows:

$$q_{si} = p_i q_{si}^* \tag{4-8}$$

where p_i = fraction of the *i*th particle size class in the active layer, and $q_{si}^* = C_{si}^* q$ = sediment transport capacity of the *i*th particle size class.

Engelund-Hansen Formula

Total sediment load is given by Engelund and Hansen (1967) as

$$C_{si}^* = 0.05 \frac{\sqrt{(S_s - 1) g D_i^3}}{q} \left(\frac{U_s}{u_*} \right)^2 \tau_{*i}^{2.5} \tag{4-9}$$

where $S_s = \rho_s/\rho$ = specific gravity of the sediment, D_i = diameter of the *i*th particle size class, U_s = depth-averaged velocity in the streamwise direction, and

$$\tau_{*i} = \frac{\tau}{(S_s - 1)\rho g D_i} \tag{4-10}$$

is dimensionless bed shear stress or Shields' parameter (*Sedimentation engineering* 1977, page 96) based on total bed shear-stress $\tau = \rho u_*^2$.

Ackers-White Formula

The sediment transport formula originally presented by Ackers and White (1973) for uniform sediments is applied to individual particle size classes to obtain

$$C_{si}^* = C \frac{D_i}{H} \left(\frac{U_s}{u_{*s}} \right)^n \left(\frac{F_{gr}}{A'} - 1 \right)^m \tag{4-11}$$

where

$$F_{gr} = \frac{u_{*s}^n}{\sqrt{(S_s - 1) g D_i}} \left[\frac{U_s}{\sqrt{32} \log\left(\frac{10H}{D_i} \right)} \right]^{1-n} \tag{4-12}$$

is a dimensionless grain mobility number, u_{*_s} = skin- or grain-friction velocity, and *C*, *n*, *A*, *m* = coefficients that depend on a dimensionless grain diameter D_{gr} defined as follows:

$$D_{gr} = D_i \left[\frac{g(S_s - 1)}{\nu^2} \right]^{1/3} \tag{4-13}$$

For fine sediment particles with $1 < D_{gr} < 60$ coefficients are as follows:

$$C = 10^{2.86 \log D_{gr} - (\log D_{gr})^2 - 3.53}$$
$$n = 1.0 - 0.56 \log D_{gr}$$
$$A = \frac{0.23}{\sqrt{D_{gr}}} + 0.14$$
$$m = \frac{9.66}{D_{gr}} + 1.34$$

For coarse particles with $D_{gr} \geq 60$ the following coefficients apply:

$$C = 0.025$$
$$n = 0$$
$$A = 0.17$$
$$m = 1.5$$

The original formula given by Ackers and White (1973) sets $A' = A$.

Ackers-White-Day Formula

A modification of the Ackers-White formula to account for individual size fractions proposed by White and Day (1983) gives

$$A' = A \left[0.4 \left(\frac{D_i}{D_A} \right)^{-0.5} + 0.6 \right] \tag{4-14}$$

where

$$D_A = 1.6\, D_{50} \left(\frac{D_{84}}{D_{16}} \right)^{-0.28} \tag{4-15}$$

is a reference particle diameter, D_{50} = particle diameter for which 50 percent of the sediment mixture is finer by weight (the median bed material diameter), D_{84} = particle diameter for which 84 percent of the sediment mixture is finer by weight, and D_{16} = particle diameter for which 16 percent of the sediment mixture is finer by weight.

Laursen Formula

Laursen (1958) correlates measured total sediment loads obtained from laboratory flume experiments with hydraulic variables to obtain the following relation:

$$C_{si}^* = 0.01 K_i \frac{\rho}{\rho_s} \left(\frac{D_i}{H} \right)^{7/6} \left(\frac{\tau_{0s}}{\tau_{ci}} - 1 \right) \tag{4-16}$$

where K_i = function based on the ratio u_{*s}/w_{si}, w_{si} = fall velocity of particles in the ith size class, u_{*s} = grain-friction velocity calculated as

$$u_{*s} = \frac{U_s}{\sqrt{58}} \left(\frac{D_{50}}{H} \right)^{1/6} \tag{4-17}$$

which gives shear stress acting on sediment grains $\tau_{0s} = \rho u_{*s}^2$, and

$$\tau_{ci} = 0.039 (S_s - 1) \rho g D_i \tag{4-18}$$

is grain shear stress needed to displace particles of diameter D_i. The graphical relation for K_i given by Laursen (1958) is closely approximated by the following expressions developed by Stevens and Yang (1989):

$$K_i = \begin{cases} 10.718 (u_{*s}/w_{si})^{0.243}; \text{ for } u_{*s}/w_{si} \le 0.3 \\ 10^{0.855 \log(u_{*s}/w_{si}) + 0.62 [\log(u_{*s}/w_{si}]^2 + 1.2}; \textit{ for } 0.3 < u_{*s}/w_{si} \le 3 \\ 4.773 (u_{*s}/w_{si})^{2.304}; \textit{ for } 3 < u_{*s}/w_{si} \le 20 \\ 10^{3.764 \log(u_{*s}/w_{si}) - 0.803 [\log(u_{*s}/w_{si})]^2 + 0.147}; \textit{ for } 20 < u_{*s}/w_{si} \le 200 \\ 9680.5 (u_{*s}/w_{si})^{0.2531}; \textit{ for } u_{*s}/w_{si} > 200 \end{cases} \tag{4-19}$$

Yang's Sand and Gravel Formula

Relating total bed-material load to the rate of energy dissipation per unit weight of streamflow or unit stream power, Yang (1972, 1973, 1984) develops the following relation for equilibrium transport of sands and gravels:

$$C_{si}^* = \frac{1}{S_s} 10^{M + N \log \left[\left(\frac{U_s - U_{ci}}{w_{si}} \right) S_e \right]} \tag{4-20}$$

where $S_e = u_*^2/gH = \sqrt{\tau_0/\rho}$ = energy gradient, M and N are coefficients, U_{ci} = depth-averaged velocity at which particles of the ith size class are set in motion, and τ_0 = total

bed shear stress. Coefficients *M* and *N* are calculated differently for sand and gravel as follows:

$$M = \begin{cases} 5.435 - 0.286 \log \dfrac{w_{si} H}{\nu} - 0.457 \log \dfrac{u_{*s}}{w_{si}} \text{ ; for sand} \\ \\ 6.681 - 0.633 \log \dfrac{w_{si} H}{\nu} - 4.816 \log \dfrac{u_{*s}}{w_{si}} \text{ ; for gravel} \end{cases} \tag{4-21}$$

and

$$N = \begin{cases} 1.799 - 0.409 \log \dfrac{w_{si} H}{\nu} - 0.314 \log \dfrac{u_{*s}}{w_{si}} \text{ ; for sand} \\ \\ 2.784 - 0.305 \log \dfrac{w_{si} H}{\nu} - 0.282 \log \dfrac{u_{*s}}{w_{si}} \text{ ; for gravel} \end{cases} \tag{4-22}$$

Critical depth-averaged velocity is found from the following expression:

$$\frac{U_{ci}}{w_{si}} = \begin{cases} \dfrac{2.5}{\log \dfrac{u_{*s} H}{\nu} - 0.06} + 0.66 \text{ ; for } 1.2 < \dfrac{u_{*s} H}{\nu} < 70 \\ \\ 2.05 \text{ ; for } 70 \le \dfrac{u_{*s} H}{\nu} \end{cases} \tag{4-23}$$

Yang's sand transport relation is used when D_i < 2 mm; otherwise, the gravel equation is used. Yang (1984) suggests that the gravel transport formula be limited to particle diameters of 10 mm or less.

Meyer-Peter and Mueller Formula

A relation developed by Meyer-Peter and Mueller (1948) based on extensive experiments with coarse sediment gives discharge-weighted concentrations as

$$C_{si}^{*} = 8 \frac{\sqrt{(S_s - 1) g D_i^3}}{q} \left(1 - \frac{0.047}{\tau_{*i}} \right) \tau_{*i}^{1.5} \tag{4-24}$$

The formulation used in *FST2DH* considers all flow resistance to be from grain roughness; a reasonable premise for coarse-bed channels for which the Meyer-Peter and Mueller formula was developed.

Garbrecht et al. Approach

A combination of sediment transport capacity formulas found by Garbrecht et al. (1995) to provide optimal estimates of total load can be used to calculate equilibrium concentrations based on particle size class diameter. Laursen's formula is used to estimate sediment load capacity when $D_i < 0.25$ mm, Yang's sand and gravel formula is used when $0.25 \text{ mm} \le D_i < 8.0$ mm, and the Meyer-Peter and Mueller formula is used when $D_i \ge 8.0$ mm. A shortcoming of this approach is that unreasonably large differences in transport rates might be calculated for consecutive particle size classes when two different formulas are used.

Combined Currents and Waves

Wave action can have a large effect on sediment motion in coastal waters and estuaries. When combined with currents, waves provide a stirring mechanism that keeps sediment grains mobile, while currents add to the stirring and produce net transport (McDowell and O'Connor 1977, page 111). Consequently, when waves are present some sediment transport will occur even in the smallest of currents because of sediment that has been entrained by wave-induced oscillatory water motion near the bed.

Sediment transport in combined current-wave flows is found by replacing τ, the bed shear stress due to current alone, by τ_m, the mean bed shear stress during a wave cycle under combined waves and currents, which is calculated as (Bijker 1966, Bijker and de Bruyn 1988)

$$\tau_m = \tau + \frac{1}{2}\tau_w \tag{4-25}$$

where τ_w = amplitude of oscillatory bed shear stress due to waves. Wave bed shear stress is obtained from the bottom orbital velocity u_w created by wave motion as

$$\tau_w = \frac{1}{2}\rho f_w u_w^2 \tag{4-26}$$

where f_w = wave friction factor. Amplitudes of orbital velocities just above beds due to monochromatic (single frequency) waves of height H_w and period T are given by

$$u_w = \frac{\pi H_w}{T \sinh(kH_w)} \tag{4-27}$$

where $k = 2\pi/L$ = wave number, and L = wave length.

Wave friction factors f_w depend on whether flows are laminar, smooth turbulent, or rough turbulent, which in turn depend on wave Reynolds number $R_w = u_w A / \nu$, the semi-orbital excursion $A = u_w T / 2\pi$, kinematic viscosity ν, and total bed roughness. Wave friction factors are calculated as (Soulsby 1997, page 79)

$$f_w = \begin{cases} 2R_w^{-0.5}; \text{for laminar flow} \\ 0.52R_w^{-0.187}; \text{for smooth turbulent flow} \\ 1.39(A/z_0)^{-0.52}; \text{for rough turbulent flow} \end{cases} \tag{4-28}$$

where z_0 = total bed roughness height. Laminar flow prevails when $R_w \le 2 \times 10^5$. When $R_w > 2 \times 10^5$, f_w = larger of the smooth and rough turbulent flow values.

Total bed roughness height needed to estimate rough turbulent flow friction factors is found as (Soulsby 1997, page 59)

$$z_0 = z_{0s} + z_{0f} + z_{0t} \tag{4-29}$$

where

$$z_{0s} = \frac{D_{50}}{12} \tag{4-30}$$

is grain roughness height for hydrodynamically rough flows,

$$z_{0f} = 0.267 \frac{\Delta_r^2}{\lambda_r} \tag{4-31}$$

is bed-form roughness height due to ripples, Δ_r = ripple height, λ_r = ripple wavelength, and

$$z_{0t} = 5.67 D_{50} \sqrt{\tau_{ws*} - 0.05} \tag{4-32}$$

is the sediment transport contribution due to momentum extracted by the flow to move sand grains, where

$$\tau_{ws*} = \frac{\tau_{ws}}{(S_s - 1)\rho g D_{50}} \tag{4-33}$$

is dimensionless grain shear stress,

$$\tau_{ws} = \frac{1}{2} \rho f_{ws} u_w^2 \tag{4-34}$$

and

$$f_{ws} = 1.39 \left(\frac{A}{z_{0s}} \right)^{-0.52} \tag{4-35}$$

is the wave friction factor for rough turbulent flows.

Sand Ripples

Apart from surf zones, ripples form on the beds of most coastal waters, although there may be dunes or sandwaves present, also. When ripples, dunes, or sandwaves occur they create form drag due to the distribution of dynamic pressure across their surfaces. Current-generated ripple wavelengths and heights are calculated as $\lambda_{rc} = 1000\ D_{50}$ and $\Delta_{rc} = \lambda_{rc}/7$, respectively. Wave-generated ripple heights and lengths are calculated as follows (Nielson 1992):

$$\Delta_{rw} = \begin{cases} (0.275 - 0.022 \Psi^{0.5}) A; \text{ for } \Psi < 156 \\ 0; \text{ for } \Psi \geq 156 \end{cases} \tag{4-36}$$

and

$$\lambda_{rw} = \begin{cases} \Delta_{rw} / (0.182 - 0.022 \tau_{ws*}^{1.5}); \text{ for } \tau_{ws*} < 0.831 \\ 0; \text{ for } \tau_{ws*} \geq 0.831 \end{cases} \tag{4-37}$$

where

$$\Psi = \frac{U_w^2}{(S_s - 1) g D_{50}} \tag{4-38}$$

is a wave mobility number. Ripple heights and wavelengths used to calculate grain roughness height for hydrodynamically rough flows are taken as the larger of current and wave-generated values.

Surf Zone Sediment Transport

The most intense sediment transport in coastal zones often takes place beneath breaking waves, either in surf zones, on beaches, or over sandbanks (Kraus and Horikawa 1990). Because surf-zone processes are complicated and difficult to simulate, sediment movement is modeled just as for non-breaking waves. Support for this approach is provided by the experiments of Deigaard et al. (1991) who show that bed shear-stresses in surf zones are not on average much different from those where waves have not broken, although they exhibit greater wave-to-wave variability. Random waves break on a beach in water of depth H when significant wave height $H_{ws} = \gamma H$, where γ takes the value 0.55 for a horizontal bed, and increases with wave period and beach slope. Monochromatic waves break in shallow water when wave height $H_w = 0.78\ H$. Bed shear-stresses used to calculate sediment transport rates within surf zones (that is, where $H < H_w/\gamma$) are found using $H_w = \gamma H$, where γ = specified ratio (usually about 0.8).

Cross-section-averaged Sediment Transport Equations

Transport of sediment in one-dimensional river channels is simulated as an option in *FST2DH* in a manner similar to two-dimensional flow. Changes in bed levels from erosion or deposition of sediment by one-dimensional cross-section-averaged flows are given by the sediment continuity equation as follows:

$$(1 - \eta_s)\, \tilde{B} \frac{\partial \tilde{z}_b}{\partial t} + \frac{\partial Q_s}{\partial x} - q_s = 0 \tag{4-39}$$

where $\tilde{B}$ = topwidth of the active bed, $\tilde{z}_b$ = average elevation of the active bed, Q_s = total volumetric sediment transport rate, and q_s = lateral inflow rate of sediment. Active beds are portions of cross sections within which sediment is transported, no sediment is carried in other parts of a section. For sediment transport calculations, the active portion of a cross section is approximated as horizontal (see Figure 4-2), and the average active bed level rises and falls as sediment is eroded or deposited uniformly across the active bed width.

Discharge-weighted sediment concentration for the *i*th particle size class $C_{si} = q_{si}/q$, expressed in volume per unit volume, is described by the following transport equation:

$$\frac{\partial (C_{si} \tilde{A})}{\partial t} + \frac{\partial (C_{si} \tilde{Q})}{\partial x} = C_{es} (C_{si}^* - C_{si}) \tag{4-40}$$

where $\tilde{A}$ = cross sectional flow area above the active bed, $\tilde{Q}$ = total flow rate within the active bed, $C_{si}^* = Q_{si}^*/\tilde{Q}$ = equilibrium discharge-weighted sediment concentration, Q_{si}^* = equilibrium volumetric sediment transport rate, and C_{es} = bed mass flux rate coefficient.

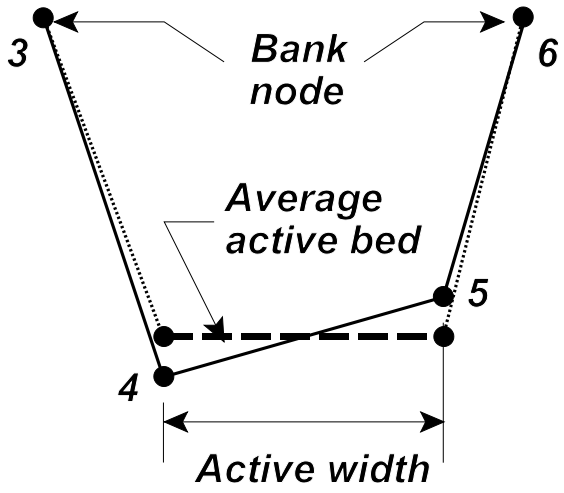

Figure 4-2. The active width of one-dimensional channels is approximated by a horizontal bed for sediment transport calculations.

Total transport rate of a mixture of particles of different sizes is calculated as

$$Q_s = \sum_{i=1}^{m} Q_{si} \tag{4-41}$$

where m = number of particle size classes, and Q_{si} = volumetric transport rate of a single class characterized by characterized by particles of diameter D_i. Total sediment flow rate of a size class is given by

$$Q_{si} = p_i Q_{si}^* \tag{4-42}$$

where p_i = fraction of the ith particle size class in the active layer, and

$$Q_{si}^* = \tilde{B} q_{si}^* \tag{4-43}$$

where q_{si}^* = unit sediment transport rates found as for two-dimensional depth-averaged flow using average velocity and depth in the active width portion of the channel.

Bridge Scour

Stream crossings are usually designed to satisfy all engineering and environmental constraints at the lowest possible cost. As a result, roadway approach embankments leading to bridge crossings often constrict flood flows at high stages, creating large velocities within and near bridge openings. Erosion of channel beds near bridges is a common result. Many bridge failures, both benign and catastrophic, have been caused by excessive erosion or scour of bed materials surrounding footings of piers and abutments [see Shirole and Holt (1991) for a summary of bridge failures in the United States and their causes]. Therefore, predicting expected depths of scour is a critical element of bridge design needed to assure a safe and reliable transportation link.

Total depth of scour (that is, the vertical distance a streambed is lowered by erosion below a reference elevation) at a bridge results from several causes and can be divided into the following three additive components: long-term degradation and lateral migration, general scour, and local scour ("Highway drainage" 1992, page VII-39; Richardson and Davis 1995, page 6). Degradation and lateral migration, which usually

take place over a long time, may be natural trends of the stream or result from artificial modifications to the stream or catchment. General or contraction scour results from constriction of streamflows by roadway approach embankments when the capacity of flow to remove or transport bed material from a bridge waterway exceeds the rate at which replacement materials are supplied. Local scour in the immediate vicinity of a bridge pier is caused by the influence of the obstruction on approaching streamflow (see Figure 4-3).

Figure 4-3. Local scour at a round-nosed bridge pier. Note protective vegetative cover of surrounding floodplain.

The pier causes flow to accelerate as it passes by, and three-dimensional vortices will form that further increase erosion. Although bed scour near abutments is often described as local in character, observation and experiment indicate the primary cause of abutment scour to be increased velocity and bed shear resulting from flow contraction by approach roadway embankments.

For either general or local scour, if no sediment is being carried by the approach flow (that is, if *clear water* conditions exist), erosion will continue until the bed shear stress reduces to a value that is unable to entrain any more material (that is, the critical shear stress). However, if sediment is actively being transported by the flow (that is, if *live bed* conditions exist) erosion will continue until a balance exists between the rates at which sediment is transported into and through the scoured area. Only clear-water general scour and local scour at bridge piers are calculated in *FST2DH*.

Clear-water Contraction Scour

Nearly 500 years ago Leonardo DaVinci noted that “where the river is constricted, it will have its bed stripped bare of earth, and the stones or tufa will remain uncovered by the soil” (MacCurdy 1938, page 84). This phenomenon is well illustrated at bridges where flow constrictions created by roadway approach embankments produce large velocities during floods that scour channel bed and bank materials.

A simple calculation of clear-water contraction scour is provided in *FST2DH*. Basically, unit flow rates are unaffected by scour that may develop. However, velocity

and shear stress may be reduced as a result of a deepening scour hole. Clearwater contraction scour depths are found by calculating the flow depth needed to reduce bed shear stress to a critical value τ_c at which erosion will cease. If bed shear stress does not exceed the critical value, no scour will occur. Deposition of sediment from upstream erosion is not accounted for in this simple treatment of scour.

Bed shear stress acting in a streamwise directions is given by Manning's relation as

$$\tau_b = \rho \frac{g n^2}{\phi_n^2 H^{1/3}} U_s^2 \tag{4-44}$$

where ρ = water mass density, n = Manning's roughness coefficient for total flow resistance, ϕ_n = units conversion factor (1.0 for SI units, 1.486 for US customary units), H = flow depth, and $U_s^2 = U^2 + V^2$ = depth-averaged velocity in the streamwise direction. Effective stress acting on erodible soil particles is found as (Temple et al. 1987)

$$\tau_{be} = \tau_b \left(\frac{n_{soil}}{n} \right)^2 \tag{4-45}$$

where n_{soil} = roughness coefficient of bare soil. Equating τ_{be} to τ_c and rearranging gives equilibrium flow depth as

$$H_{sc} = \left(\frac{\rho g n_{soil}^2 q^2}{\phi_n^2 \tau_c} \right)^{3/7} \tag{4-46}$$

where q = unit flow rate in the streamwise direction. Considering q and n_{soil} to remain constant as contraction scour develops, clear-water contraction scour depth $d_{sc} = H_{sc} - H$ is given by

$$d_{sc} = \left(\frac{\rho g n_{soil}^2 q^2}{\tau_c} \right)^{3/7} - H \tag{4-47}$$

Two critical shear stresses can be specified: one for soil τ_{cs}, and one for a protective soil cover τ_{cp}, where $\tau_{cp} > \tau_{cs}$. Protective soil covers are considered to have negligible thickness. No scour takes place when protective soil covers are present and $\tau_b \le \tau_{cp}$. However, when $\tau_b > \tau_{cp}$ protective covers are completely removed and general clear-water scour depth is calculated with $\tau_c = \tau_{cs}$. Critical shear stresses for several types of protective soil covers are given in Table 4-1.

Live-bed Contraction Scour

Live bed contraction scour can be found as part of a general sediment transport simulation. Erosion of river beds within constrictions created by bridge crossings will take place as velocities and depths increase. For given channel flow rates and water depths, live bed contraction scour will decrease as sediment concentration increases.

Local Scour at Bridge Piers

Local pier scour can be calculated automatically in *FST2DH* by computing approach flow velocity, approach flow depth, and the degree of alignment of the pier and approach flow at the center of a pier. Using the equation suggested by Richardson and Davis (1995) in the *FHWA Hydraulic Engineering Circular 18* (*HEC-18*), depth of local scour below the ambient bed elevation around a bridge pier is calculated as

Table 4-1. Critical shear stresses for various protective soil covers[a].

Protective soil cover	Critical shear stress τ_{cp}	
	in lb/ft^2	in N/m^2
Vegetation[b]:		
Class A	3.7	180
Class B	2.1	100
Class C	1	48
Class D	0.6	28
Class E	0.35	17
Woven paper	0.15	7.1
Jute net	0.45	22
Single fiberglass	0.6	29
Double fiberglass	0.85	41
Straw mulch with net	1.5	69
Curled wood mat	1.6	74
Synthetic mat	2	96
Straw mulch without net[c]:		
0.025 lb/ft^2 (0.12 kg/m^2)	0.012	0.6
0.05 lb/ft^2 (0.24 kg/m^2)	0.063	3
0.10 lb/ft^2 (0.49 kg/m$^{2)}$	0.29	14

[a]Unless otherwise noted, all data are from Chen and Cotton (1988).
[b]See Table 4-2 for a description of vegetation classes.
[c]Foster (1982)

$$d_{sl} = 2.0 K_1 K_2 K_3 K_4 b^{0.65} y_a^{0.35} Fr_a^{0.43} \tag{4-48}$$

where K_1 = pier shape factor, K_2 = flow alignment factor, K_3 = bed condition factor, K_4 = bed armoring factor, b = pier width, y_a = approach flow depth, $Fr_a = V_a / \sqrt{g y_a}$ = approach flow Froude number, and V_a = depth-averaged velocity of the approach flow. Local pier scour depth given by the *HEC-18* equation represents a conservative estimate that can be used for design, not the actual scour depth expected for the given pier and approach flow parameters. Heights of dunes in sand-bed channels needed to assign the bed condition factor K_3 can be calculated using Yalin's (1964) formula as follows:

$$h_{dune} = \frac{H}{6}\left(1 - \frac{\tau_{*c}}{\tau_*}\right)\left(1 - Fr^2\right) \tag{4-49}$$

where τ_{*c} = 0.045 = dimensionless critical shear stress,

$$\tau_* = \frac{\tau_{0s}}{(S_s - 1)\rho g D_{50}} \tag{4-50}$$

is dimensionless shear stress, $\tau_{0s} = \rho u_{*s}^2$ = shear stress acting on sediment grains, and u_{*s} = grain-friction velocity calculated as

Table 4-2. Description of vegetation retardance classes[a].

Retardance Class	Vegetal cover	
	Type	Condition
A (very high)	Weeping lovegrass	Excellent stand, tall (average height = 0.75 m)
	Yellow bluestem ischaemum	Excellent stand, tall (average height = 0.9 m)
B (high)	Kudzu	Dense growth, uncut
	Bermuda grass	Good stand, tall (average height = 0.3 m)
	Native grass mixture including little bluestem, bluestem, blue gamma, and other short and longstem Midwest grasses	Good stand, unmowed
	Weeping lovegrass	Good stand, tall (average height = 0.6 m) or mowed (average height = 0.3 m)
	Lespedeza sericea	Good stand, not woody, tall (average height = 0.5 m)
	Alfalfa	Good stand, uncut (average height = 0.3 m)
C (moderate)	Crab grass	Fair stand, uncut (height = 0.25 to 1.2 m)
	Bermuda grass	Good stand, unmowed (average height = 0.15 m)
	Common lespedeza	Good stand, uncut (average height = 0.3 m)
	Grass-legume mixture: summer (orchard grass, redtop, Italian rye grass, and common lespedeza)	Good stand, uncut (height = 0.15 to 0.2 m)
	Centipede grass	Dense cover (average height = 0.15 m)
	Kentucky bluegrass	Good stand, headed (height = 0.15 to 0.3 m)
D (low)	Bermuda grass	Good stand, cut to a height of 0.06 m
	Common lespedeza	Excellent stand, uncut (average height = 0.1 m)
	Buffalo grass	Good stand, uncut (height = 0.08 to 0.3 m)
	Grass-legume mixture: fall, spring (orchard grass, redtop, Italian rye grass, and common lespedeza)	Good stand, uncut (height ≈ 0.1 m)
	Lespedeza sericea	Good stand (height = 0.05 m)
E (very low)	Bermuda grass	Good stand (height = 0.04 m)
	Bermuda grass	Burned stubble

[a] After "Handbook of channel design" (1954)

$$u_{*s} = \frac{U_s}{6.73}\left(\frac{D_{50}}{H}\right)^{1/6} \tag{4-51}$$

As an option, expected local pier scour depth and a design scour depth can be calculated using Froehlich's (1988) expression

$$d_{sl} = 0.32\, K_1\, \tilde{b}^{0.62}\, y_a^{0.47}\, Fr_a^{0.22}\, D_{50}^{-0.09} \tag{4-52}$$

where

$$K_1 = \begin{cases} 0.7, \textit{for sharp-nosed piers} \\ 1.0, \textit{for round-nosed piers} \\ 1.3, \textit{for square-nosed piers} \end{cases}$$

is a pier shape factor, $\tilde{b}$ = pier width projected normal to the approach flow, and D_{50} = median diameter of bed material surrounding the pier. Scour depths given by Froehlich's (1988) equation are expected responses to the specified pier, approach flow, and bed material parameters, and, consequently, are uncertain estimates. However, scour depths that have small probabilities of being exceeded might be wanted to design pier foundations that are unlikely to fail. Therefore, an upper prediction limit of scour depth is also calculated for a specified confidence level. The default design confidence level is 99% (that is, there is a 99% probability that the scour depth would be less than the predicted value). However, either larger or smaller confidence levels yielding larger or smaller design scour depths can be specified.

Pier Rock Riprap

Sizes of rock riprap needed to resist scour at bridge piers are calculated automatically if pier scour is evaluated. Median rock diameter is found as (Richardson and Davis 1995, page 199)

$$D_{50} = K_p \frac{1}{(S_s - 1)} \frac{V_a^2}{2g} \tag{4-53}$$

where

$$K_p = \begin{cases} 1.6; \text{ for round-nosed or sharp-nosed piers} \\ 2.0; \text{ for square-nosed piers} \end{cases}$$

This page has been left blank intentionally.

5. Application Steps

The steps generally taken to simulate surface-water flow and sediment transport using *FST2DH* are as follows: (1) Data collection, (2) network design, (3) model calibration, (4) model testing, and (5) model application. These five steps, illustrated in Figure 5-1, are common to the operation of almost any type of numerical model and are described in this section. Notice that direction lines suggesting modification or control of the application process are shown in the diagram. For example, during model calibration you might find that additional data topographic data are needed to simulate flow more accurately in one or more areas covered by your mesh. Or while testing your model further you might decide that additional calibration is needed to improve simulation results.

Data Collection

After a surface-water flow problem has been defined, the first step in the operation of the modeling system consists of gathering data. Needed data are classified as either topographic or hydraulic data. Topographic data describe the geometry of the physical system and include an evaluation of surface roughness to be used in estimating bed friction coefficients. Hydraulic data include measurements of stage and flow hydrographs; spot measurements of stage, flow, and velocity; high-water marks left by floods; rating curves; limits of flooding; and wind measurements. Hydraulic data are used to establish model boundary conditions, and to calibrate and test a model. Data needs are summarized in Table 5-1.

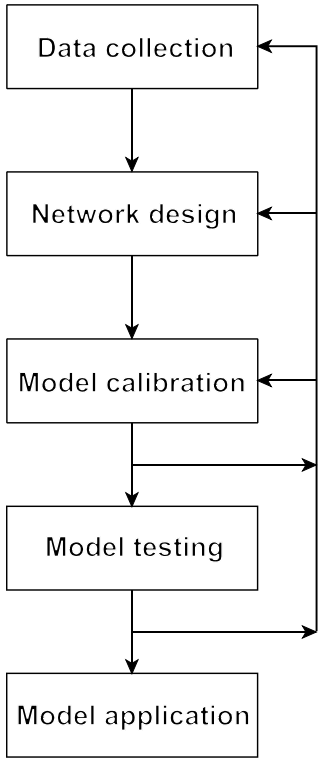

Figure 5-1. Modeling steps usually taken when applying *FST2DH* to simulate depth-averaged surface-water flow.

The type and amount of data needed to design a network properly and to apply a model mainly depend on the purpose of the model. The more data that can be obtained the better, and all of the data can be used to improve the quality of a model's output. Theoretically, any surface-water flow can be simulated as accurately as wanted provided the important physical processes are represented adequately by the governing equations. However, the purpose of a model needs to be considered when deciding what and how much data is needed to provide results of the desired accuracy. For example, a computational resolution of centimeters (or less) might be needed to

Table 5-1. Summary of data that might be needed to apply the modeling system.

Data item	Use of data	Source(s) of data
Ground-surface elevations	Assignment of ground-surface elevations to node points; layout of a finite element network.	Topographic and hydrographic charts, maps, and surveys.
Bridge, culvert, weir, pier, and drop inlet structure dimensions.	Layout of a network; assignment of bridge, culvert, weir, pier, and drop inlet structure parameters.	Design drawings and surveys.
Channel and floodplain surface characteristics, vegetative cover, and sediment composition.	Evaluation of bed friction coefficients and eddy viscosity.	Aerial and ground photographs, topographic maps, and on-site inspection.
Water-surface elevations.	Establishment of boundary conditions, calibration of model coefficients, and testing model accuracy.	On-site measurements, high-water marks, and streamgage records.
Current velocity and flow rate.	Establishment of boundary conditions, calibration of model coefficients, and testing model accuracy.	On-site measurements, indirect estimates based on measured high-water marks, and streamgage records.
Wind velocity.	Calculation of wind stresses at the water surface.	On-site measurements and weather station records.
Water temperature and salinity.	Calculation of water density.	On-site measurements and streamgage records.
Latitude.	Calculation of the Coriolis force.	Map.
Astronomical tide stages.	Boundary conditions for time-dependent simulations affected by ocean levels.	NOAA tide tables and computer programs.
Tropical cyclone windfield parameters.	Calculation of storm surge and generation of surface shear stresses caused by tropical cyclone winds.	NOAA Technical Report NWS-38 (Ho et al. 1987) and historic records.
Bed material size and gradation.	Initial and boundary conditions for sediment transport solutions.	Onsite samples and boring logs from nearby construction projects such as bridges.

provide the desired results for a model of a laboratory flume. On the other hand, a model of a tidal estuary might require a computational resolution of a kilometer or more.

Minimum data needs for a particular application are difficult to estimate in advance. Objectives of the study and the available time, personnel, and funding need to be considered before model construction (that is, network design, calibration, and testing) and subsequent application. Because time, personnel, and funding always have finite limits, decisions need to be made regarding how much detail to be represented by the model and the extent of a calibration and testing to be carried out. If a high level of detail is provided

by a network, risk of not representing a physical system properly will be reduced, but difficulty (in time and expense) of obtaining a solution will be increased. On the other hand, if a simple network is designed, the risk of not accurately representing a physical system will be increased, but the difficulty of obtaining a solution will be reduced. Knowledge of important physical processes that govern the response of a system under study is needed to evaluate the tradeoff between risk of not accurately representing the system and difficulty of obtaining a solution. Sometimes constraints on time, human resources, or funding will predetermine how much detail can be included in a model and the amount of calibration and testing to be carried out. Consequently, a larger amount of risk would be accepted than would otherwise be wanted.

Mesh Design

The next step in applying *FST2DH* is to design a finite element mesh. Mesh design can be defined simply as the process by which the surface-water body being modeled is subdivided into an assemblage of finite elements. The basic goal of mesh design is to create a representation of the water body that provides an adequate approximation of the true solution of the governing equations at a reasonable cost. No set rules exist for achieving this goal because of the many different conditions encountered from one problem to the next. Design of a satisfactory mesh depends largely on the use of sound engineering judgment gained from previous modeling experience. However, some helpful guidelines are presented in this section.

General Mesh Layout

Decisions as to the number, size, shape, and pattern of elements used to provide an adequate representation of the water body that is to be modeled need to be made when designing a finite element mesh. If the elements obey some basic requirements for a convergent solution, the accuracy of the solution will improve as the size of the elements in a mesh is reduced. However, increasing the number of elements in a mesh also increases computational expenses. Elements need to be made small enough to provide a solution of sufficient detail and accuracy, yet large enough to obtain the solution at a reasonable cost.

Next, the limits of the area to be modeled are defined. As a rule, model boundaries are placed where water-surface elevations and flows can be specified accurately. The effect that boundary condition errors will have on a solution needs to be considered. If the accuracy of boundary conditions is not certain, the limits of a model can be placed as far away as possible from areas of primary interest so that any errors introduced at the boundaries will have little influence at the points of interest.

After boundaries have been defined, subdivision of the solution domain continues by dividing the area to be modeled into large regions that have similar topographic and surface cover characteristics. Subdivision lines between the regions are placed, as much as possible, where abrupt changes in topography or surface cover occur. The large regions then are divided into elements, the size and shape of which will depend on the desired level of detail in that particular area.

FST2DH will accept any combination of six-node triangular, eight-node quadrilateral, or nine-node quadrilateral elements that have straight or curved sides so that complex geometries can be modeled in detail. Curved-side elements are created by simply specifying the coordinates of the midside node of sides that are curved. If midside-node coordinates are omitted, element sides are considered straight and the midside node coordinates are interpolated halfway between the two adjacent vertex nodes.

Some conditions regarding the shape of an element need to be satisfied so that the determinant of the Jacobian matrix will not vanish within the element (that is, the

isoparametric mapping between a global element and its parent element needs to be one-to-one). It is a good idea to make sure that a midside node is placed within the middle third of the curved element side that it defines as shown in Figure 5-2. Also, it is suggested that internal angles of quadrilateral elements be kept between 60° and 120° as shown in Figure 5-2. For triangles, well-shaped elements can be assured by keeping interior angles between 5° and 120°, which means avoiding long, thin elements that come to a sharp point, especially when curved sides are used.

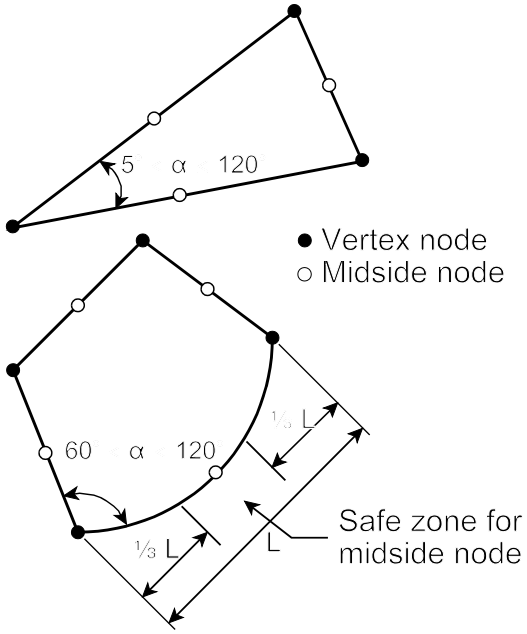

Figure 5-2. Some rules to ensure one-to-one mapping of two-dimensional isoparametric finite elements.

Meshes in which all the elements have about the same size and shape throughout might be easy to construct but will usually not be practical. The ability to vary the size and shape of elements within a single mesh is a major advantage of the finite element method. In regions where the gradients of dependent variables are expected to be large, small elements will provide a more accurate solution than large elements. Locations where gradients of velocities and depth might be large include stream channels, constrictions, and areas near large inflows or outflows. Small elements also need to be used to model boundaries that have irregular shapes. In regions where solution variables are expected to change very slowly, or in areas of the model that are of minor interest, large elements can provide a solution of sufficient accuracy. Transition between a section of a mesh composed of large elements and a section of a network composed of smaller elements needs to be gradual; that is, it is best if very large elements are not connected to very small elements. Also, it is a good idea to position nodes at locations where point inflows or outflows are to be applied.

The question of which type of element to use to construct a mesh (that is, a six-node triangle, an eight-node quadrilateral, or a nine-node quadrilateral) is not answered easily. The ease of approximating a two-dimensional region with an assemblage of arbitrary triangular elements has been shown in many applications. The two kinds of quadrilateral elements are similar except for the presence of an internal node in the nine-node Lagrangian element. The additional node in a nine-node quadrilateral element creates a little more computational effort, but provides a more accurate solution than an eight-node quadrilateral element. For most meshes, mixtures of six-node triangular elements and nine-node quadrilateral elements will provide the best representation of the water bodies being modeled.

Another characteristic of mesh design that affects a finite element solution is the aspect ratio of elements. The aspect ratio of a two-dimensional element is the ratio of the longest element dimension to the shortest element dimension as shown in Figure 5-3. A well-designed mesh will usually be composed of elements that have a variety of shapes, sizes, and a wide range of aspect ratios. However, elements that have aspect ratios that are

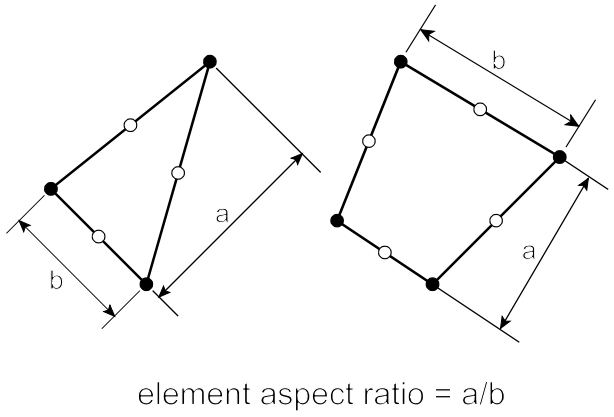

Figure 5-3. Aspect ratios of triangular and quadrilateral elements.

much greater than unity need to be designed cautiously. The optimal aspect ratio for a particular element depends on the local gradients of the solution variables. If the gradients can be estimated in advance, aligning the longest element dimension to the direction of the smallest gradient and the shortest element dimension to the direction of the largest gradient is best. For example, in stream channels where the longitudinal variation of velocity and depth is gradual and the transverse variation is large, elements can be much longer in the longitudinal direction than in the transverse direction. If the interior angles of triangular elements are kept between 5° and 120°, the maximum aspect ratio that can result is about 12.5. For most networks it is probably a good idea to keep the aspect ratio of both triangular and quadrilateral elements below 12.5.

Two-Dimensional Bridges

Two-dimensional flow through a bridge or a culvert is modeled exactly as ordinary free-surface flow when the water surface is not in contact with the top of the bridge or culvert opening. However, when the water surface is in contact with the top of an opening pressure flow exists. When pressure flow conditions can occur at a bridge or culvert, special consideration needs to be given to the design of a finite element mesh near the structure. Elements need to be constructed to conform to the two-dimensional plan of the bridge deck as shown in Figure 5-4. The elevation of the ceiling (that is, the underside of the bridge deck) also needs to be specified for each of the vertex nodes contained in elements that conform to the bridge deck. More than two rows of elements within an opening might be needed to model pressure flow accurately. Increased resistance to flow caused

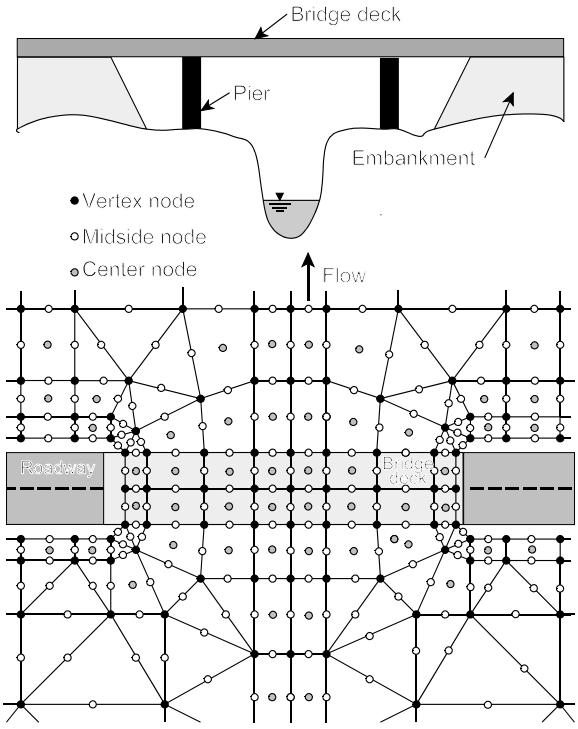

Figure 5-4. A finite element network at a bridge where pressure flow within the bridge opening is modeled.

by shear along the underside of bridge decks is included when pressure flow occurs.

To avoid ambiguous definition of bridge deck elements when two parallel bridges are separated by a single row of uncovered elements, you also need to specify the element property type applied to bridge deck elements as potential pressure flow elements. Consequently, when assigning property types to elements you will want to create property types that are applied only to bridge deck elements.

Bridge decks need to begin and end at closed boundaries, which usually represent the bridge abutments, as shown in Figure 5-4. When flow over approaching roadway embankments is modeled as one-dimensional weir flow (see the following section "One-dimensional Weirs and Culverts"), this condition will be satisfied. However, if an approach roadway is completely level with the surrounding floodplain, and a mesh is constructed on the roadway to model depth-averaged flow over it, you will need to leave a small vacant area next to the end of the bridge deck so that the deck will terminate at a solid boundary as shown in Figure 5-5.

Combined pressure flow through a bridge opening and weir flow over the bridge deck can be modeled by specifying weir segments that define the top of a bridge deck. Bridge openings can be either completely or partially submerged. The two nodes on either side of a weir segment that defines the top of a bridge deck will be the nodes on the upstream and downstream sides of the bridge that correspond to the location of the weir segment. These nodes will always be internal nodes, except where the bridge deck intersects a network boundary. However, weir flow over a bridge deck is treated as a source/sink term in the continuity equation, even when the upstream and downstream nodes are boundary nodes.

While simulating the effect of a bridge pier by constructing the network around it might be possible, usually elements would be needed that are much smaller than those in the surrounding mesh, requiring more work to construct the mesh and greater computational expense. However, the effect of drag forces on bridge piers can be accounted for indirectly by distributing the force evenly across the surface of the element containing the pier. If a pier occupies more than one element, the drag force is applied to the element at the center of the pier. More than one pier can occupy an element. Therefore, the total pier drag force distributed on an element might be an accumulation of drag forces acting on several piers.

One-Dimensional Weirs and Culverts

One-dimensional weirs and culverts are described by a set of parameters and two node points, one on either side of a weir or on either end of a culvert. Flow over weirs or through culverts is calculated based on the water-surface elevations and velocities at the two node points and the specified parameters. The node points may be placed on the

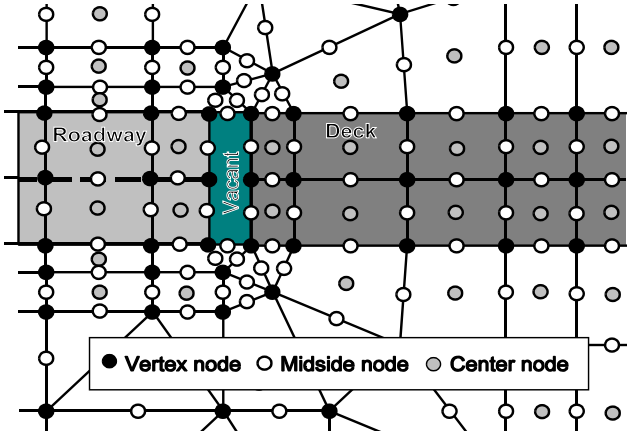

Figure 5-5. Bridge decks need to begin and end at closed boundaries. When approach roadways are covered by two-dimensional meshes, you will need to leave a "vacant" area at the end of the deck to create a closed boundary there.

boundary or in the interior of the finite element network. If water is allowed to leave a network at a weir or culvert and not return, then only one node point is needed.

Flow over roadway embankments is modeled best as one-dimensional weir flow. To model weir flow over roadway embankments, a finite element mesh needs to be designed so that solid boundaries are positioned on both sides of an embankment as shown in Figure 5-6. The embankment is divided into weir segments, and appropriate parameters assigned to each segment. The number of segments to use depends on the variation of the roadway elevation along the embankment and the spacing of node points on the solid boundaries that define the embankment. Node points that define the sides of a weir segment need to be placed at approximately the center of the weir segment. Flow will be allowed to leave the mesh at the upstream node (that is, the node with the highest water surface elevation) and reenter the network at the downstream node. If water flows over the weir segment and does not return to the mesh, only the upstream node needs to be specified. The location of a weir segment needs to be considered during initial design of a finite element network near a roadway embankment. It is a good idea to match up node points on opposite sides of the roadway that define the two sides of a weir segment. Also, a single node point can be used to define the side (end) of more than one weir segment (culvert). The same two node points can be used for both a weir segment and a culvert as shown in Figure 5-7.

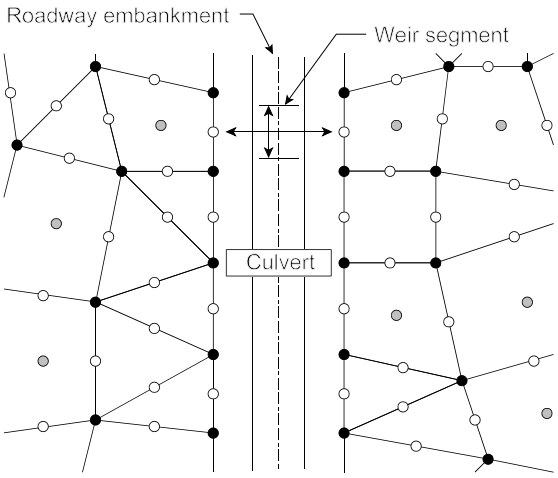

Figure 5-6. Modeling one-dimensional weir and culvert flow at roadway embankments.

When assigning weir segment lengths two-thirds of the side length of an element is assigned to the midside node, and one-sixth of the side length is assigned to each vertex node of that side. This apportionment will provide equal amounts of flow across the network boundary at each node if the water-surface elevation is constant along the element side. Following this rule, the resulting weir segment lengths assigned to adjacent nodes will not be equal but will alternate in size. If all elements along a boundary that defines one side of a roadway embankment over which water can flow have sides of length L, then all midside nodes along that boundary will be assigned weir segment lengths of ⅔L, and all vertex nodes will be assigned weir segment lengths of ⅓L (one-half of which is assigned from each element containing the vertex node).

One-dimensional flow modeled at weirs, culverts, and small bridges is treated as either a point flow on the boundary of a finite mesh network when the nodes defining the structure are mesh boundary nodes, or a sink/source term when the nodes defining the structure are interior nodes. A point flow is the total flow that crosses the mesh boundary because of flow at a single node point. However, if one node at a weir or culvert is wet, and the other node in an element that is dry and, therefore, has been excluded from the mesh, even temporarily, computational difficulties may arise. Therefore, both nodes are best placed in locations that will be wet if they are expected to convey flow for reasons of numerical stability.

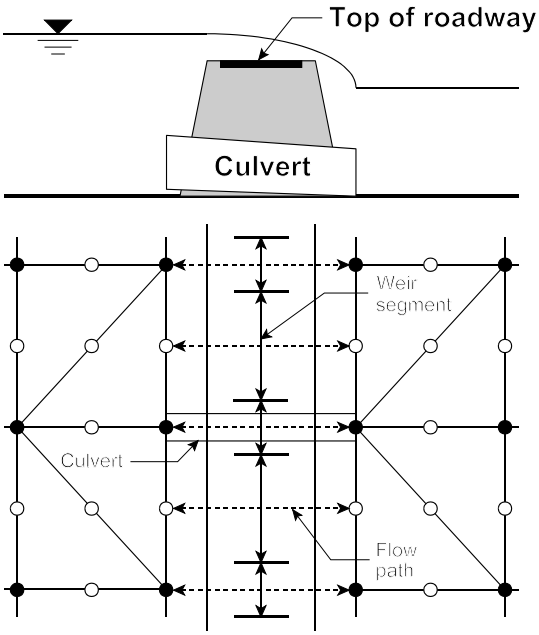

Figure 5-7. A roadway embankment with a culvert through it and the top divided into weir segments. Nodes match on opposite sides of the embankment. Midside nodes are assigned two-thirds of a weir crest segment length, vertex nodes are each assigned one-sixth of the length.

Drop Inlet Structures

Flows through drop inlet structures are treated as point flows on the boundary of a finite element mesh when the nodes defining the structure are placed on the mesh boundary, or as sink/source terms when the nodes are placed in the interior of the mesh. Drop inlet structures are described by a set of parameters and two node points, one at the entrance of the drop inlet and one at the outlet of the conduit. Therefore, when laying out the mesh, node points need to be positioned close to the entrance and outlet of each drop inlet structure as shown in Figure 5-8. Flow rates through the structures are computed based on the water-surface elevations and velocities at the two node points and the specified parameters. Tailwater elevation is specified at conduit outlets if flows are allowed to leave the networks through the drop inlet and not return. The same node point can be used to define more than one drop inlet structure and weir segments and culverts.

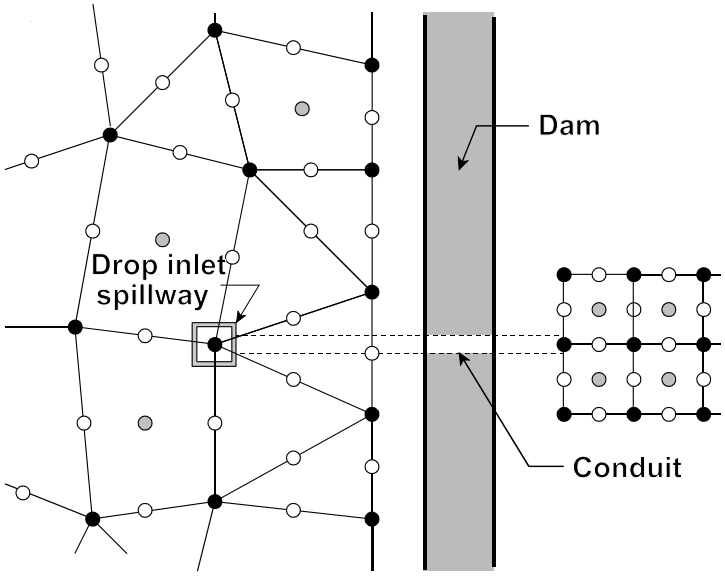

Figure 5-8. Meshes need to be designed with consideration of the locations of the drop inlet spillway entrances and outlets.

1D/2D Junctions

One-dimensional channel elements can be used to connect separate sections of two-dimensional meshes. One-dimensional sections of meshes join two-dimensional sections at "junctions" as shown in Figure 5-9. Junctions are specified at single nodes in the *BOUN* data set, and for entire boundary cross sections in the *BSEC* data set. Water-surface elevations will be the same at all nodes

forming a junction, and mass continuity will be assured there (that is, the rate at which water or sediment leaves/enters the two-dimensional mesh will equal the rate at which water enters/leaves the one-dimensional mesh).

Model Calibration

Finite element models are simplified, discrete representations of complex and continuous physical flow systems. Three-dimensional topographic features are represented by two-dimensional elements, and the physics of flow are considered to obey differential equations in which several empirical coefficients appear. When models produces useful results, they need to be calibrated if enough data are available. Model calibration is the process of adjusting the dimensions of simplified geometric elements and empirical

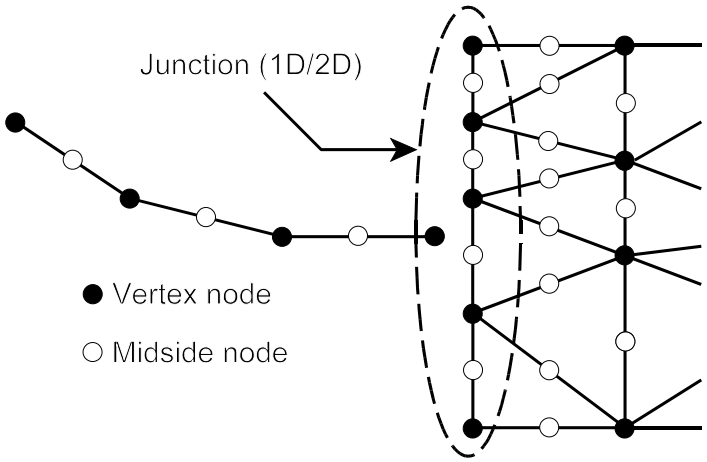

Figure 5-9. One-dimensional and two-dimensional meshes join at junctions.

hydraulic coefficients so that values computed by a model reproduce as closely as possible measured values.

The ability of a model to reproduce and predict measured values depends on the amount and quality of topographic, topologic, and hydraulic data collected. Although model parameters can be adjusted to obtain close agreement between computed and measured values, an adjustment may not be extended beyond physically reasonable values. For example, if good agreement can be obtained only by using Manning roughness coefficients three times as large as estimated initially, the finite element network probably is a poor representation of the physical region being modeled. The purpose of model calibration is to obtain an accurate mathematical representation of reality, not a forced fit of a poorly constructed model.

Model calibration proceeds by adjusting parameters systematically so that computed and measured values agree as closely as possible. Measured values of water-surface elevation, total flow rates, and velocities can be used to calibrate a model. An impression of the sensitivity of computed values to changes in model data can be obtained from initial adjustment runs. Sensitivity of results to changes in model data suggests a need to measure more accurately those parameters for which small changes affect model output.

Roughness (or discharge) coefficients are empirical coefficients that affect a solution the most. Roughness coefficients estimated during the initial design of a network will not have to be adjusted much if sufficient and accurate topographic data have been collected. Changes to roughness coefficients need to be made carefully so that adjusted values are appropriate for the bed material, channel slope, and vegetative cover that exist in

the area covered by a particular element. For example, two channel reaches that have about the same bed material and cross section shape, or two flood plains that have about the same vegetative cover and topographic characteristics, need to be assigned roughness coefficients of approximately the same value.

Eddy viscosity coefficients usually affect a solution much less than roughness coefficients. The influence of eddy viscosity is greatest in a finite element network where velocity gradients are large. Increasing eddy viscosity coefficients will cause velocity gradients to be reduced, and the horizontal velocity distribution will become more uniform. Reducing eddy viscosity coefficients will cause velocity gradients to increase.

If close agreement between measured and computed water-surface elevations, flow rates, and velocities cannot be obtained using roughness and eddy viscosity coefficients that are within reasonable ranges, then model discretization and the accuracy of topographic and hydraulic data need to be examined. However, if a model cannot reproduce measured values satisfactorily, one or more of the following reasons might be the cause of discrepancies:

- The time step or element sizes might be too large to resolve short wave components in unsteady flow simulations. Time steps need to be made small enough to model time-dependent boundary conditions accurately. The only definite way to decide whether the time step is too large is to simulate the same event using successively smaller time steps. If the size of the time step significantly affects calculated water depths and unit flow rates, the time step is too large and needs to be reduced.

- The data measurement techniques or frequency of observations could be inaccurate. Errors might be caused by inaccurate leveling, incorrect high-water marks, or faulty gauges.

- Tributary inflows might be significant and may need to be measured or estimated.

- Phenomena that affect the flow significantly might not be accounted for in the model. Possibly surface wind stresses, bed variation caused by erosion or sedimentation, or seasonal variation of roughness resulting from changes in vegetative cover need to be considered.

Model Testing

Testing a calibrated model to see if computed values compare favorably to measured values used to adjust coefficients is a useful, but not always possible, step in the modeling process. If a model reproduces the additional measured values closely without any further adjustment of model parameters or redesign of the finite element network, the model can be used to simulate conditions outside the range of a calibration with more confidence than if no additional testing were carried out. However, often model testing is not possible because of insufficient data or because of time or funding constraints. Nevertheless, if even limited data are available, models need to be tested to make sure that results are reasonable.

Model Application

After preliminary steps have been completed, models can be used to simulate a variety of flow conditions. Models still need to be applied with care, especially if they are used to evaluate conditions far outside ranges of calibration and testing. However, if a model has been calibrated and tested properly, it can be used to gain valuable insights to the response of a surface-water flow system to natural or artificial changes.

This page has been left blank intentionally.

6. Solution Responses to Parameter Changes

Several simple test channels are used to show the effects of changes in Manning's roughness coefficients and kinematic eddy viscosities on water-surface elevations and flow distributions in this chapter. Understanding the effects of changes in these parameters helps to make reasonable and prudent adjustment of model parameters needed to improve agreement between calculated and measured water-surface elevations and velocities.

Longitudinal Depth Changes in a Channel of Uniform Width

A test channel 800 m long and 100 m wide that has a level bottom is discretized using five rows of elements, each 20 m wide and 80 long, that span the channel width is shown in Figure 6-1. All elements are nine-node quadrilaterals. A water depth of 1.0 m is applied at the left end of the channel as an essential boundary condition, and an inflow rate of 100 m^3/s is applied at the right end. Semi-slip conditions are applied along all closed boundaries. A single element type is applied to the entire channel.

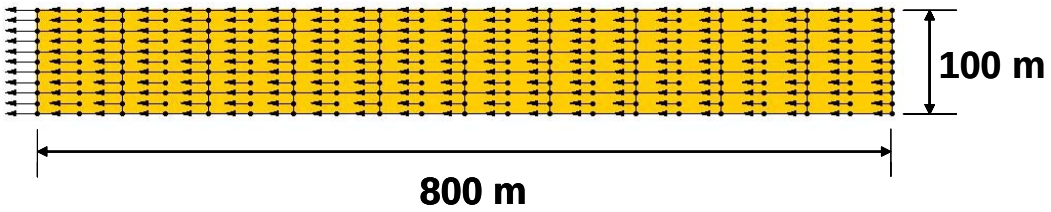

Figure 6-1. The horizontal test channel is 800 m long and 100 m wide and is discretized using nine-node quadrilateral elements each 80 m long and 20 m wide. Water flows from right to left.

Effect of Roughness Coefficient

Effects of changes in Manning's roughness coefficient on longitudinal variation of water-surface elevations were studied by carrying out steady-state simulations with roughness coefficients n = 0.015, 0.025, 0.035, 0.045, and 0.055 and kinematic eddy viscosity ν = 1.0 m^2/s. Since semi-slip conditions are applied along the sides of the channel (that is, the vertical sides provide no resistance to flow), water depths and velocities are uniform across the channel. Water-surface profiles along the center of channel for each simulation are shown in Figure 6-2. Not surprisingly, larger roughness

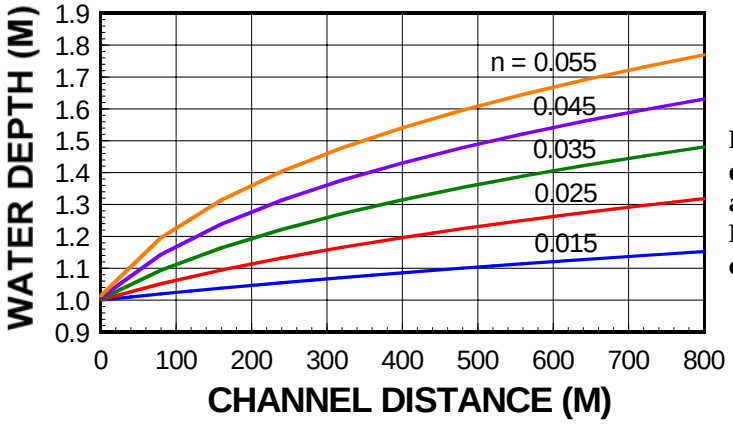

Figure 6-2. Water-surface elevations along the channel are sensitive to changes in Manning's roughness coefficient.

coefficients lead to higher water-surface elevations along the test channel. Water depth at the upstream end varies from 1.14 m when n = 0.015 to 1.77 m when n = 0.055. Even comparatively small changes in Manning's n can produce significant changes over the 800 m length of the channel.

Effect of Eddy Viscosity

With n = 0.035, steady-state simulations were carried out with kinematic eddy viscosity ν_t = 1, 10, and 100 m^2/s. The two largest values are unreasonable for the dimensions of the test channel and the water depths and velocities that occur. The resulting longitudinal water-surface profiles are shown in Figure 6-3. Because turbulent shear stresses depend on velocity gradients as well as eddy viscosity, the effect of eddy viscosity will be greatest where velocity gradients are largest. Consequently, differences caused varying eddy viscosity are apparent only near the downstream end of the channel where velocity gradients are largest.

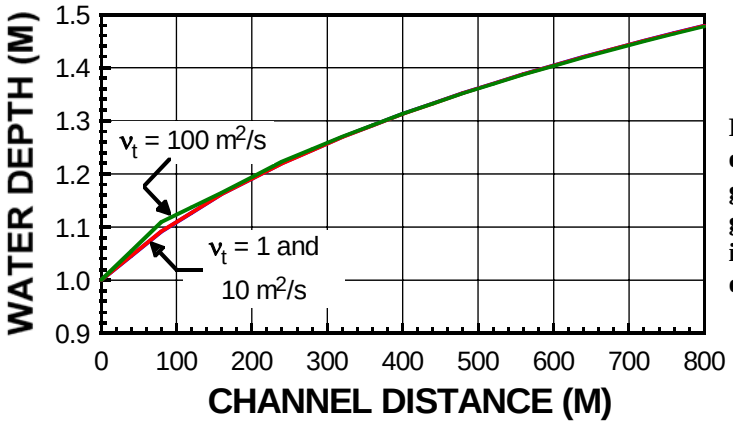

Figure 6-3. The effect of eddy viscosity will be greatest where velocity gradients are largest, which is near the downstream end of the channel.

What the Test Shows

Results from this test show that large increases in eddy viscosity raise upstream water-surface elevations far less than large increases in roughness coefficients. This finding is true in general based on numerous applications in rivers where high-water marks were available and compared to calculated values. Therefore, reasonable adjustments to roughness coefficients will likely improve agreement between calculated and measured water-surface elevations far more than changes to eddy viscosities that are kept within sensible limits.

Longitudinal Depth Changes in a Channel of Variable Width

A second test channel also 800 m long having a width that varies from 100 m at the upstream and downstream ends, to 20 m in a central section is shown in Figure 6-4. The channel has a level bottom and is again discretized using five rows of elements. However, elements widths vary, ranging from 20 m at the ends to 4 m within the narrow central portion of the channel. All elements are nine-node quadrilaterals. A water depth of 1.0 m is applied at the left end of the channel as an essential boundary condition, and an inflow rate of 100 m^3/s is applied at the right end. Semi-slip conditions are applied along all closed boundaries. A single element type is applied to the entire channel.

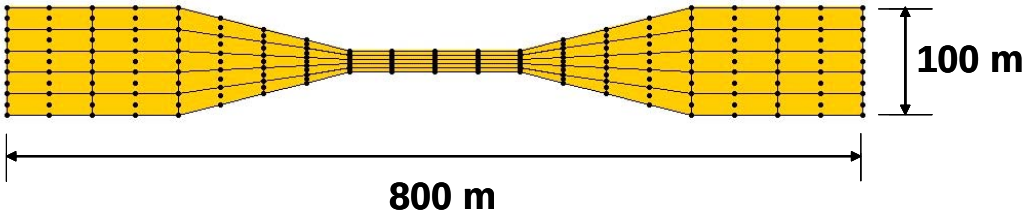

Figure 6-4. An 800 m long test channel having a width that varies from 100 m at the upstream and downstream ends, to 20 m in a central section .

Effect of Roughness Coefficient

Solutions were obtained for Manning roughness coefficients n = 0.015, 0.035, and 0.055 with ν_t = 1.0 m^2/s. Water-surface profiles along the center of the channel for each simulation are shown in Figure 6-5. Again, larger roughness coefficients produce higher water-surface elevations along the test channel. Water depth at the upstream end of the test channel varies from 2.4 m when n = 0.015 to nearly 3.0 m when n = 0.055.

Effect of Eddy Viscosity

Because of the constriction in the central portion of the channel, longitudinal and transverse velocity gradients are larger than in the previous test. Consequently, eddy

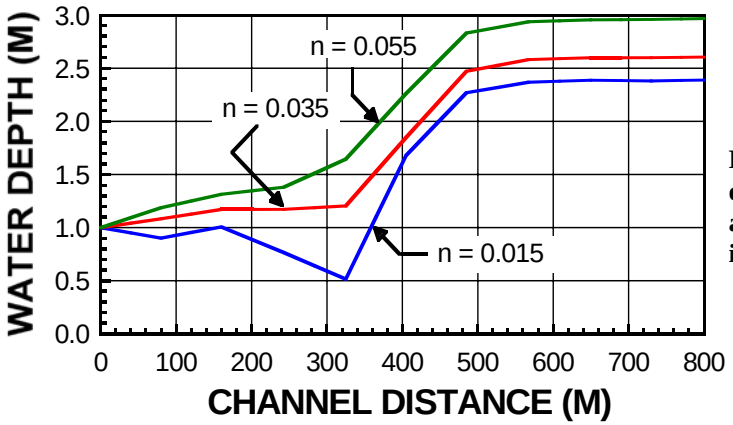

Figure 6-5. Water elevations along the channel are very sensitive to changes in roughness coefficients.

viscosity has a larger effect on water depth as shown by the profiles in Figure 6-6. With n = 0.035, little difference exists between solutions with ν_t = 1 and 10 m^2/s. However, water depths are significantly larger at the upstream end when ν_t = 100 m^2/s, and unreasonably large value for flow conditions in the channel.

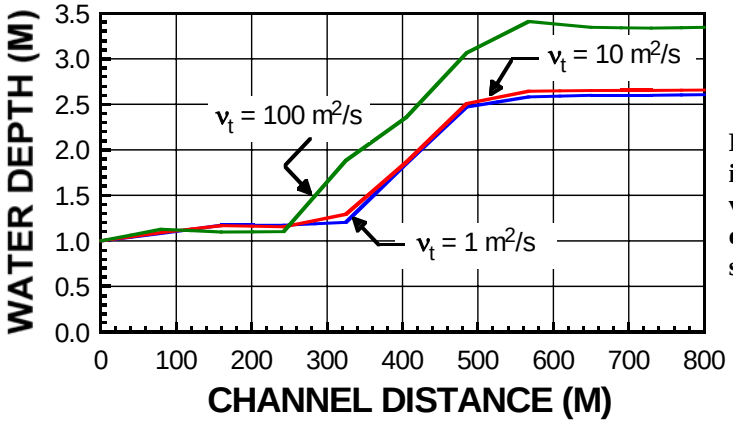

Figure 6-6. Eddy viscosities in the range of reasonable values for the test channel conditions yield nearly the same results.

What the Test Shows

Although large increases in eddy viscosity raise upstream water-surface elevations as much or more than increases in roughness coefficients, eddy viscosities in the range of reasonable values for the test channel conditions yield nearly the same results. Therefore, changes in eddy viscosity that are kept within sensible limits still have much less influence on water-surface elevations than do changes in roughness coefficients. When trying to match calculated water-surface elevations to measured highwater marks, make sure that eddy viscosities values are reasonable for the flow conditions, then make prudent changes to flow resistance coefficients.

Effects of Lateral Roughness Variations and Eddy Viscosity

A third test channel with the same dimensions and boundary conditions as the first test channel, but with two different roughness coefficients dividing it, a large roughness coefficient (n = 0.055) on the right side representing a more flow resistant surface cover, and a smaller roughness coefficient on the left side (n = 0.035), is shown in Figure 6-7.

Distribution of velocity laterally across the channel at its midsection for several values of constant kinematic eddy viscosity ranging from 0.1 m^2/s to 100 m^2/s is shown in Figure 6-8. Eddy viscosity clearly has a large effect on lateral velocity distribution. Small values of eddy viscosity produce the smallest lateral shear stress, and velocity across the channel is affected most by the variation in bed roughness coefficients. Flow on the right

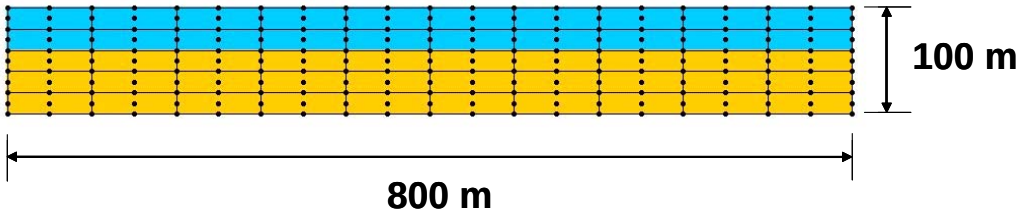

Figure 6-7. A test channel similar to the first that has a higher flow resistance of the right side (n = 0.055) than on the left side (n = 0.035).

side of the channel is slowed because of the higher resistance. Even though a large velocity gradient exists in a transverse channel direction, lateral shear stresses are functions of both velocity gradients and eddy viscosity. Effect of increased kinematic eddy viscosity

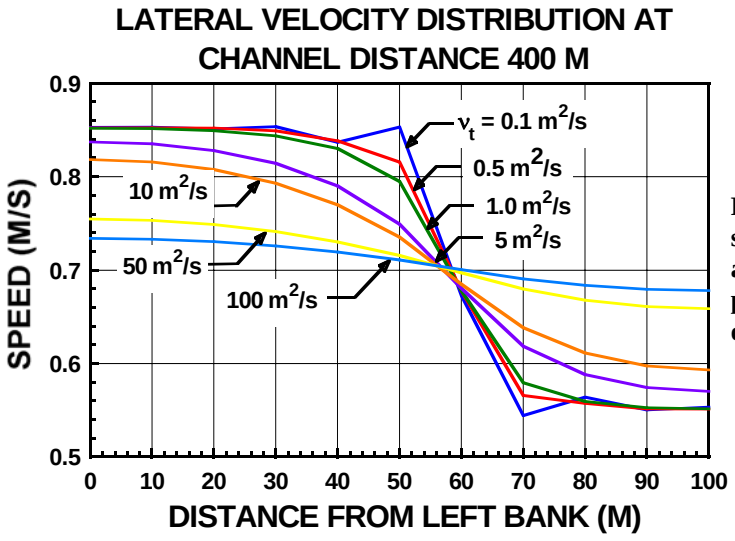

Figure 6-8. Effect of lateral shear stresses on velocity across the channel is pronounced for large values of kinematic eddy viscosity.

becomes noticeable for values of $\nu_t > 1.0$ m^2/s, as the lateral shear stress tends to make velocities more uniform across the channel. However, when viscosities appropriate for the physical channel are considered ($\nu_t \leq 1.0$ m^2/s), differences in velocity profiles are comparatively small.

What the Test Shows

This test shows the effect of kinematic eddy viscosity on velocity distribution in shear flows (flows with large velocity gradients). Using unrealistically large eddy viscosities makes velocity more uniform across the channel, but likely does not reflect true physical conditions. When modeling flow through constrictions, such as bridge openings, accurate depictions of velocity variation across the openings will depend largely on applying reasonable values of eddy viscosity.

Effects of Vertical Wall Shear Stress on Velocity

The next test channel has the same dimensions and inflow and outflow boundary conditions as the firs; however, vertical wall shear is applied to closed boundaries (that is, the "semi-slip" condition is applied) as shown in Figure 6-9.

Lateral velocity distribution at the channel midpoint with $\nu_t = 1.0$ m^2/s both with lateral wall shear (a "semi-slip" boundary condition) and without lateral wall shear (a "slip" boundary condition) are shown in Figure 6-10. The effect of wall shear is clearly significant. With a slip condition applied, velocity is uniform

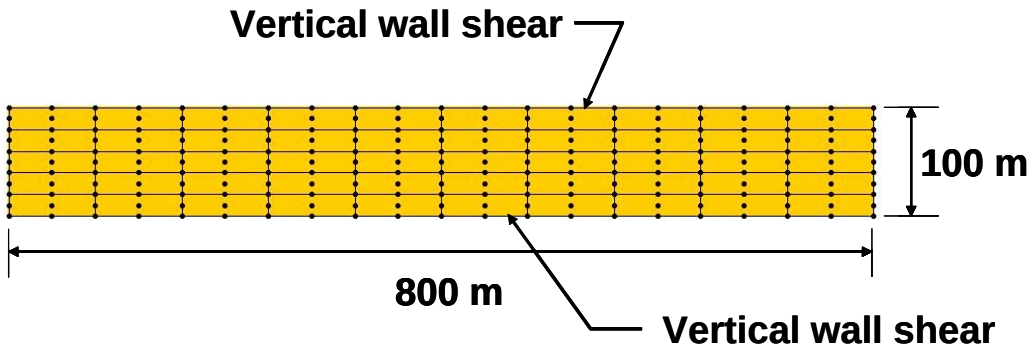

Figure 6-9. Vertical wall shear is applied by means of the "semi-slip"boundary condition.

across the channel, Wall shear retards flow along the sides of the channel, causing a peak velocity to occur at the center.

What the Test Shows

When modeling flows in channels that have vertical or nearly vertical side walls, semi-slip boundary conditions will likely be needed to capture the effect of shear stresses along the channel sides. Accurate simulation of velocities in lateral directions will probably not be possible if these effects are ignored.

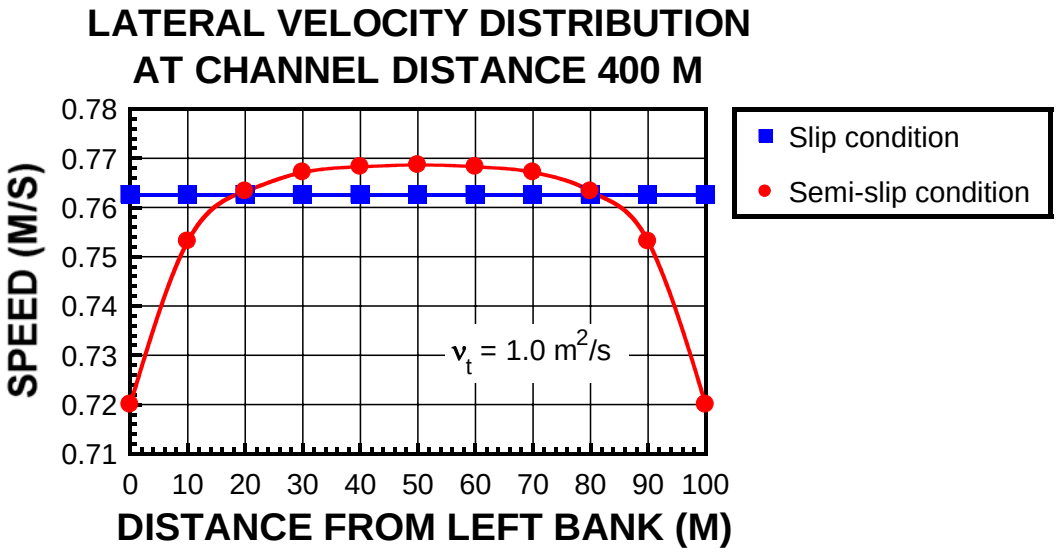

Figure 6-10. Lateral wall shear stress applied by the "semi-slip" condition on closed boundaries can have a significant influence on velocity. Without lateral shear stress (that is, with a 'slip" condition on closed boundaries, velocity is uniform across the test channel.

Effects of Wind Shear Stress on Water Depth

A test channel with the same dimensions as the first, but with closed boundaries all around, is shown in Figure 6-11. Wind blows in the longitudinal channel direction from left to right (that is, in the positive *x* direction) at a constant speed.

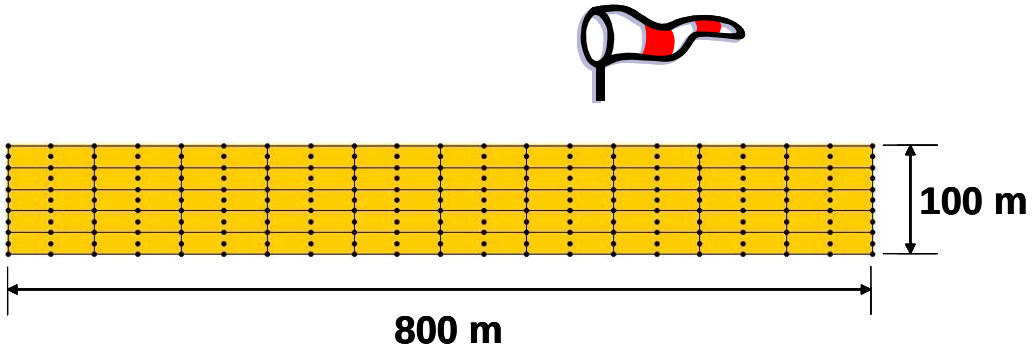

Figure 6-11. Wind blows from left to right along the channel, creating surface shear stresses.

Water-surface elevations along the center of the channel for applied wind speeds ranging from 10 m/s to 50 m/s are shown in Figure 6-12. From one end of the 800 m channel to the other, a wind speed of 50 m/s produces a water-surface elevation difference of 0.25 m. Sustained winds blowing across large distances can raise water surfaces considerable heights. Velocities are affected as well, as large volumes of water can be moved by the applied surface forces.

What the Test Shows

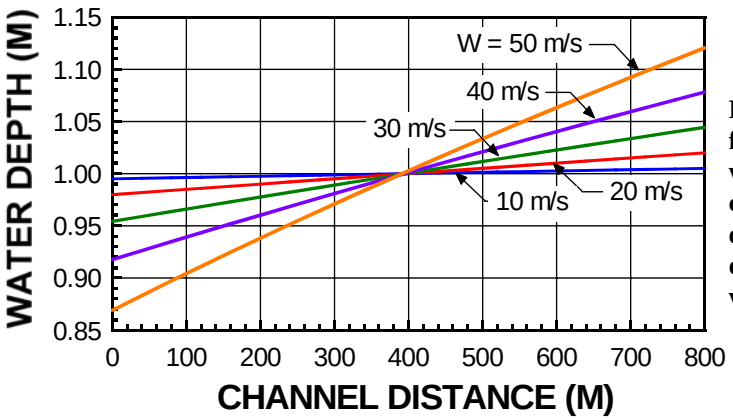

Figure 6-12. Wind blowing from left to right creates a water-surface elevation change of 0.25 m from one end of the channel to the other. The change increases with wind speed.

Wind shear can have a significant influence on water-surface elevations and velocities in open channels. Sustained winds caused by tropical cyclones, for example, can push large volumes of water upstream in an estuary or river, which is in addition to upstream flows caused by coastal storm surge.

This page has been left blank intentionally.

7. Program Operation

Operation of *FST2DH*, which is the same on any computer system, is as follows: (1) the program is executed, (2) it reads input data files at the start and possibly during a simulation, (3) it carries out the requested calculations, and (4) it writes output data files during and at the end of a simulation. Names of all input and output data files are contained in a *FST2DH* project file, which is usually given the filename extension *.fpr* (for example *Alexander.fpr*). Project file formats are explained in Appendix A. A typical *FST2DH* project file is shown in Figure 7-1. Data file names are terminated by a slash in each line, and short descriptions of the data follow.

```
FST2DH,3
Alexander.dat       /Control data
Alexander.msh       /Mesh data
Alexander(01).flo   /Flow input data
Alexander(01).sed   /Sediment input data
Alexander.bcs       /Boundary condition data
Alexander.wnd       /Wind data
Alexander.wve       /Wave data
Alexander.tim       /Time-dependent data
Alexander.rpt       /Report data
Alexander(02).flo   /Flow output data
Alexander(02).sed   /Sediment output data
Alexander.rsr       /Restart-recovery data
Alexander.upp       /Upper coefficient matrix
Alexander.low       /Lower coefficient matrix
Alexander.scl       /Scalar output data
Alexander.vec       /Vector output data
Alexander.pro       /Profile output data
Alexander.sta       /Run status data
```

Figure 7-1. Contents of a *FST2DH* project file. Filenames are terminated before the forward slashes, which are followed by brief descriptions of the data files.

Input Data Files

Several data files may be read by *FST2DH* during a simulation. The number and type of input files depends on the information you need and how you organize your data. A control data file is needed for every simulation. All other input data files are optional. Input data files read by *FST2DH* are described briefly in the following sections. Detailed data format descriptions are presented in Appendix A.

Control Data File

All information needed to run *FST2DH* for an application can be entered in a control data file. However, because large amounts of data are usually required, control data files most often contain only program options, general parameter values, boundary conditions, and modifications to other data. Other input data are placed in separate files that are read by *FST2DH* as they are needed. These data include network geometry, initial flow and sediment transport solutions, boundary conditions, wind parameters, wave parameters, and time-dependent data.

Mesh Data File

Finite element mesh data consisting of two-dimensional node and element data, and one-dimensional node, element, and cross section data can be read from a mesh ata file. Although all mesh data can be entered in an application's control data file, the amount of information will typically be large. Therefore, the preferred approach to storing mesh data is to place them in a separate mesh data file.

Flow Data File

Flow data files contain depth-averaged flow solution values at node points. Flow solution values consist of water depth, depth-averaged velocities in the *x* and *y* coordinate directions, and time-derivatives of these quantities. Calculated flow variables are written to flow data files after the last iteration of steady-state solutions, and after the last iteration of selected time steps of time-dependent simulations. Time-derivatives are not written for steady-state simulations. *FST2DH* can read flow data files to obtain initial conditions. Flow data files may be created in either text or binary format.

Sediment Data File

Sediment data files contain depth-averaged sediment transport solution values at node points consisting of bed elevation, time-derivative of bed elevation, thicknesses of bed sediment layers (active, deposition, and original), number of particle size classes for which concentrations and composition fractions are provided, discharge-weighted concentrations by particle size class, time-derivatives of concentrations by particle size class, and bed layer fractional compositions by particle size class. Calculated sediment transport variables are written to sediment data files after the last iteration of selected time steps. *FST2DH* can read sediment data files to obtain initial sediment concentrations, bed-layer thicknesses, and bed-layer compositions. Sediment data files may be created in either text or binary format.

Boundary Condition Data File

Boundary condition data files contain specifications of water flow and sediment transport variables along finite element network boundaries. Data files for time-dependent simulations contain sequential specifications of updated boundary conditions. Boundary condition data files may be in either text or binary format.

Wind Data File

Wind data files contain wind speed and direction angle at all node points. Data files for time-dependent simulations contain sequential specifications of updated wind parameters. Wind data files may be created in either text or binary format.

Wave Data File

Wave data files contain wave height, period, and direction angle at all node points. Data files for time-dependent simulations contain sequential specifications of updated wave parameters. Wave data files may be created in either text or binary format.

Time-dependent Data File

Boundary, wind, and wave data may be updated periodically during time-dependent simulations. When reading from *FST2DH* control data files, all time-dependent data sets need to appear in chronological order at the end of the data streams. Optionally, these data sets can be placed in other files called *Time Data Files*. Time Data Files can be in only text format.

Output Data Files

Several output files may be created by *FST2DH* during a run. Only the report data file, coefficient matrix files, and run status data file are created automatically. All other output files are optional.

Report Data File

Report data files contain a printed reports of all control data, network data reports (optional), solution convergence parameters, and solution reports (optional). Several types of solution reports can be requested. Report data files are generated automatically; however, sizes of report data files can vary significantly depending on the optional items requested.

Flow Data File

Output flow data files contain the same data in the same format as input flow data files. They are optional, but will almost always be created during a simulation. Results from the final iteration of steady-state solutions, and the final iteration of selected time steps during time-dependent solutions, are saved to the data file in either binary or text format. Output flow data files can be used as input flow data files for subsequent runs.

Sediment Data File

Output sediment data files contain the same data in the same format as input sediment data files. They are optional, but will almost always be created during a sediment transport simulation. Results from the final iteration of selected time steps during time-dependent solutions are saved to the data file in either binary or text format. Output sediment data files can be used as input sediment data files for subsequent runs.

Restart-recovery Data File

Restart-recovery data files contain results from the last completed iteration only, and are overwritten at the end of each iteration. The files are used to store intermediate results that can be used to restart a solution in case calculations are halted by a power outage or some other reason. Use of restart-recovery files is optional, but might be of value when many iterations that require long computation times are needed to achieve solution convergence.

Upper and Lower Coefficient Matrix Files

The linear system of algebraic equations formed by applying the finite element method to the governing hydrodynamic and sediment transport equations are solved by a process known as Gaussian elimination. During the solution the coefficient matrix is factored into a product of upper and lower triangular matrices. Decomposition of the coefficient matrix is useful because the solution of triangular matrices is easily accomplished by successive substitution in the corresponding linear equations. Files are created automatically for each of the triangular matrices during a run. Because they can be used in subsequent runs if a modified-Newton iteration strategy is applied, upper and lower coefficient matrices can be saved as an option.

Scalar Data File

Many values having only magnitude, but not direction, can be calculated from the basic solution variables and other mesh parameters and be written to a scalar data file at the end run. Scalar data files can be read by the *Surface-water Modeling System (SMS)* pre-

and post-processing computer program (*SMS reference manual*, 2002) to display solution results.

Vector Data File

Several values having both magnitude and direction can be calculated from the basic solution variables and other mesh parameters and be written to a vector data file at the end run. Vector data files can be read by the *Surface-water Modeling System (SMS)* pre- and post-processing computer program (*SMS reference manual*, 2002) to display solution results.

Profile Data File

Profiles along designated lists of connected nodes can be calculated and stored at the end of a steady-state simulation, or at the end of printed time steps during unsteady flow and sediment transport simulations. Profile data files can be read directly by spreadsheet and other computer programs, and the data can be plotted to help illustrate the solution.

Run Status Data File

Solution convergence parameters are written to a run status data file at the end of every iteration during a run. You can read run status data files at any time during a run to check on convergence.

Running FST2DH from Microsoft Windows

FST2DH runs as a console application that does not require screen graphics output. It looks about the same whether run on a personal computer, a workstation, or a terminal connected to a mainframe computer. When running under the Microsoft Windows operating system (Figure 7-2), you can execute the program using the Windows Run command or by double-clicking the file in Windows Explorer. When using the Run command, you can include the name of the *FST2DH* project file on the command line separated from the executable file name by a space. *FST2DH* will prompt you for the

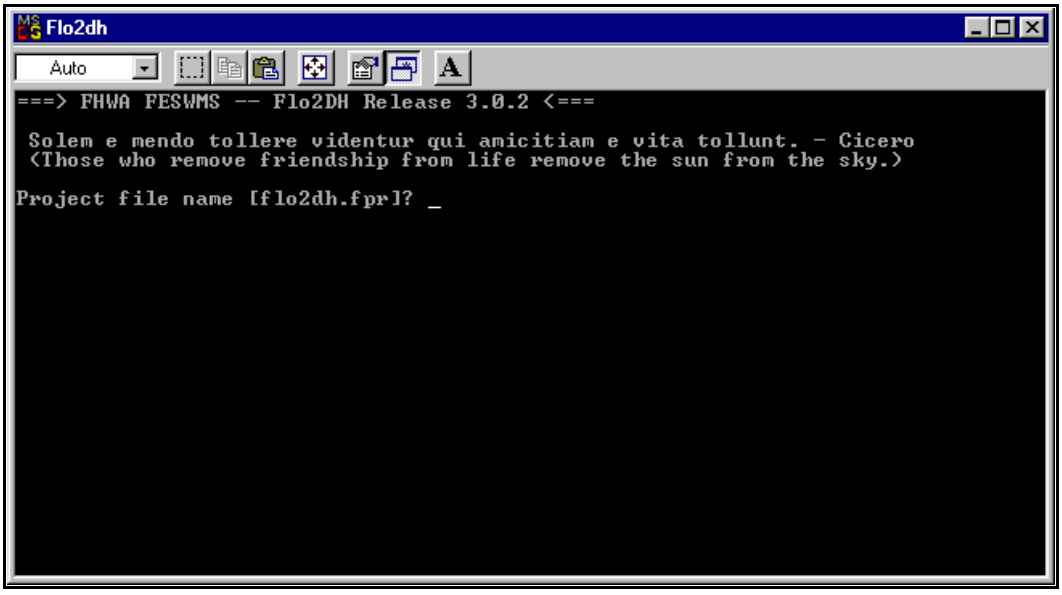

Figure 7-2. *FST2DH* runs under Microsoft Windows operating system as a console application. You will be prompted for the name of the *FST2DH* project file if you have not included it in the command line.

project file name if you do not enter one on the command line. The default project file name is shown in brackets.

Data Flow

The logical flow of data through *FST2DH* from the entry of input data to the generation of output data and the major functions of the program is illustrated in Figure 7-3. Program control data records are read first, and then network data, initial condition data, boundary condition data, and wind data files are read if needed. Any remaining input data records for an initial solution then are read. Data entered on data records will override information that was previously read from data files. Preliminary computations and an initial flow check are made next. A degree-of-freedom array that relates every nodal variable to an equation number is constructed, and solution parameters (number of equations, and maximum and root-mean-square frontwidth) are computed.

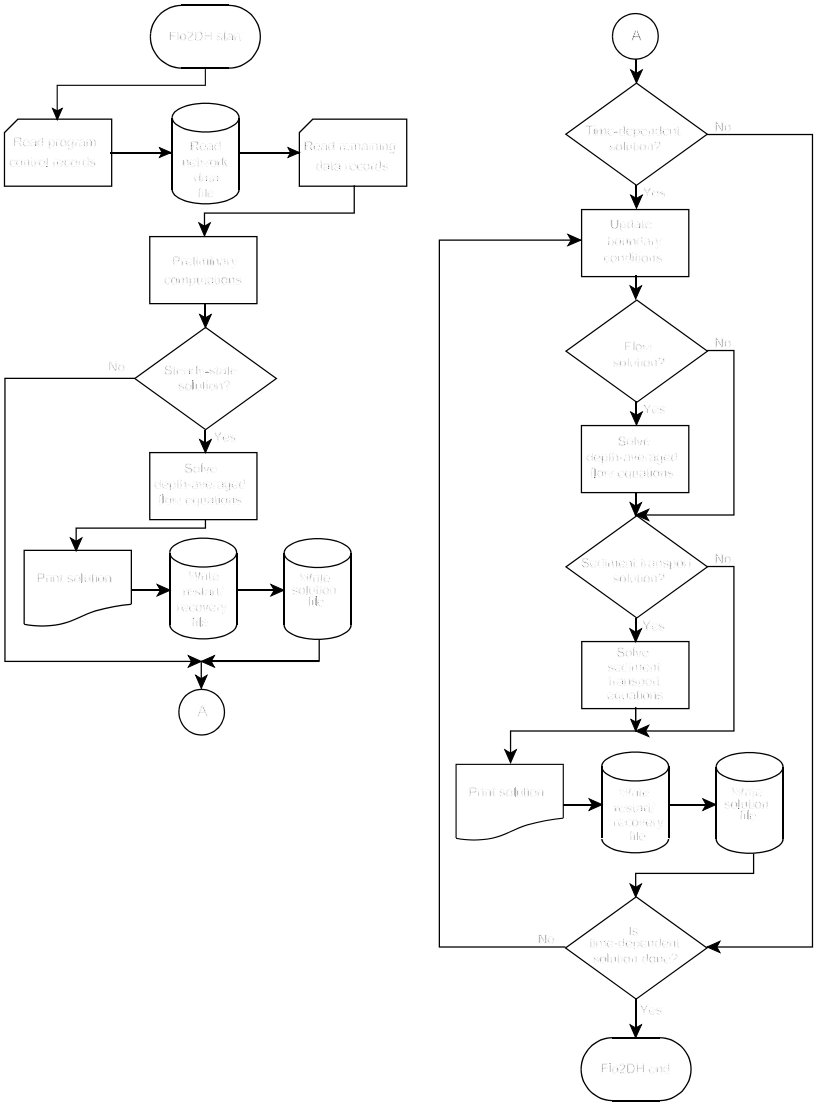

Figure 7-3. The logical flow of data through *FST2DH* and the major functions carried out by the program is shown in the diagram.

A steady-state solution is carried out next. Intermediate solution results are written to a restart/recovery file (if requested) after every iteration. If a run terminates abnormally, the run can be restarted using the intermediate results stored in a restart/recovery file. The computed flow data (depth-averaged velocities and the flow depths at node points) can be printed after selected iterations. The results of the final iteration of a steady-state solution are written to a flow data file. A flow check is made and element continuity norms are computed.

A time-dependent solution, if one is requested, follows. Preparations are made and boundary conditions are updated to the current time. Time-dependent data can be read from data records or from data files. If time-dependent data records are read, they need to be arranged in chronological order at the end of the input stream. Results can be printed at the end of every iteration or only at the end of selected iterations for every time step or only for selected time steps. Results are written to a flow data file at the end of each time step. Intermediate results are written to a restart/recovery file (if requested) at the end of every iteration. A flow check is made and element continuity norms are computed at the end of every time step.

Some Computational Aspects of *FST2DH*

Several computational aspects of *FST2DH* operation are discussed in this section including automatic boundary adjustment, assigning initial conditions, possible steps to take if you experience convergence problems, and assignment of boundary conditions.

Specifying Boundary Conditions

Boundary conditions need to be specified at all node points that form the boundary of a network. Slip, no-slip, or semi-slip conditions are specified automatically at all closed boundary node points of a network. Boundary conditions can be specified on open boundaries at each node or at groups of nodes that form a boundary cross section.

Boundary Conditions at Node Points

Water-surface elevation, velocity, unit flow rate, or total flow normal to a boundary are the values that can be specified as boundary conditions for flow solutions. Although all boundary conditions except total flow can be specified at any node point in a finite element network, generally boundary conditions will be specified only at node points that actually form part of the network boundary. The two types of boundaries (closed and open) and boundary conditions that are appropriate for each type of boundary are described in Chapter 3.

Codes are used to define the type(s) of boundary condition(s) that is (are) specified at a node point. Slip (tangential flow), no-slip (zero flow), or semi-slip (tangential shear stress) conditions can be applied automatically to all closed-boundary node points. Slip and no-slip conditions can be overridden by specifications in the boundary condition data set.

Special consideration needs to be given a node point where a closed boundary and an open boundary meet (a boundary interface node). Boundary type (closed or open) needs to change always at a vertex node and never at a midside node. If unit flow or velocity is specified at a boundary interface node, the resulting velocity vector needs to be parallel to the closed boundary. If a velocity vector at a boundary interface node is not parallel to the closed boundary, flow will "leak" into or out of the network depending on the direction of the vector. If water-surface elevation is specified at a boundary interface node, either a slip condition or a no-slip condition also needs to be specified, otherwise accidental "leaks" will exist along the closed boundary adjacent to the node.

Total flow normal to either a closed or an open boundary resulting from flow at a boundary node also can be specified. Prescribing total flow normal to a closed boundary can be used to simulate inflows from small tributaries or withdrawals at a point. Total flow normal to an open boundary is specified where major known inflows or outflows occur, such as at the upstream end of a river reach.

Total flow normal to both closed and open boundaries might need to be specified at a boundary interface node. If a non-zero flow normal to an open boundary is specified at a boundary interface node, and a slip condition is specified along the closed boundary, the velocity vector at the boundary interface node will be directed into the network parallel to the closed boundary.

Boundary Conditions at Cross Sections

Boundary conditions can be specified at cross sections that form part of an open boundary of a finite element network. Either total flow, water-surface elevation, or an invariant quantity that allows waves to pass through the boundary with essentially no reflection can be specified at a boundary cross section. Cross section boundary conditions are specified in the *BSEC* data set.

Total flow. An open boundary where total flow at a cross section is specified usually will represent the upstream end of a river/flood plain model where total flow has been measured. The specified total flow at a cross section is distributed among the nodes that define the cross section on the basis of conveyance. Positive flows represent inflows to a network, and negative flows represent outflows from a network.

Weakly-reflecting invariant. An open boundary through which long-period waves (such as those generated by tidal variation) can pass with minimal reflection can be used to represent the entrance of a river to an estuary. Since flow entering (or leaving) the network at such a boundary is affected by tidal conditions, it is not known in advance. However, flow conditions at a point far upstream in the river which is not tidally-influenced might be know and can be specified at the boundary in the form of an invariant quantity.

Water-surface elevation. A level or sloping water-surface elevation at a cross section that forms part of an open boundary of a network can be specified as a boundary condition. An open boundary where water-surface elevation at a cross section is specified usually will represent the downstream end of a river/flood plain model where high-water marks have been collected, or a channel in a model of a bay or estuary where stage has been recorded. The water-surface elevation may be specified directly, calculated using the slope-area method, or found from a rating-curve. If a level water-surface is specified, a single water-surface elevation and a boundary condition code need to be specified. Two elevations are needed to specify a sloping water-surface, one elevation at each end node of the cross section. Intermediate water-surface elevations along the cross section are interpolated based on a linear variation. If the slope-area method is used, the total flow rate through the section and the total energy slope need to be specified along with the boundary condition code that will be assigned to each node point of the cross section, and the calculated elevation is applied to all node points of the cross sections (that is, a level water surface is assigned). If a rating-curve is used, a tabular relation between the water-surface elevation and the flow rate needs to be defined using the *RATE* data set.

Assigning Initial Conditions

Initial conditions (that is, starting values) need to be specified at each node point in an active network at the beginning of a run. Initial conditions consist of depth-averaged velocities in the x and y directions and flow depth (water-surface elevation minus ground-surface elevation) at vertex nodes, just depth-averaged velocities at midside and

center nodes, and time-derivatives of each of the variables if the simulation is time-dependent (unsteady).

Cold Starts

Estimating reasonable starting values if a solution has not been obtained previously might at first seem to be a difficult or an impossible task. However, a cold start procedure can be used whereby a constant water-surface elevation and zero velocities are assigned. A cold start is the only practical way of beginning a simulation on a new network.

During a cold start, the water-surface elevation is initially constant, and velocities are set to zero at all node points. A constant water-surface elevation is specified in the *SWMS* data set on the system-parameters record (*SWMS.5*). Because *FST2DH* solves for depth of flow, the ground-surface elevation is subtracted from the constant water-surface elevation to obtain the depth of flow at all vertex nodes. A constant water-surface elevation can be overridden at any node point by specifying a water-surface elevation as an initial condition at that node point. Initial velocities at node points are considered always to equal zero unless an initial condition value is specified.

When starting cold, the initial constant water-surface elevation needs to be greater than the ground-surface elevation at the node points where boundary conditions are to be specified. Usually computations will need to be started using an initial water surface that is much higher than the final solution water surface at most node points in the finite element network. Dry elements are permitted to exist in a network if the boundary of the network is adjusted automatically. If the boundary of a network is not adjusted automatically to account for dry elements, all active elements in the network always need to be wet (that is, have positive flow depths at all node points).

Hot Starts

A solution from a previous run can be used to assign initial conditions for a subsequent run. This way of specifying initial conditions is referred to as a hot start. Because computed velocities and depths usually are written to a data file, a flow data file from a run can thus become an initial condition data file for a subsequent run.

Achieving Convergence

A solution might not converge if the initial conditions are not sufficiently close to the true solution, regardless of the type of start. If a cold start is attempted and convergence problems develop, the difference between specified boundary conditions and the initial conditions is probably too great. The relaxation factor, ω, can be decreased so that the solution change from one iteration to the next will be reduced. Try setting l equal to 0.5 or less for a few iterations if solution convergence is a problem.

Another way of solving a convergence problem is to temporarily increase kinematic eddy viscosity to a large value. Large eddy viscosities encourage solution convergence because of their dissipative effect when velocity gradients are large. Large values of eddy viscosity probably need to be maintained for two or three iterations before they are reduced to physically appropriate values.

If convergence problems persist and a plot of the finite element network has been inspected carefully for geometric inconsistencies, then the network probably needs to be refined. Areas in need of refinement probably will be located where velocities and variations in velocities are extremely large, such as near constrictions (bridge openings).

Incremental Load Strategy

Convergence can often be obtained for difficult problems by gradually increasing inflow rates or gradually lowering a downstream water-surface elevation, the hydraulic

"loads" acting on a model, beginning from some "known" solution. Indeed, "cold starts" are known solutions, with level water surfaces and no motion throughout a mesh. By choosing suitably small increments of the loads, convergence can usually be assured and results of a reasonable kind will generally be available. Furthermore, the intermediate results often provide useful information. You can implement an incremental loading strategy automatically using the *LOAD* data set. An incremental-load data set immediately precedes boundary condition data that are changed in an incremental fashion in the course of achieving solution convergence. Incremental load data sets are needed for each set of data changes you want to make, the data sets forming *load data packets*.

Continuity Norms

A potential problem caused by the use of mixed interpolation (that is, linear interpolation of depth and quadratic interpolation of velocities) is that mass conservation is not well enforced because the ratio of discrete continuity constraints to discrete momentum equations is much smaller than the continuum ratio of 0.5. Computing the mass flux at model cross sections in steady-state simulations is one method for determining whether mass conservation errors are within acceptable limits. At cross sections where the mass flux differs substantially from the inflow, the finite element network can be refined to reduce the errors. An even better way to determine which parts of a network can be refined to improve mass conservation is to compute a continuity norm for each element in the network.

Letting R_H denote the continuity equation residual,

$$R_H = \frac{\partial H}{\partial t} + \frac{\partial q_1}{\partial x} + \frac{\partial q_2}{\partial y} \tag{7-1}$$

the continuity norm for an element, N_e , is computed as

$$N_e = \frac{1}{A_e}\left(\int_{A_e} R_H^2 \, dA_e \right)^{1/2} \tag{7-2}$$

where A_e = element area. Continuity norms will be large for elements in which continuity equation residuals are large. Calculation of continuity norms is optional. Continuity norms greater than a specified value are flagged with an asterisk in the printed output so that elements that need to be refined to obtain a more accurate solution can be identified easily.

Automatic Boundary Adjustment

Automatic boundary adjustment in *FST2DH* allows elements that are not covered completely by water to exist in a finite element network. If the boundary is not allowed to adjust automatically then all nodes in a network need to be "wet" at all times (that is, water depth always needs to be greater than zero at a node point) otherwise computational problems will result when a node becomes "dry" (that is, when water depth becomes less than or equal to zero). A conceptually simple algorithm is used to determine automatically the boundary of a finite element network so that no dry nodes exist. The procedure excludes from an active network all elements that are connected to one or more dry node points.

To explain how the algorithm determines whether or not an element is to be included in an active network, several terms need to be defined. An element is said to be "on" if it is included in the active network, and is said to be "off" if it is not included. A "dry" element is an element that is connected to at least one node point that is dry. A "wet" element is an element in which all node points are wet.

At the beginning of each iteration, every element that is currently on is checked to find out if it is dry. If found to be dry, the element is turned off. In addition, each element that is currently off is checked to determine if it can be turned on. The decision to turn on an element is based on the minimum water depth at wet nodes and the maximum ground-surface elevation at the dry node points connected to the element. If the minimum water-surface elevation is greater than the maximum ground-surface elevation, plus a small depth tolerance, the element is turned on. The need for a depth tolerance is twofold. First, because of friction losses, there probably will be some change in the water-surface elevation across an element when it is turned on. Second, the condition of an element (wet or dry) can oscillate from one iteration to the next, and cause the solution to converge slowly or not at all. A depth tolerance of 0.5 feet (0.15 meters) has been found to provide good results and is the default value used in *FST2DH*. However, the best depth tolerance to use will depend on the size of the elements in a network, and on the flow conditions.

It is possible that an element that would actually be wet is turned off in the final solution. However, the depth of flow in the element would be small, and the effect of not including the element in the active network would be negligible. The possibility of a wet element being turned off in a final solution can be minimized by constructing smaller elements in areas where the active network boundary is expected to occur.

The automatic boundary-adjustment feature allows a finite element network to be designed without too much concern for the location of boundaries. However, ground-surface elevations still need to be assigned carefully. If the automatic boundary-adjustment feature is used and a high node point (located on a channel bank in the middle of a flood plain, for example) becomes dry, all the elements connected to that node point will be turned off for the next iteration. Removal of a large number of elements from an active network could affect significantly the solution unless all the elements turned off were quite small.

Either slip or no-slip conditions (as specified by a user) are applied automatically at all existing or newly created boundary nodes. However, if a velocity, unit flow rate, or depth boundary condition is specified at a node point that is eliminated from an active network, and the node later is readmitted to the active network, the boundary conditions that were specified for that node will not be applied again. If a velocity, unit flow rate, or water-surface elevation is specified at a node, a user needs to be certain that the node will not be removed from the active network even temporarily.

8. References

Ackers, P, and White, W. R. (1973). "Sediment transport: new approach and analysis." *Journal of the Hydraulics Division, ASCE*, 99(HY11), 2041-2060.

Alonso, C. V., Neibling, W. H., and Foster, G. R. (1981). "Estimating sediment transport capacity." *Transactions of the ASAE*, 24(5), 1211-1220.

American National Standards Institute (1978). *American National Standard Programming Language FORTRAN, ANSI X3.9-1978*.

Arcement, G. J., and Schneider, V. R. (1984). "Guide for selecting Manning's roughness coefficients for natural channels and flood plains." *Report No. FHWA-TS-84-204*, Federal Highway Administration, McLean, Virginia.

Armanini, A., and Di Silvio, G. (1988). "A one-dimensional model for transport of a sediment mixture in non-equilibrium conditions." *Journal of Hydraulic Research*, 26(3), 275-292.

Barnes, H. H., Jr. (1967). "Roughness characteristics of natural channels." *U.S. Geological Survey Water-Supply Paper 1849*, Washington, D.C.

Bennett, J. P., and Nordin, C. F. (1977). "Simulation of sediment transport and armouring." *Hydrological Sciences Bulletin*, 22(4), 555-569.

Bijker, E. W. (1966). "Erosion around a pile due to current and breaking waves." *Proceedings of the 10th International Conference on Coastal Engineering*, American Society of Civil Engineers, New York, NY, 746-765.

Bijker, E. W. (1967). "Some considerations about scales for coastal models with movable bed." *Publication No. 50*, Delft Hydraulics Laboratory, Delft, Netherlands.

Bijker, E. W., and de Bruyn, C. A. (1988). "Erosion around a pile due to current and breaking waves." *Proceedings of the 21st International Conference on Coastal Engineering*, American Society of Civil Engineers, New York, NY, 1369-1381.

Bodhaine, G. L. (1968). "Measurement of peak discharge at culverts by indirect measurements." *U.S. Geological Survey Techniques of Water Resources Investigations, Book 3, Chapter A3*, Washington, D.C.

Bradley, J. N. (1978). "Hydraulics of bridge waterways (2nd ed.)." *Federal Highway Administration Hydraulic Design Series, No. 1*.

Buell, W. R., and Bush, B. A. (1973). "Mesh generation -- a survey." *Transactions of the American Society of Mechanical Engineers, Journal of Engineering for Industry, ser. B.*,95(1), 332-338.

Chaudhry, M. H. (1993). *Open-channel flow*. Prentice Hall, Englewood Cliffs, New Jersey.

Chen, Y. H., and Cotton, G. K. (1988). "Design of roadside channels with flexible linings." *Publication No. FHWA-IP-87-7, Hydraulic Engineering Circular No. 15,* Federal Highway Administration, McLean, Virginia.

Chow, V. T. (1959). *Open-channel hydraulics.* McGraw-Hill, New York, New York.

"Coastal flooding hurricane surge model - volume 1, methodology." (1988). *FEMA Report,* Federal Emergency Management Agency, Office of Risk Assessment, Federal Insurance Administration, Washington, D.C.

Corry, M. L., Thompson, P. L., Watts, F. J., Jones, J. S., and Richards, D. L. (1983). "Hydraulic design of energy dissipaters for culverts and channels." *Hydraulic Engineering Circular No. 14*, Federal Highway Administration, Washington, D.C.

Cunge, J. A., Holly, F. M., and Verwey, A. (1980). *Practical aspects of computational river hydraulics*. Pitman, Boston.

Deigarrd, R., Bro Mikkelson, M., and Fredsøe, J. (1991). "Measurements of the bed shear stress in a surf zone." *Progress Report 73*, Institute of Hydrodynamic and Hydraulic Engineering, Technical University of Denmark, Lyngby, Denmark.

Defina, A., D'Alpaos, L., and Matticchio, B. (1994). "A new set of equations for very shallow water and partially dry areas suitable to 2D numerical models." In *Modelling of Flood Propagation Over Initially Dry Areas*, P. Molinaro and L. Natale (eds.), Proceedings of the Specialty Conference held in Milan, Italy, June 29-July 1, 1994, American Society of Civil Engineers, New York, New York.

"Design and construction of urban stormwater management systems." (1996). *Manuals and Reports of Engineering Practice No. 77*, American Society of Civil Engineers, New York, New York.

Dyer, K. R. (1986). *Coastal estuarine sediment dynamics*. John Wiley & Sons, Chichester, England.

Edge, B. L., Scheffner, N. W., Fisher, J. S., and Vignet, S. N. (1998). "Determination of Velocity in Estuary for Bridge Scour Computations." *Journal of Hydraulic Engineering*, 124(6), 619-628.

Engelman, M. S., Strang, G., and Bathe, K.-J. (1981). "The application of quasi-Newton methods in fluid mechanics." *International Journal for Numerical Methods in Engineering*, 17(5), 707-718.

Engelund, F. and Hansen, E. (1967). *A monograph on sediment transport in alluvial streams*. Teknisk Vorlag, Copenhagen, Denmark.

Fischer, H. B., List, E. J., Koh, R. C. Y., Imberger, J., and Brooks, N. H. (1979). *Mixing in inland and coastal waters.* Academic Press, New York.

Foster, G. R. (1982). "Modeling the erosion process." Chapter 8 in *Hydrologic modeling of small watersheds*, C. T. Haan, H. P. Johnson, and D. L. Brakensiek, eds., American Society of Agricultural Engineers, St. Joseph, Michigan.

Froehlich, D. C. (1988). "Analysis of on-site measurements of scour at piers." *Proceedings of the 1988 National Conference on Hydraulic Engineering*, Colorado Springs, Colorado, August 15-19, 1988, American Society of Civil Engineers, New York, NY, 826-831.

Froehlich, D. C. (1989). "Local scour at bridge abutments." *Proceedings of the 1989 National Conference on Hydraulic Engineering*, New Orleans, Louisiana, August 14-18, 1989, American Society of Civil Engineers, New York, NY, 13-18.

Garbrecht, J., Kuhnle, R. A., and Alonso, C. V. (1995). "A sediment transport capacity formulation for application to large channel networks." *Journal of Soil and Water Conservation*, 50(5), 527-529.

Garratt, J. R. (1977). "Review of drag coefficients over oceans and continents." *Monthly Weather Review*, 105(7), 915-929.

"Handbook of channel design" (1954). *Publication No. SCS-TP-61*, U.S. Soil Conservation Service, Stillwater Outdoor Hydraulic Laboratory, Stillwater, Oklahoma.

Hicks, B. B. (1972). "Some evaluations of drag and bulk transfer coefficients over water bodies of different sizes." *Boundary-Layer Meteorology*, 3(1), 201-213.

Hicks, B. B., Drinkrow, R. L., and Grauze, G., (1974). "Drag and bulk transfer coefficients associated with a shallow water surface." *Boundary-Layer Meteorology*, 6(1), 287-297.

"Highway drainage guidelines." (1992). American Association of State Highway Officials, Inc., Washington, D. C.

Ho, F. P., Su, J. C., Hanevich, K. L., Smith, R. J., and Richards, F. (1987). "Hurricane climatology for the Atlantic and Gulf coasts of the United States." *NOAA Technical Report NWS-38*, National Weather Service, National Oceanic and Atmospheric Administration, Washington, D.C.

Hood, P. (1976). "Frontal solution program for unsymmetric matrices." *International Journal for Numerical Methods in Engineering*, 10(2), 379-399.

Hood, P. (1977). "Note on frontal solution program for unsymmetric matrices." *International Journal for Numerical Methods in Engineering*, 11(6), 1055.

Hulsing, Harry (1976). "Measurement of peak discharge at dams by indirect method." *Techniques of Water-Resources Investigations of the U.S. Geological Survey, Book 3, Chapter A5*, Washington, D. C.

Jansen, P. P., van Bendegom, L., van den Berg, J., deVries, M., and Zanen, A. (1979). *Principles of river engineering -- the non-tidal alluvial river*. Pittman, London.

Kaplan, J., and DeMaria, M. (1995). "A simple empirical model for predicting the decay of tropical cyclone winds after landfall." *Journal of Applied meteorology*, 34(11), 2499-2512.

King, H. W., and Brater, E. F. (1963). *Handbook of hydraulics (5th ed.)*. McGraw-Hill, New York, New York.

King, I. P., and Norton, W. R. (1978). "Recent applications of RMA's finite element models for two-dimensional hydrodynamics and water quality." in Brebbia, C. A., Gray, W. G., and Pinder, G. F. (eds.), *Finite Elements in Water Resources*, Proceedings of the 2nd International Conference on Finite Elements in Water Resources, London, 1978, Proceedings, London, Pentech Press, 2.81-2.99.

Kraus, N. C., and Horikawa, K. (1990). "Nearshore sediment transport." *The Sea, Vol. 9B: Ocean Engineering Science*, B. Le Mehauté, and D. Hanes (eds.), 775-814, John Wiley and Sons, New York, NY.

Laursen, E. M. (1958). "The total sediment load of streams." *Journal of the Hydraulics Division, ASCE*, 84(HY1).

Longuet-Higgins, M. S. (1970). "Longshore currents generated by obliquely incident sea waves." *Journal of Geophysical Research*, 75, 6778-6801.

Lee, J. K. and Froehlich, D. C. (1986). "Review of literature on the finite-element solution of the equations of two-dimensional surface-water flow in the horizontal plane." *U.S. Geological Survey Circular 1009*, Washington, D. C.

MacCurdy, Edward (1938). *The notebooks of Leonardo DaVinci*, Reynal and Hitchcock, New York.

Madsen, P. A., Sørenson, O. R., and Schäffer, H. A. (1997). "Surf zone dynamics simulated by a Boussinesq type model. Part I. Model description and cross-shore motion of regular waves." *Coastal Engineering*, 32(3), 255-287.

McDowell, D. M., and O'Connor, B. A. (1977). *Hydraulic behavior of estuaries*. John Wiley and Sons, New York, New York.

Meyer-Peter, E., and Mueller, R. (1948). "Formula for bed-load transport." *Proceedings of the 2nd International Conference of the International Association for Hydraulic Research*, Stockholm, Sweden.

Nielson, P. (1992). *Coastal bottom boundary layers and sediment transport. Advanced series on ocean engineering, Vol. 4*. World Scientific Publishing, Singapore.

Normann, J. M., Houghtalen, R. J., and Johnston, W. J. (1985). "Hydraulic design of highway culverts." *Hydraulic Design Series No. 5, Report No. FHWA-IP-85-15*, Federal Highway Administration, Washington, D.C.

Novak, P., Moffat, A. I. B., Nalluri, C., and Narayanan, R. (1996). *Hydraulic structures, (2nd ed.)*, E & FN Spon, London, United Kingdom.

Raudkivi, A. J. (1990). *Loose boundary hydraulics*. Pergamon Press, Oxford, England.

Richardson, E. V. and Davis, S. R. (1995). "Evaluating scour at bridges." *Publication No. FHWA-IP-90-017, Hydraulic Engineering Circular No. 18, 3rd ed.*, Federal Highway Administration, U.S. Department of Transportation, McLean, Virginia.

"Roadway and traffic design standards for design, construction, maintenance and utility operations on the state highway system." (1998). Florida Department of Transportation, Tallahassee, Florida.

Rodi, Wolfgang (1982). "Hydraulics computations with the k-ε turbulence model." in Smith, P. E., ed., *Applying Research to Hydraulic Practice*, Proceedings of the Conference of the Hydraulics Division of the American Society of Civil Engineers, Jackson, Miss., 1982, 44-54.

Scheffner, N. W., Mark, D. J., Blain, C. A., Westerink, J. J., and Luettich, R. A., Jr. (1994). "A tropical storm data base for the east and Gulf of Mexico coasts of the United States," *Technical Report*, U.S. Army Corps of Engineers, Coastal Engineering Research Center, Vicksburg, Mississippi.

Sedimentation engineering (1975). Vito A. Vanoni (ed.), Manuals and reports on Engineering Practice No. 54, American Society of Civil Engineers, New York, New York.

Shirole, A. M., and Holt, R. C. (1991). "Planning for a comprehensive bridge safety assurance program." *Transportation Research Record No. 1290, Volume 1*, National Research Council, Washington, D.C., 39-50.

Smagorinsky, J. (1963). "General circulation experiments with the primitive equations, I. The basic experiment." *Monthly Weather Review*, 91(2), 99-164.

SMS (Surface Water Modeling System) reference manual, version 8.0 (2002). Brigham Young University, Engineering Computer Graphics Laboratory, Provo, Utah.

Sokolnikoff, I. S., and Redheffer, R. M. (1966). *Mathematics of physics and modern engineering (2nd ed.)*. McGraw-Hill, New York.

"Some fundamentals of particle size analysis: a study of methods used in measurement and analysis of sediment loads in streams." (1957). *Report No. 12*, Subcommittee on Sedimentation, Interagency Committee on Water Resources, Saint Anthony Falls Hydraulic Laboratory, Minneapolis, Minnesota.

Soulsby, R. L. (1997). *Dynamics of marine sands*. Thomas Telford, London, England.

Stevens, H. H., and Yang, C. T. (1989). "Summary and use of selected fluvial sediment-discharge formulas." *U.S. Geological Survey Water Resources Investigation Report 89-4026*, Denver, Colorado.

Strang, G., and Fix, G. J. (1973). *An analysis of the finite element method*. Prentice-Hall, Englewood Cliffs, New Jersey.

Temple, D. M., Robinson, K. M., Ahring, R. M., and Davis, A. G. (1987). "Stability design of grass-lined open channels." *Agricultural Handbook No. 667*, U.S. Department of Agriculture, Washington, D.C.

Wang, J. D., and Connor, J. J. (1975). "Mathematical modeling of near coastal circulation." *Ralph M. Parsons Laboratory for Water Resources and Hydrodynamics Report No. 200*, Massachusetts Institute of Technology, Department of Civil Engineering, Cambridge, Massachusetts.

White, W. R., and Day, T. J. (1982). "Transport of graded gravel bed material." in *Gravel Bed Rivers*, R. D. Hey, J. C. Bathurst, and C. R. Thorne (eds.), John Wiley and Sons, Chichester, United Kingdom, 181-223.

Yalin, M. S. (1964). "Geometrical properties of sand waves." *Journal of the Hydraulics Division, ASCE*, 90(HY5), 105-119.

Yang, C. T. (1972). "Unit stream power equation and sediment transport." *Journal of the Hydraulics Division, ASCE*, 98(HY10), 1805-1826.

Yang, C. T. (1973). "Incipient motion and sediment transport." *Journal of the Hydraulics Division, ASCE*, 99(HY10), 1679-1704.

Yang, C. T. (1984). "Unit stream power equation for gravel." *Journal of Hydraulic Engineering*, 110(12), 1783-1797.

Zienkiewicz, O. C. (1977). *The finite element method (3rd ed.)*. McGraw-Hill, London, England.

Zienkiewicz, O. C., and Taylor, R. L. (1991). *The finite element method (4th ed.), volume 2, solid and fluid mechanics, dynamics, and non-linearity*. McGraw-Hill, London, England.

Appendix A - FST2DH Input Data

Introduction

Data files and formats of data needed to run *FST2DH* are described in this Appendix. The primary data file, called the *control data file*, contains, at a minimum, basic information needed to operate *FST2DH,* including parameters that control reading and writing of auxiliary data files. While all input data can be placed in an application's control data file, data for ordinary applications will likely be stored in one or more additional files. Some input and output data files may be in either text or binary format.

List-directed Input

*A*ll data contained in text files are read using list-directed, sequential read statements that translate data from character to binary form using the data types of the corresponding input/output (I/O) list items to decide the forms of the data. Translated data are then assigned to the entities in the I/O list in their order of appearance, from left to right.

Both numeric values and text strings need to be separated. Separators may be any number of blank spaces, or a single comma preceded or followed by any number of blank spaces. Text strings need delimiting double quotation marks (for example, "text string") if they contain blank spaces, commas, or slash marks. Unless noted otherwise, nondelimited text strings are terminated by the first blank, comma, slash, or end-of-record encountered. Apostrophes and quotation marks within nondelimited text strings are transferred just as they are.

Unless specified otherwise, default values of all optional numeric values are zero. All unspecified text strings default to a blank string.

FST2DH Project File

A *FESWMS* project consists of files containing an application's associated data. You can specify names of files from which data are read and to which data are written by *FST2DH* in a *FESWMS* project file. *FST2DH* will prompt you for the name of the project file at the start of a simulation. Default data file names will be used if you do not enter a project file name. Project files contain the program name (*FST2DH*) and release number followed by the names of all data files used by *FST2DH* listed in the specified order given in Table A-1. The default name of a *FESWMS* project file is "feswms.fpr".

Table A-1. FST2DH Data Files

File order[a]	Data file description	Data file type	Default file name
1	FST2DH control data file	Input	FST2DH.dat
2	Mesh (network) data	Input	FST2DH.msh
3	Flow data[b] (initial)	Input	FST2DH.flo
4	Sediment data[c] (initial)	Input	FST2DH.sed
5	Boundary condition data	Input	FST2DH.bcs
6	Wind data	Input	FST2DH.wnd
7	Wave data	Input	FST2DH.wve
8	Time data	Input	FST2DH.tim
9	Printed reports	Output	FST2DH.rpt
10	Flow data (output)	Output	FST2DH.flo
11	Sediment data (output)	Output	FST2DH.sed
12	Restart/recovery data	Output	FST2DH.rsr
13	Upper coefficient matrix	Output	FST2DH.upp
14	Lower coefficient matrix	Output	FST2DH.low
15	Scalar data	Output	FST2DH.scl
16	Vector data	Output	FST2DH.vec
17	Profile data	Output	FST2DH.pro
17	Run status file	Output	FST2DH.sta

[a]Order in which file names need to appear in *FST2DH* project data files.
[b]Flow initial data files are usually flow solution files generated by previous runs.
[c]Sediment initial data files are usually solution files generated by previous runs.

FST2DH Control Data File

Control data files for *FST2DH* are text files containing all or part of the information needed to carry out depth-averaged flow and sediment transport simulations. Data are grouped in sets of related information. Each data set consists of one or more data records. The first record in a data set contains a mnemonic code that identifies the data set. Some data records and sequences of data records are repeated as many times as needed within data sets. All of the data sets read by *FST2DH* are listed in Table A-2 and are described in detail in following sections.

Table A-2. *FST2DH* Data Sets

Data set name (mnemonic identifier)	*Data description*
SWMS[a]	Program control data
MEMO	Memo data.
NODE	Node data
ELEM	Element data
PROP	Element properties set data
NODE1D	Node data (one-dimensional flow)
ELEM1D	Element data (one-dimensional flow)
XSEC1D	Cross section data (one-dimensional flow)
COND1D	Closed-conduit cross section data (one-dimensional flow)
FLOW	Flow initial condition data
BOUN	Boundary condition data
BSEC	Boundary cross section data
WIND	Wind data
WAVE	Wave data
CYCL	Tropical cyclone data
SURGE	Storm surge data
WEIR	Weir segment data
CULV	Culvert data
GATE	Gate structure data
DROP	Drop inlet spillway data
LINK	Channel link data
RATE	Rating curve data
PIER	Bridge pier data
FLUX	Flux (water flow or sediment flow) check data
GAGE	Gage data
SEDI	General sediment data.
BEDS	Bed sediment composition initial data
SEDC	Sediment concentration initial data
RESE	Element resequencing data
PROF	Profile data
LOAD[b]	Incremental load data
TIME[c]	Time-dependent data
LAST[d]	Last record in the data stream

[a]Needs to be the first data set in the file.
[b] Incremental load data sets need to appear in sequential order at the end of the input data stream and prior to time-dependent data sets.
[c] Time-dependent data sets need to appear in chronological order at the end of the file.
[d] Needs to be the first data set in the input data stream.

First Record

The first record of the *FST2DH* control data file needs to contain the model name and version number as follows:

FST2DH,3

Comment Records

Data records in the control data file having an asterisk or an exclamation point ("*" or "!") as the first character are regarded as comments and are not processed. Comment records may be placed anywhere within the data file.

Program Control Data Set

Program control data records immediately follow an SWMS data set identification record. The identification record contains the data set identifier and a code that controls the format of printed output. The other eight records of the data set contain information that controls the overall operation of the program. Record 1 contains the project title used in printed output headings; Record 2 contains run option codes; Record 3 contains input/output file specifications; Record 4 contains iteration control parameters; Record 5 contains time-step parameters used in time-dependent solutions; Record 6 contains general system specifications; Record 7 contains general wind stress parameters; and Record 8 contains finite element network orientation data.

SWMS Identification Record

Order	*Value*	*Description*
1	"SWMS"	Data set identifier.
2	0 or 1	Printed output code: 0 = Printed output will be 80 columns wide. 1 = Printed output will be 132 columns wide.
3	0 or 1	Interactive message code: 0 = Messages that describe program operations will be written to the screen during program execution. 1 = No messages will be written to the screen during program execution.
4	+	Number of beeps to be sounded at the completion of a run. Maximum = 10. Default = 0.
5	0 or 1	Restart/recovery code: 0 = A normal steady-state or time- dependent solution is to be carried out. 1 = A restart/recovery run is to be carried out. Initial conditions will be read from a restart/recovery file "FST2DH.rsr".

SWMS.1 Record

1	"text"	Project stamp (32 characters maximum). This text string will be written as a heading to all output data files generated by *FST2DH*, and will need to be matched by headings of all input data files read by *FST2DH* to assure consistency of finite element network and solution data.

SWMS

Order	*Value*	*Description*
2	"text"	Variant description used to describe differences in boundary conditions and other factors from other simulations using the same network data (48 characters maximum).

SWMS.2 Record

1	0 to 2	Solution type option code as follows: 0 = A flow solution only will be carried out. 1 = A time-dependent sediment transport solution only will be carried out. Flow data from a previous simulation will be used to drive sediment movement. 2 = A time-dependent, semi-coupled flow and sediment transport solution will be carried out. Hydrodynamic equations and sediment transport equations will be solved sequentially at each time step.
2	0 to 511	Sum of the codes of the following printed output options that are desired.

Code	*Option Description*
0	Control data, error messages, and solution results will be printed.
1	All input data read from data records will be echo printed.
2	Element and node data will be printed.
4	Initial condition data will be printed.
8	Element assembly sequence will be printed.
16	Degree-of-freedom array that contains equation numbers that correspond to each nodal variable will be printed.
32	Scalar data consisting of water-surface elevation, water depth, velocity magnitude, Froude number, mechanical energy head (that is, potential head plus kinetic head) elevation, average bed shear stress magnitude, and vorticity magnitude at node points will be printed at the end of a steady-state solution and at the end of each printed time step of a time-dependent solution.
64	Vector data consisting of velocity, unit flow rate, and bed shear stress at node points will be printed at the end of a steady-state solution and at the end of each printed time step of a time-dependent solution.

Order	*Value*	*Description*
		128 Local scour depth at bridge piers will be calculated and printed at the end of a steady-state solution and at the end of each time step. General clear-water scour at piers will also be calculated and total scour depths printed.
		256 General clear-water scour will be calculated at all node points and printed at the end of a steady-state solution and at the end of each time step.
3	0 or 1	Computational units option code as follows:
		0 = US customary units will be used in all computations and for printed output.
		1 = International System (SI) units will be used in all computations and for printed output.
4	0 or 1	Bed shear stress formula option code as follows:
		0 = Bed shear stresses will be calculated using the Manning formula. All flow resistance coefficients specified in the PROP data set will be considered Manning roughness coefficients.
		1 = Bed shear stresses will be calculated using the Chézy formula. All flow resistance coefficients specified in the PROP data set will be considered Chézy discharge coefficients.
5	0 to 2	Wind shear stress option code as follows:
		0 = Wind-induced surface stresses will not be considered.
		1 = General wind parameters or wind parameters read from the WIND data set or wind data file will be used to calculate wind-induced surface stresses.
		2 = A tropical cyclone windfield will be simulated using parameters specified in the STORM data set.
6	0 or 1	Wave-induced bed shear stress option code as follows:
		0 = Wave-induced bed stresses will not be considered.
		1 = General wave parameters or wave parameters read from the WAVE data set or wave data file will be used to calculate wave-induced bed stresses.
7	0 to 2	Closed boundary condition option code as follows:

SWMS

Order *Value* *Description*

0 = Slip (tangential flow/zero tangential shear) conditions will be applied automatically to all closed boundary nodes.

1 = No-slip (zero flow) conditions will be applied automatically to all closed boundary nodes.

2 = Semi-slip (tangential flow/tangential wall shear)

Slip conditions are appropriate for most river and floodplain networks where physical boundaries are formed by the edges of floodplains or sloped embankments. Semi-slip conditions might be best where the boundary is formed by a vertical or nearly vertical wall.

8 0 to 2 Numerical integration option code as follows:

0 = Low-order numerical integration will be used on all elements.

1 = High-order numerical integration will be used on all curve-sided elements.

2 = High-order numerical integration will be used on all elements.

9 0 to 3 Sum of the codes of the following continuity norm options that are desired.

Code	*Option Description*
0	Continuity norms will not be computed.
1	Continuity norms will be computed at the end of a steady-state solution.
2	Continuity norms will be computed at the end of every time-step of a time-dependent solution.

10 0 or 1 Element on/off option code as follows:

0 = Elements will be turned on and off during a run.

1 = Elements will *not* be turned on and off during a run. If water-surface elevation falls below the elevation of the bed at any node computations will be halted.

Automatic boundary adjustment allows elements that are not covered entirely by water to be included in a network. If used, all elements that are found to have at least one *dry* node point will be excluded from the *active* network. A dry node point has a calculated water surface elevation that is lower than the *effective* bed

Order	*Value*	*Description*
		elevation. Effective bed elevations are found from the *fixed* bed elevation at a node and the assigned *flow storativity depth*, described in the PROP data set.
11	0 or 1	Solution matrix option code as follows: 0 = Files that contain the upper and lower decompositions of the coefficient matrix will be deleted at the end of a run. 1 = Files that contain the upper and lower decompositions of the coefficient matrix will be saved at the end of a run.
12	0 or 1	Network geometry check option code as follows: 0 = Network geometry will not be checked. 1 = Network geometry will be checked for consistency and completeness at the start of a solution.
13	0 to 2	Element resequencing option code as follows: 0 = Element resequencing will not be carried out. 1 = Element resequencing will be carried out only at the start of a solution. 2 = Element resequencing will be carried out at the start of a solution and after every iteration during which at least one element has switched on or off.
14	0 or 1	Node point report option code as follows: 0 = Node point reports will include the following flow variables: depth averaged velocities in the *X* and *Y* coordinate directions, water-surface elevation, and water depth. 1 = Node point reports will include unit flow rates in the *X* and *Y* coordinate directions in addition to the variables listed above.
15	0 to 1	Initial water-surface elevation for cold starts option code as follows: 0 = Default initial water-surface elevation will be assigned to all nodes for which initial conditions have not been specified. 1 = Storm surge elevation will be assigned to all nodes for which initial conditions have not been specified.
16	-2 to 1	Frontal solver pivoting strategy option code as follows:

SWMS

Order	*Value*	*Description*
		0 = Partial pivoting (just rows).
		1 = Full pivoting (rows and columns).
		-1 = No pivoting (first complete equation eliminated).
		-2 = No pivoting (equation with largest diagonal element eliminated).

SWMS.3 Record

1	-1 to 1	Mesh data file option code as follows:
		0 = All finite element mesh data will be entered on data records.
		±1 = Finite element mesh data will be read from a data file. However, additional mesh data that will supercede values read from the mesh data file may be entered on data records. Data will be read in "text" form if the value is positive, or in "binary" form if the value is negative. The default name of the mesh data file is "FST2DH.msh".
2	-1 to 1	Initial condition data file option code as follows:
		0 = All initial flow condition data will be entered on data records.
		±1 = Initial flow condition data will be read from a data file. However, additional initial flow condition data that will supercede values read from the initial flow condition data file may be entered on data records. Data will be read in "text" form if the value is positive, or in "binary" form if the value is negative. The default name of the initial flow condition data file is "FST2DH.flo".
		 An initial flow condition data file usually will be a flow solution output file created by a previous run.
3	-1 to 1	Boundary condition data file option code as follows
		0 = All boundary condition data will be entered on data records.
		±1 = Boundary condition data will be read from a data file. However, additional boundary condition data that will supercede values read from the boundary condition data file may be entered on data records. Data will be read in "text" form if the value is positive, or in "binary" form if

Order	*Value*	*Description*
		the value is negative. The default name of the boundary condition data file is “FST2DH.bcs”.
4	-1 to 1	Wind data file option code as follows: 0 = All wind data will be entered on data records. ±1 = Wind data will be read from a data file. However, additional wind data that will supercede values read from the wind data file may be entered on data records. Data will be read in “text” form if the value is positive, or in “binary” form if the value is negative. The default name of the wind data file is “FST2DH.wnd”.
5	-1 to 1	Wave data file option code as follows: 0 = All wave data will be entered on data records. ±1 = Wave data will be read from a data file. However, additional wave data that will supercede values read from the wave data file may be entered on data records. Data will be read in “text” form if the value is positive, or in “binary” form if the value is negative. The default name of the wind data file is “FST2DH.wve”.
6	0 or 1	Time data file option code as follows: 0 = All time data will be entered on data records. 1 = All time data will be read from a data file in “text” form. The default name of the time data file is “FST2DH.tim”.
7	-1 to 1	Flow solution output data file code as follows: 0 = Flow solutions will not be written to a data file. ±1 = Flow solutions will be written to a data file at the end of a steady-state run and at the end of selected time-steps during a time-dependent run. If a positive value is entered, the solution will be written in “text” form; if a negative value is entered, the solution will be written in “binary” form. The default name of the flow solution data file is “FST2DH.flo”.
8	-1 to 1	Restart/recovery file option code as follows: 0 = A restart/recovery file will not be used. ±1 = Intermediate results will be written to a restart/recovery file after every iteration to allow a run to be restarted from

Order	*Value*	*Description*
		the last successful iteration if the run terminates abnormally. Results will be written in "text" form if the value is positive, or in "binary" form if the value is negative. The default name of the restart/recovery file is "FST2DH.rsr".
9	0	A scalar output data file will not be written.
	1 to 65535	Sum of the codes of the following items to be written to the scalar output data file:

Code	*Item Description*
1	Water-surface elevation
2	Water depth
4	Ground elevation
8	Depth-averaged velocity magnitude.
16	Unit flow rate magnitude
32	Froude number
64	Mechanical energy head elevation
128	Bed shear stress magnitude (node average)
256	Vorticity magnitude (node average)
512	Wind speed
1024	Depth of general scour
2048	Scoured bed elevation (that is, bed elevation less depth of general scour)
4096	Sediment concentration (discharge-weighted)
8192	Sediment volumetric transport rate.
16384	Sediment volumetric transport capacity (that is, the equilibrium sediment transport rate)
32768	Sediment transport rate deficit (that is, the transport capacity minus the transport rate)

Selected scalar values at every node point in the network will be written to a data file. If the value is positive, scalar data will be written in "text" form; if the value is negative, scalar data will be written in "binary" form. The default name of the scalar output data

Order	*Value*	*Description*
		file is “FST2DH.scl”.
10	0	A vector output data file will not be written.
	1 to 63	Sum of the following codes of items to be written to the vector output data file:

Code	*Item Description*
1	Depth-averaged flow velocities.
2	Unit flow rates (velocities × water depth)
4	Bed shear stresses
8	Tropical cyclone wind velocities.
16	Sediment volumetric transport rates.
32	Sediment volumetric transport capacities (that is, equilibrium transport rates).

Selected vector values at every node point in the network will be written to a data file. If the value is positive, data will be written in “text” form; if the value is negative, data will be written in “binary” form. The default name of the vector output data file is “FST2DH.vec”.

SWMS.4 Record

1	1 to 99	Solution iteration code read as *KKJJII* where:
		II = maximum number of initial full-Newton iterations to be carried out (usually from 5 to 20).
		JJ = maximum number of quasi-Newton iterations to be carried out after all the initial full- Newton iterations, and after each additional full-Newton iteration.
		KK = maximum number of additional full-Newton iterations to be carried out.
		 The maximum allowable number of iterations for a steady-state solution or for a time step of a time-dependent solution is 99. Therefore, $II + JJ + KK \times (1 + JJ)$ needs to be less than or equal to 99. The solution may be stopped before the maximum number of iterations are completed if convergence criteria are satisfied.
2	+	Convergence tolerance for maximum absolute changes to *X* and *Y* direction unit flow rates, in ft^2/sec (m^2/s).

SWMS

Order	*Value*	*Description*
3	+	Convergence tolerance for maximum absolute changes to water-surface elevation, in ft (m).
		If the convergence tolerances for velocity and flow depth are satisfied, the steady-state solution or the time-dependent solution for the current time step will be considered to have converged and calculations will be halted.
4	+	Relaxation factor $0 < \omega_r \leq 2$ used in equation solution. Default $\omega_r = 1$.
5	+	Printed iteration control code. Results from every *i*th iteration during a steady-state solution and at every printed time step of a time-dependent solution will be printed, where *I* is the specified value. Results from the last iteration are always printed for a steady-state solution and for printed time steps of a time-dependent solution. Default = 1.
6	+	Number of ranked changes included in printed output. Up to the 10 largest changes at node points for each solution variable will be printed. Default = 1.
7	+	Default flow storativity depth. Flow storativity depth is specified as an element property in the PROP data set. This default value that will be specified for an element if a non-zero value is not specified in the PROP data set.
8	+	Global minimum element storativity coefficient *a*.
9	+	Global storativity depth multiplier η used to set the lower limit of element storativity.

SWMS.5 RECORD

1	hhhh:mm:ss	Starting simulation time.
2	hhhh:mm:ss	Length of simulation for a time dependent solution. A steady-state solution will carried out if this value is zero.
3	hhhh:mm:ss	Length of each time step used in a time-dependent solution Δt.
4	+	Time integration factor θ ($0.5 \leq \theta \leq 1.0$). Default $\theta = 0.667$.
5	hhhh:mm:ss	Printed report time interval. Flow solutions will be reported at this incremental time during time-dependent simulations. Default = “0000:00:00”.
6	hhhh:mm:ss	Output time interval. Flow solutions will be written to output files at this incremental time during time-dependent simulations. Default = “0000:00:00”.

Order	*Value*	*Description*
7	+	Starting data of simulation entered as *ccyymmdd* where *cc* = century (00 to 99), *yy* = year of the century (00 to 99), *mm* = month of year (01 to 12), and *dd* = day of month (01 to 31).

SWMS.6 Record

1	+	Default water-surface elevation, in ft (m). This value is assigned to each node point in a network that has not been assigned an initial water-surface elevation. Usually the *cold start* water-surface elevation is assigned using this parameter.
2	0	Effect of the Coriolis force will not be considered.
	±	Average local latitude of the surface-water body being modeled, in degrees. The latitude is positive in the Northern hemisphere and negative in the Southern hemisphere.
3	+	Average water mass density ρ, in slugs/ft^3 (kg/m^3). Default ρ = 1.937 slug/ft^3 (999.0 kg/m^3).
4	+	Coefficient β_0 used to compute the momentum correction coefficient. Default β_0 = 1.0.
5	+	Coefficient c_β used to compute the momentum correction coefficient. Default c_β = 0.
6	+	Continuity norm flag value. Continuity norms greater than this value will be denoted by an asterisk. Appropriate values are problem dependent. Default = 1.0e+35 (that is, continuity norms will not be flagged).
7	+	Depth tolerance, in ft (m), used during automatic boundary adjustment to decide whether or not to turn on an element. Default = 0.5 ft (0.15 m).

SWMS.7 Record

1	+	Default wind speed, in ft/sec (m/s). This value is assigned to each node in the network unless superceded by a value specified in the WIND data set.
2	+	Default wind direction angle, in degrees measured clockwise from true north. Wind direction is the direction *from which* the wind is blowing. This value is assigned to each node in the network unless superceded by a value specified in the WIND data set.
3	+	Air mass density ρ_{air}, in slugs/ft^3 (kg/m^3). Default ρ_{air} = 0.00237 slug/ft^3 (1.225 kg/m^3).

SWMS

Order	*Value*	*Description*
4	+	Coefficient c_{w1} used to calculate the wind stress coefficient. Default $c_{w1} = 1$.
5	+	Coefficient c_{w2} used to calculate the wind stress coefficient. Default $c_{w2} = 0$.
6	+	Minimum wind velocity W_{min}, in m/s, used to calculate the wind shear stress coefficient. Default $W_{min} = 0$ m/s.
7	+	Breaking water wave height to depth ratio γ_w . Default $\gamma_w = 0.78$.

SWMS.8 Record

1	+	Angle between the positive *x*-axis of the network coordinate system and true north, measured in degrees clockwise from true north.
2	±	Reference point latitude, in degrees (northern latitudes are positive, southern latitudes are negative.)
3	±	Reference point longitude, in degrees (western longitudes are positive, eastern longitudes are negative).
4	±	Reference point network *X* coordinate, in ft (m).
5	±	Reference point network *Y* coordinate, in ft (m).

Reference point geodetic and network coordinates are used to establish the geodetic coordinates of the network origin, which may be needed to calculate tropical cyclone pressure and wind fields. While the reference point may be the network origin, a point near the center of the finite element network would be best.

MEMO

Memorandum Data Set

Memorandum data records immediately follow a MEMO data set identification record. Memo records are simply character strings that become part of the FST2DH data file. They provide a means of describing the project and its variants and will be written to printed report files.

MEMO Identification Record

Order	*Value*	*Description*
1	"MEMO"	Data set identifier.
2	0	Number of memo records to follow.

MEMO Record

1	text	Up to 256 characters per record may be entered. The entire record is considered a character string and, therefore, does not need to be delimited. Records may be truncated when printed in reports. Repeat the memo record the specified number of times. Memo records may be blank.

NODE

Node Data Set

Node data records immediately follow a NODE data set identification record. The identification record contains the data set identifier and factors used to convert node point coordinates and ground and ceiling elevations read from data records to the desired units (either feet or meters). A node data record contains the identification number of a node, the horizontal X-Y coordinates of the node, and the node's ground-surface and ceiling elevations. Node data records are needed for all vertex nodes and for midside nodes of curved element sides. Curved element sides are defined by entering coordinate data for their midside nodes. Because bed and ceiling elevations are interpolated within elements using linear functions, values for these quantities are needed at only vertex nodes. Therefore, bed and ceiling elevations specified at midside and center nodes will be ignored. Optionally, node records may be read from a separate data file. The data set is terminated with one or more blank data records.

NODE Identification Record

Order	*Value*	*Description*
1	"NODE"	Data set identifier.
2	+	Multiplication factor used to convert *X* coordinates read from data records to feet (meters). Default = 1.
3	+	Multiplication factor used to convert *Y* coordinates read from data records to feet (meters). Default = 1.
4	+	Multiplication factor used to convert ground and ceiling elevations read from data records to feet (meters). Default = 1.
5	+	Feet (meters) to be added to all *X* coordinates read from data records after they are multiplied. Default = 0 ft (0 m).
6	+	Feet (meters) to be added to all *Y* coordinates read from data records after they are multiplied. Default = 0 ft (0 m).
7	+	Feet (meters) to be added to all ground and ceiling elevations read from data records after the they are multiplied. Default = 0 ft (0 m).
8	0 or 1	Node data record option code as follows: 0 = All node data records will follow in the data stream. 1 = All node records will be read from a separate data file. Enter the complete name of the node data file on the following record.

NODE Record

1	+	Node identification number.
2	±	*X* coordinate of the node.

NODE

Order	*Value*	*Description*
3	±	*Y* coordinate of the node.
4	±	Ground-surface elevation at the node.
5	±	Ceiling (lower bridge deck) elevation at the node.
		Coordinates and elevations are converted to feet (meters) by the factors specified on the data set identification record. Therefore, any system of units can be used to record node coordinates and elevations.

Terminate the NODE data set with one or more blank data records.

ELEM

Element Data Set

Element data records immediately follow an ELEM data set identification record. One record is required for each element. An element data record contains the identification number of an element, the sequence of nodes connected to the element (the element connectivity list), the element properties set number, and the element assembly sequence. Optionally, element records may be read from a separate data file. The data set is terminated with one or more blank data records.

ELEM Identification Record

Order	*Value*	*Description*
1	"ELEM"	Data set identifier.
2	0 or 1	Element data record option code as follows: 0 = All element records will follow in the data stream. 1 = All element records will be read from a separate data file. Enter the complete name of the element data file on the following record.

ELEM Record

1	+	Element identification number.
2 to 10	+	Element connectivity list. The sequence of nodes connected to the element. Enter six node numbers for a triangular element, eight node numbers for a "serendipity" quadrilateral element, or nine node numbers for a "Lagrangian" quadrilateral element. Begin the list at any vertex node and proceed in a counter-clockwise direction around the element as shown in the adjacent figure. Enter the center node last for a nine-node quadrilateral element.

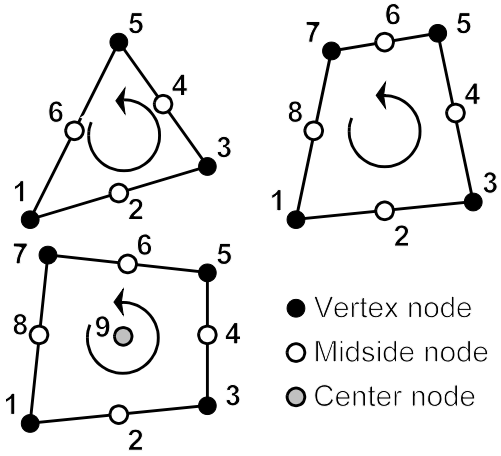

ELEM

Order	*Value*	*Description*
11	±	Element property set number. The number corresponds to a set of element properties or parameters that are entered in the **PROP** data set. If the number is negative, the element will be turned off (that is, the element will not be used in computations).
12	+	Element assembly sequence. The sequence number of the element for processing by the frontal method. An efficient element sequence can be generated using the resequencing option.

Terminate the ELEM data set with one or more blank data records.

PROP

Element Properties Data Set

Two-dimensional element properties data records immediately follow a PROP data set identification record. Three data records are needed for each set of element properties. An element properties data set contains information that describes the erosion and flow resistance of the element surface, the presence of a bridge deck, and turbulence parameters. The data entered on these records are applied to all elements that have been assigned the property set number. Optionally, element properties data may be read from a separate data file. The data set is terminated with one or more blank data records.

PROP Identification Record

Order	*Value*	*Description*
1	"PROP"	Data set identifier.
2	+	Default wall roughness coefficient n_{wall} or dimensionless discharge coefficient C'_{wall}. Default values: n_{wall} = 0.035, C'_{wall} = 11.
3	+	Default bridge deck roughness coefficient n_{deck} or dimensionless discharge coefficient C'_{deck}. Default values: n_{deck} = 0.035, C'_{deck} = 11.
4	+	Default bare soil roughness coefficient n_{soil} or dimensionless discharge coefficient C'_{soil}. Default values: n_{soil} = 0.016, C'_{soil} = 20.
5	+	Default protective soil cover roughness coefficient n_{cover} or dimensionless discharge coefficient C'_{cover}. Default values: n_{cover} = 0.040, C'_{cover} = 8.
6	0 or 1	Property data record option code as follows: 0 = All element properties data records will follow in the data stream. 1 = All element properties data records will be read from a separate data file. Enter the complete name of the element properties data file on the following record.

Use of Manning roughness or Chézy discharge coefficients is specified on the SWMS.2 data record. Dimensionless Chézy discharge coefficients $C' = C/\sqrt{g}$, where C = Chézy coefficient for the appropriate system of units being used, and g = gravitational acceleration.

PROP.1 Record

1	0 to 99	Property set number.

Elements can be removed from the network for computational purposes by setting the property code to a negative value. All elements assigned a negative property set code will always be "turned off" during the computations. This feature can be used to

Order	*Value*	*Description*
		evaluate the effect of a bridge crossing on water-surface elevations by constructing the "without roadway" network with elements that conform to the new roadway approach embankment. Elements occupied by approach roadways can then be easily turned off by assigning them unique property set codes and then setting the codes negative.
2	0 or 1	Potential pressure flow code as follows: 0 = Elements assigned this property set are not potential *pressure flow* elements. 1 = Elements assigned this property code are potential *pressure flow* elements.
		If ceiling elevations are specified at all vertex nodes of a potential pressure flow element (for example, to represent the underside of a bridge deck) a ceiling will be added and pressure flow will be simulated if the water-surface is in contact with the ceiling.
3	+	Critical shear stress of bed soil τ_{cs} , in lb/ft^2 (N/m^2), used in general clear-water scour calculations. Set this value to zero if the bed will not be allowed to erode.
4	+	Critical shear stress of a protective bed cover τ_{cp} , in lb/ft^2 (N/m^2), used in general scour calculations. Set this value to zero if a protective lining does not exist.
		A thin protective cover, such as gravel, grass, or a synthetic fabric, may extend over ground surfaces. No erosion will be calculated until bed shear stresses exceed the critical shear stresses of protective covers. When failure of linings occur, depth of clear-water scour will be calculated based on critical shear stresses of the underlying bed material.
5	"text"	Comment string describing the element type.
		PROP.2 Record
1	+	Manning roughness coefficient or dimensionless Chézy discharge coefficient applied to all water depths less than or equal to the depth entered in the next data item.
2	+	Water depth, in ft (m), below which the flow resistance coefficient entered in the previous data item is applied.
3	+	Manning roughness coefficient or dimensionless Chézy discharge coefficient applied to all depths greater than or equal to the depth in the next data item.

PROP

Order	*Value*	*Description*
4	+	Water depth, in ft (m), above which the flow resistance coefficient entered in the previous data item is applied.
	☞	For depths greater than the first depth and less than the second depth entered above, the roughness coefficient is interpolated linearly. If the second coefficient is zero or blank, the first coefficient is applied to all depths.
	☞	Use of Manning roughness or Chézy discharge coefficients is specified on the SWMS.2 data record. Dimensionless Chézy discharge coefficients $C' = C/\sqrt{g}$, where C = Chézy coefficient for the appropriate system of units being used, and g = gravitational acceleration.
5	+	Manning roughness coefficient n_{wall} used to calculate "wall" shear stress.
6	+	Manning roughness coefficient n_{deck} used to calculate "ceiling" shear stress from a bridge deck.
7	+	Manning roughness coefficient n_{soil} used to calculate "bare soil" shear stress.
8	+	Manning roughness coefficient n_{liner} used to calculate "soil liner" shear stress.
		PROP.3 Record
1	+	Turbulence model base kinematic eddy viscosity ν_o, in ft^2/sec (m^2/s).
2	+	Turbulence model coefficient $c_{\mu 1}$ (dimensionless).
3	+	Turbulence model coefficient $c_{\mu 2}$ (dimensionless).
4	+	Eddy diffusivity ϵ_o, in ft^2/sec (m^2/s).
5	+	Flow storativity depth, in ft (m). Flow storativity depth is the distance below the fixed bed elevation at a node to which the water-surface can fall before the node is considered dry
6	+	Wind shear reduction factor $C_{\tau w}$ $(0 \le C_{\tau w} \le 1)$. This value is used to reduce wind shear at the water surface caused by the presence of vegetation such as trees and brush. Default = 1 (that is, no reduction is applied). Default = 0 ft (0 m). Ranges of coefficients for several different types of land cover are given in the table below.

Order *Value* *Description*

Wind Stress Reduction Coefficients[a]

Land Cover	Coefficient Range
Wooded land	0.1 to 1.0
Marsh land	0.7 to 0.9
Open water	1
Developed areas	0.1 to 1.0
Open land	0.7 to 0.9

[a]From "Coastal flooding" (1988, p. 4-42)

7 + Water wave height H_w , in ft (m).

8 + Water wave period T_w, in sec.

0 Water wave period is calculated as $T_z = \alpha_w \sqrt{H_w / g}$, where α_w = 11.

- Negative value of the dimensionless coefficient α_w used to calculate wave periods using the above formula.

9 + or -1 Sediment erosion rate coefficient K_{es}. Default = 1.0

-1 Sediment erosion rate coefficient K_{es} will be calculated using the expression developed by Armanini and Di Silvio (1988).

Repeat the PROP.1-PROP.2-PROP.3 data record sequence for each set of element properties.

Terminate the PROP data set with one or more blank data records.

NODE1D

Node Data Set (for One-dimensional Flow)

One-dimensional node data records immediately follow a NODE1D data set identification record. The identification record contains the data set identifier and factors used to convert node point coordinates and ground and ceiling elevations read from data records to the desired units (either feet or meters). One-dimensional node data records contain node numbers, values of measured coordinates, the name of a cross section associated with the node point, and an optional comment. A node data record is needed for each element end node. Curved one-dimensional elements are specified by also entering coordinate data for the midside node of the element side. Because cross section geometry is interpolated within elements using linear functions, sections are specified only at end nodes. Optionally, one-dimensional node records may be read from a separate data file. The data set is terminated with one or more blank data records.

NODE1D Identification Record

Order	*Value*	*Description*
1	"NODE1D"	Data set identifier.
2	+	Multiplication factor used to convert *X* coordinates read from data records to feet (meters). Default = 1.
3	+	Multiplication factor used to convert *Y* coordinates read from data records to feet (meters). Default = 1.
4	+	Feet (meters) to be added to all *X* coordinates read from data records after they are multiplied. Default = 0 ft (0 m).
5	+	Feet (meters) to be added to all *Y* coordinates read from data records after they are multiplied. Default = 0 ft (0 m).
6	0 or 1	One-dimensional node data record option code as follows: 0 = All one-dimensional node data records will follow in the data stream. 1 = All one-dimensional node records will be read from a separate data file. Enter the complete name of the one-dimensional node data file on the following record.

NODE1D Record

1	+	One-dimensional node number.
2	±	*X* coordinate of the node.
3	±	*Y* coordinate of the node.
4	"text"	Identifier of the cross section associated with the end node. Required only for end nodes because cross section properties are interpolated linearly between end nodes within an element. Cross section data are entered in the **XSEC1D** data set.

NODE1D

Order	*Value*	*Description*
5	"text"	Comment string.
		Coordinates and elevations are converted to feet (meters) by the factors specified on the data set identification record. Therefore, any system of units can be used to record node coordinates and elevations.

Terminate the NODE1D data set with one or more blank data records.

ELEM1D

Element Data Set (for One-dimensional Flow)

One-dimensional element data records immediately follow an ELEM1D data set identification record. One record is required for each element. A one-dimensional element data record contains the identification number of an element, the sequence of nodes connected to the element (the element connectivity list), the element type code, the element assembly sequence, and a comment string. Optionally, element records may be read from a separate data file. The data set is terminated with one or more blank data records.

ELEM1D Identification Record

Order	*Value*	*Description*
1	"ELEM1D"	Data set identifier.
2	0 or 1	Element data record option code as follows: 0 = All element records will follow in the data stream. 1 = All element records will be read from a separate data file. Enter the complete name of the element data file on the following record.

ELEM1D Record

1	+	Element identification number.
2 to 4	+	Element connectivity list. The sequence of three nodes that define the one-dimensional element. Begin the list at an end node and proceed to the other end. (Also, make sure to read the note at the end of this section regarding topological consistency.)

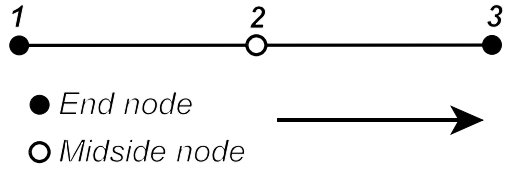

5	0 to 3	One-dimensional element type code as follows: 0 = Channel element 1 = Bridge element (not currently functional) 2 = Culvert element (not currently functional) 3 = Roadway element (not currently functional)

☞ Only one-dimensional channel elements are currently supported. Support for other one-dimensional element types will be added in the future.

Order	*Value*	*Description*
6	+	Element assembly sequence. The sequence number of the element for processing by the frontal method. An efficient element sequence can be generated using the resequencing option.
7	+	Kinematic eddy viscosity, in ft^2/sec (m^2/s).
8	"text"	Comment string (32 characters maximum).

Flow within an element is considered positive when proceeding from the element's first vertex node to its second, and negative when moving in the opposite direction. To maintain topological consistency, all one-dimensional elements connecting two boundaries (including junction boundaries) need to be numbered in sequential fashion, beginning at one boundary node and concluding at the other as shown in the figure below. The order in which nodes are numbered defines the direction of positive and negative flow rates. Choose the direction that best suits the application.

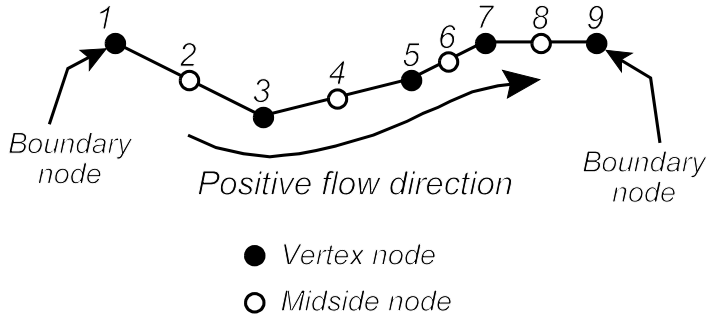

Terminate the ELEM1D data set with one or more blank data records.

XSEC1D

Open-channel Section Data Set (for One-dimensional Flow)

One-dimensional open-channel section data records immediately follow an XSEC1D data set identification record. Three records are required for each cross section. The first record contains coordinates of the section origin (that is, the first ground point), the azimuth of the section, roughness coefficients of the left and right overbanks and the main channel, and a comment. The second data record contains horizontal distances from the origin of exactly eight section points, which correspond to eight ground elevations entered on the third data record. Optionally, cross section records may be read from a separate data file. The data set is terminated with one or more blank data records.

XSEC1D Identification Record

Order	*Value*	*Description*
1	"XSEC1D"	Data set identifier.
2	0 or 1	Cross section data record option code as follows: 0 = All cross section records will follow in the data stream. 1 = All cross section records will be read from a separate data file. Enter the complete name of the cross section data file on the following record.

XSEC1D.1 Record

1	"text"	Cross section identifier (8 characters maximum).
2	±	Section origin *X* coordinate, in ft (m).
3	±	Section origin *Y* coordinate, in ft (m).
4	±	Section azimuth, in deg. The section is considered straight.
5	+	Manning roughness coefficient of the left overbank.
6	+	Manning roughness coefficient of the main channel.
7	+	Manning roughness coefficient of the right overbank.
8	"text"	Comment string (32 characters maximum).

XSEC1D.2 Record

1 to 8	+	Horizontal distances corresponding to bed elevations specified on the following record, in ft (m).

XSEC1D.3 Record

1 to 8	±	Bed elevations corresponding to horizontal distances specified on the preceding record, in ft (m).

Order *Value* *Description*

Each cross section is defined by exactly eight ground points as shown in the following figure. The third and sixth points represent the two channel banks. *Active width* of the section (that is, the portion of the section within which sediment can be transported) is between points four and five as shown.

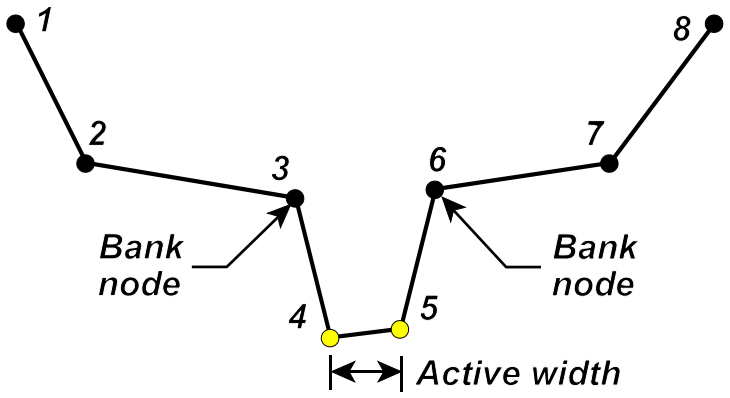

Terminate the XSEC1D data set with one or more blank data records.

COND1D

Closed-conduit Section Data Set (for One-dimensional Flow)

One-dimensional closed-conduit data records immediately follow an COND1D data set identification record. Four data records are required for each closed conduit section. The first record contains coordinates of the section origin (that is, the first ground point), the azimuth of the section, roughness coefficients of the left and right overbanks the main channel, and the ceiling, and a comment. The second data record contains horizontal distances from the origin of exactly eight section points, which correspond to eight ground elevations entered on the third data record, and eight ceiling elevations entered on the fourth record. Optionally, closed conduit section records may be read from a separate data file. The data set is terminated with one or more blank data records.

COND1D Identification Record

Order	*Value*	*Description*
1	"COND1D"	Data set identifier.
2	0 or 1	Closed conduit section data record option code as follows: 0 = All closed conduit section records will follow in the data stream. 1 = All closed conduit section records will be read from a separate data file. Enter the complete name of the closed conduit section data file on the following record.

COND1D.1 Record

1	"text"	Closed conduit section identifier (8 characters maximum).
2	±	Section origin *X* coordinate, in ft (m).
3	±	Section origin *Y* coordinate, in ft (m).
4	±	Section azimuth, in deg. The section is considered straight.
5	+	Manning roughness coefficient of the left overbank bed.
6	+	Manning roughness coefficient of the main channel bed.
7	+	Manning roughness coefficient of the right overbank bed.
8	+	Manning roughness coefficient of the conduit ceiling.
9	"text"	Comment string (32 characters maximum).

COND1D.2 Record

1 to 8	+	Horizontal distances corresponding to bed elevations and ceiling elevations specified on the following two records, in ft (m).

Order	*Value*	*Description*
		COND1D.3 Record
1 to 8	±	Bed elevations corresponding to horizontal distances specified on the COND1D.2 data record, in ft (m).
		COND1D.3 Record
1 to 8	±	Ceiling elevations corresponding to horizontal distances specified on the COND1D.2 data record, in ft (m).

Each closed conduit section is defined by exactly eight ground points as shown in the following figure. The third and sixth points represent the two channel banks. *Active width* of the section (that is, the portion of the section within which sediment can be transported) is between points four and five as shown. Vertical sidewalls are assumed to exist at the first and last station points if their ground elevations are less than their ceiling elevations.

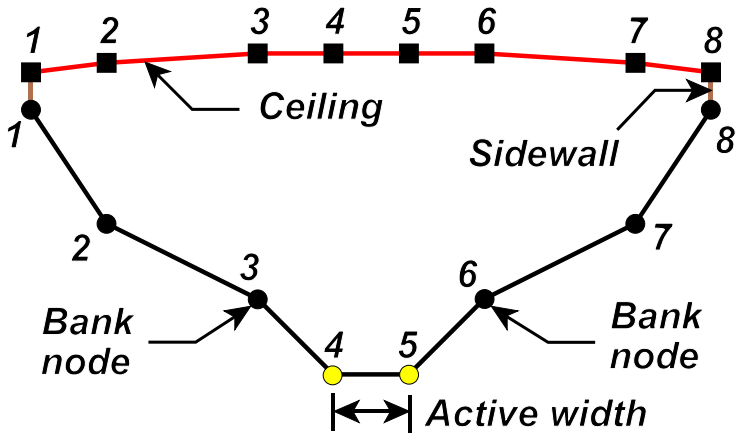

Terminate the COND1D data set with one or more blank data records.

FLOW

Flow Initial Condition Data Set

Flow initial condition data records immediately follow an FLOW data set identification record. One record is needed for each node at which initial conditions are specified. Flow initial condition data consist of node numbers, initial velocities in the *x* and *y* directions, water-surface elevations, and time derivatives of the *x* and *y* velocities and water-surface elevations. Values entered on data records will override those read from an initial condition data file. The data set is terminated with one or more blank data records.

FLOW Identification Record

Order	*Value*	*Description*
1	"FLOW"	Data set identifier.

FLOW Record

1	+	Node number.
2	±	Initial velocity in the *x* direction, in ft/sec (m/s).
3	±	Initial velocity in the *y* direction, in ft/sec (m/s).
4	+	Initial water-surface elevation, in ft (m).
5	±	Initial *x* velocity rate of change, in ft/sec (m/s).
6	±	Initial *y* velocity rate of change, in ft/sec (m/s).
7	±	Initial water-surface elevation rate of change, in ft/sec (m/s).

Terminate the FLOW data set with one or more blank data records.

BOUN

Boundary Condition Data Set

Boundary condition data records immediately follow a BOUN data set identification record. Two records are needed for each boundary node at which conditions other than slip/no-slip/semi-slip are specified. For a time-dependent (unsteady) simulation, only values that change from the previous time step need to be specified. Boundary condition data consist of the number of the node to which the data apply, boundary condition codes, a comment, and specified values. Either tangential flow (slip) or zero flow (no-slip) conditions (as specified on the SWMS.2 data record) are applied automatically at all boundary nodes unless specified otherwise. Values entered on data records will override those read from a boundary condition data file. The data set is terminated with one or more blank data records.

BOUN Identification Record

Order	*Value*	*Description*
1	"BOUN"	Data set identifier.

BOUN.1 Record

1	+	Node number.
2	0 to 6	Flow specification in the *x-direction*, the *tangent direction*, or *normal* to the *open* boundary as follows: 0 = No specification. 1 = Velocity in the *x* direction. 2 = Unit flow (velocity × depth) in the *x*-direction. 3 = Velocity *tangent* to the boundary. 4 = Unit flow *tangent* to the boundary. 5 = Total flow *normal* to the *open* boundary. 6 = Weakly-reflecting boundary invariant quantity $U_{n\infty} + 2\sqrt{gH_{n\infty}}$ where $U_{n\infty}$ = velocity in a fictitious channel far away from the boundary, g = gravitational acceleration, and $H_{n\infty}$ = flow depth in the fictitious channel.
3	0 to 6	Flow specification in the *y-direction*, the *normal direction*, or *normal* to the *closed* boundary as follows: 0 = No specification. 1 = Velocity in the *y* direction. 2 = Unit flow (velocity × depth) in the *y*-direction.

BOUN

Order	*Value*	*Description*
		3 = Velocity *normal* to the boundary.
		4 = Unit flow *normal* to the boundary.
		5 = Total flow *normal* to the *closed* boundary.
		6 = Velocity *tangent* to the *open* boundary.
		 Zero flow (no-slip) conditions are applied at a boundary node by setting data items 2 and 3 to "1" and specifying the *x* and *y* velocities to be zero. Tangential flow (slip) conditions are applied at a boundary node by setting data item 2 "0" and data item 3 to "5" and specifying the total flow normal to the boundary to be zero.
		 Special consideration needs to be given nodes where closed and open boundaries meet. Specified unit flow or velocity needs to be parallel to closed boundaries at these nodes. If water-surface is specified, tangential or zero flow needs to be specified.
4	0 to 9	Water-surface elevation specification code as follows:
		0 = No specification.
		1 = Water-surface elevation will be applied as an *essential* boundary condition.
		2 = Water-surface elevation will be applied as a *natural* boundary condition.
		3 = *Supercritical* flow exists at the *outflow* boundary node. Water-surface elevation is not specified.
		4 = Water-surface elevation *plus* an additional rise due to cyclonic storm pressure deficit will be applied as a *natural* boundary condition.
		5 = A *source* (inflow) or *sink* (withdrawal) is specified. The node does not have to lie on the network boundary.
		7 = Stormtide elevations (that is, storm surge plus astronomic tide elevation) calculated based on storm surge and tide parameters specified in the SURGE and STORM data sets will be applied as essential conditions. The boundary node does not need to be repeated as time-dependent data.
		9 = The node is a *junction node*. Water-surface elevations at all nodes assigned to a junction will be required to be the same. The junction identifier is the specified value.

Order	*Value*	*Description*
		Only one junction may be attached to an element. Where two or more junctions are close to one another, elements may need to be subdivided to satisfy the "one junction per element" limit.
5	0 to 2	Bed elevation specification for sediment transport solutions as follows: 0 = No specification. 1 = Bed elevation is specified. 2 = Initial bed elevation is fixed and will not change.
6	0 to 5	Sediment volumetric flow rate specification for sediment transport solutions as follows: 0 = No specification. 1 = Sediment discharge-weighted volumetric concentrations are specified as essential conditions. 2 = Sediment discharge-weighted volumetric concentrations are specified as natural conditions. 3 = Sediment volumetric transport rates are specified for each size class, and average discharge-weighted volumetric concentrations are specified as essential conditions. 4 = Sediment transport rates are specified for each size class, and average discharge-weighted volumetric concentrations are specified as natural conditions. 5 = Equilibrium total sediment transport rates are applied. Transport rates will be calculated using flow parameters and properties of the active layer.
7	"text"	Boundary node comment string.

BOUN.2 Record

1	+	Specified velocity, in ft/sec (m/s), or unit flow, in ft^2/sec (m^2/s), in the *x* direction or tangent to the boundary at the node point. Or, for a weakly reflecting boundary, the invariant quantity, in ft/sec (m^2/s).
2	+	Specified velocity, in ft/sec (m/s); unit flow, in ft^2/sec (m^2/s); or total flow, in ft^3/sec (m^3/s), in the *y* direction or normal to the boundary at the node point. Or, if total flow normal to an *open* boundary is specified, the velocity tangent to the *open* boundary.

BOUN

Order	*Value*	*Description*
		If total flow is specified, a positive value indicates flow into a network and a negative value indicates flow out of a network resulting from flow.
3	± or "text"	Specified water-surface elevation, in ft (m), or total flow, in ft^3/sec (m^3/s) if a source (inflow) or sink (withdrawal) is specified. Total flow is positive for a source, and negative for a sink. For junction nodes, the specification is a junction identifier (that is, a unique text string of up to 8 characters that identifies the junction).
4	±	Bed elevation, in ft (m).
5 to 12	+	Discharge-weighted sediment concentrations in volume per unit volume $\times 10^6$, or unit volumetric sediment transport rates in ft^2/s (m^2/s), for each size class in order.

Terminate the BOUN data set with one or more blank data records.

BSEC

Boundary Cross Section Data Set

Boundary cross section data records immediately follow a BSEC data set identification record. Boundary cross section data consist of boundary conditions that apply to all the node points that define a "channel cross section" forming part of a finite element network's *open* boundary. Boundary conditions that can be specified include total flow normal to the boundary, water-surface elevation, weakly reflecting conditions, or the presence of a junction. Two records are needed to specify boundary conditions, and a variable number of records are needed to list cross section nodes. Up to 1000 nodes can be entered for each boundary section. Only values that change from the previous time step need to be specified for time-dependent (unsteady) simulations. The boundary cross section data set is terminated with one or more blank data records.

BSEC Identification Record

Order	*Value*	*Description*
1	"BSEC"	Data set identifier.

BSEC.1 Record

1	"text"	Boundary cross section identification string. An alpha/numeric character string that is used to identify the cross section.
2	0, 5, or 6	Normal flow specification along the open boundary as described below: 0 = No specification. 5 = Total flow *normal* to the open boundary cross section will be specified. 6 = A *weakly-reflecting* boundary condition will be specified along the open boundary cross section. The invariant quantity $\frac{Q_{n\infty}}{A_{n\infty}} + 2\sqrt{g\frac{A_{n\infty}}{B_{n\infty}}}$ in ft/sec (m/s) needs to be specified where $Q_{n\infty}$ = total flow in a fictitious channel far away from the boundary, $A_{n\infty}$ = cross section area of the fictitious channel far away from the boundary, $B_{n\infty}$ = cross section top width far away from the boundary, and g = gravitational acceleration.
3	0	No specification. Always enter zero for consistency with node point boundary condition codes.
4	0 to 9	Water-surface elevation specification along the boundary section as follows: 0 = No specification.

BSEC

Order *Value* *Description*

1 = Water-surface elevation will be specified as an *essential* boundary condition at each node of the cross section.

2 = Water-surface elevation will be specified as a *natural* boundary condition at each node of the cross section.

Water-surface elevations need to be specified on the BSEC.2 data record if codes 1 or 2 are entered.

3 = *Supercritical* flow exists at each node of the cross section. The cross section is considered to form an *outflow* boundary and water-surface elevation is not specified.

4 = Water-surface elevation *plus* an additional rise due to cyclonic storm pressure deficit will be applied as an essential condition.

5 = Water-surface elevation will be calculated based on the slope-area method using the specified friction slope and total flow rate. Total cross section flow rate and friction slope need to be specified on the BSEC.2 data record.

6 = Water-surface elevation will be calculated based on a stage-discharge relation using the specified rating curve and total flow rate. Total cross section flow rate and a rating curve identifier need to be specified on the BSEC.2 data record.

7 = Stormtide elevations (that is, storm surge plus astronomic tide elevation) calculated based on storm surge and tide parameters specified in the SURGE and STORM data sets will be applied as essential conditions. The boundary cross section does not need to be repeated as time-dependent data.

9 = The boundary section is part of a *junction*. Water-surface elevations at all nodes assigned to a junction will be required to be the same. The junction identifier is the specified value.

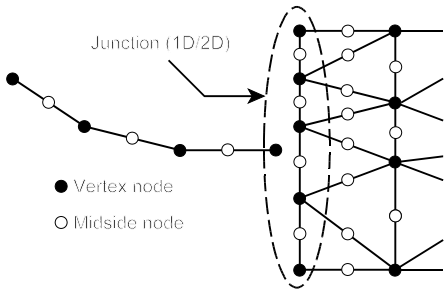

Order	*Value*	*Description*
	☞	Only one junction may be attached to an element. Where two or more junctions are close to one another, elements may need to be subdivided to satisfy the "one junction per element" limit.
5	0 or 2	Bed elevation specification along the boundary section as follows: 0 = No specification. 2 = Initial bed elevation is fixed and will not change.
6	0 to 5	Sediment volumetric flow rate specification for sediment transport solutions as described below: 0 = No specification. 1 = Sediment discharge-weighted volumetric concentrations are specified as essential conditions. 2 = Sediment discharge-weighted volumetric concentrations are specified as natural conditions.
	☞	Cross-section averaged discharge-weighted sediment concentrations for each particle size class need to be specified on the following data record if codes 1 or 2 are entered.
		3 = Sediment volumetric transport rates are specified for each size class, and average concentrations are applied as essential conditions. 4 = Sediment volumetric transport rates are specified for each size class, and average discharge-weighted concentrations are applied as natural conditions.
	☞	Total cross-section volumetric transport rates for each particle size class need to be specified on the following data record if codes 3 or 4 are entered.
		5 = Equilibrium total sediment volumetric transport rates are applied at all nodes in the cross section. Transport rates are calculated using flow parameters and properties of active layers at cross section node points.
7	"text"	Boundary cross section comment string.

BSEC.2 Record

1	±	Total flow normal to the boundary cross section, in ft^3/sec (m^3/s), or the weakly-reflecting boundary invariant quantity in ft/sec (m/s). Total flow rate needs to be specified if water-surface elevations are calculated by the slope-area method.

BSEC

Order	*Value*	*Description*
	☞	Flows into finite element networks through open boundaries (inflows) are positive, and flows out of networks through open boundaries (outflows) are negative.
2	± or "text"	Water-surface elevation, in ft (m), or friction slope used in the slope-area method.. For junction nodes, the specification is a junction identifier (that is, a unique text string of up to 8 characters that identifies the junction).
3	±	Second water-surface elevation, in ft (m), if a linearly- varying water-surface elevation is specified along the cross section.
	☞	If the data item 3 water-surface elevation ≠ 0, water-surface elevations at node points between the two cross section end nodes are interpolated linearly on the basis of distance between the two end nodes.
	☞	If the slope-area method is used, water-surface elevation will be calculated using the friction slope and total flow rate specified in for the cross section.
4	"text"	Rating curve identifier. The rating curve is used along with the total cross section flow rate to establish a water-surface elevation that is assigned to every node point of the cross section.
5 to 12	+	Cross-section-averaged discharge-weighted sediment concentrations in volume per unit volume $\times 10^6$, or total cross-section sediment transport rates in ft^3/s (m^3/s), for each particle size class in order.
		BSEC.3 Record
3 to 1000	+	A list of node numbers that define a connected series of element sides on a section of the network boundary that is *open* (that is, through which flow can enter or leave the network). The list is terminated by a negative entry. Up 1000 node points may be used to define a cross section. When the boundary cross section is used repeatedly as time-dependent data, only a single "-1" entry is needed so that the list of boundary section nodes does not need to be repeated.

Terminate the BSEC data set with one or more blank records.

WIND

Wind Data Set

Wind data records immediately follow a WIND data set identification record. *One* record is prepared for *each* node at which conditions other than general wind specifications are desired. For a time-dependent (unsteady) run, only values that change from the previous time step need to be specified. Wind data consist of the node number and the specified wind direction and velocity. The data set is terminated with one or more blank data records.

WIND Identification Record

Order	*Value*	*Description*
1	"WIND"	Data set identifier.

WIND Record

1	0	Node number at which the following wind data are to be applied.
2	+	Wind velocity, in ft/sec (m/s).
3	+	Wind direction angle, in degrees measured counterclockwise from East. The wind direction is interpreted as the direction *to which* the wind is blowing. For example, a wind blowing to the northeast (45^o clockwise from true north) would be coming from the southwest, and would have a direction angle of 135^o measured counter clockwise from east as shown in the diagram below.

Previous versions of this document defined the wind direction as the conventional meteorological definition of a wind (i.e. the direction *from which* the wind is blowing measured clockwise from true north. In this convention, the wind described above would have a direction of 235^o.) This has been changed to reflect how the FESWMS engine computes wind.

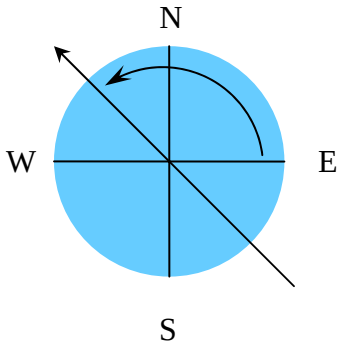

Terminate the WIND data set with one or more blank data records.

WAVE

Wave Data Set

Wave data records immediately follow a WAVE data set identification record. *One* record is prepared for *each* node at which wave data are to be specified. Only values that change from the previous time step need to be specified for a time-dependent (unsteady) simulation. Wave data consist of the node number and the specified wave height, period, and direction. The data set is terminated with one or more blank data records.

WAVE Identification Record

Order	*Value*	*Description*
1	"WAVE"	Data set identifier.

WAVE Record

1	0	Node number at which the following wave data are to be applied.
2	+	Wave height, in ft (m).
3	0	Wave period, in seconds.
4	+	Wave direction angle, in degrees measured counter-clockwise from the positive x-axis.

Terminate the WAVE data set with one or more blank data records.

CYCL

Tropical Cyclone Data Set

A tropical cyclone data record immediately follows a CYCL data set identification record. The identification record contains information describing the storm initial position and the landfall location. The tropical cyclone data record contains data information used to calculate movement of the storm, wind speeds, and wind directions. Storm coordinates in time-dependent tropical cyclone data sets are not read.

CYCL Identification Record

Order	*Value*	*Description*
1	"CYCL"	Data set identifier.
2	0 or 1	Storm coordinates code as follows: 0 = Geodetic coordinates (latitude and longitude). 1 = Universal Transverse Mercator (UTM) system coordinates (Northing and Easting)
3	±	Storm latitude (for geodetic coordinates) in degrees, or Northing (for UTM coordinates) in meters.
4	±	Storm longitude (for geodetic coordinates) in degrees, or Easting (for UTM coordinates) in meters.
		Northern latitudes are positive, southern latitudes are negative; western longitudes are positive, eastern longitudes are negative. UTM coordinates (Northing and Easting) are in meters.
5	0 or 1	Storm position code as follows: 0 = Coordinates are the initial position of the storm center. 1 = Coordinates are the *landfall* location of the storm. The initial position of the storm will be calculated based on the landfall location and the landfall time, along with storm track angle and forward speed (which are considered constant).
6	0 or +	0 Landfall will not be considered and wind speeds will not be adjusted. + Landfall time, in hours (simulation time, not actual clock time). Wind decay after landfall will be calculated using the procedure in Kaplan and DeMaria (1995)

CYCL Record

1	+	Forward storm speed V_f, in nautical mi/hr (km/hr).
2	+	Storm track azimuth, in degrees measured clockwise from true north, is the direction *from which* the storm is moving.

CYCL

Order	*Value*	*Description*
3	+	Radius to maximum winds R_{max}, in nautical mi (km).
4	+	Central pressure P_c, in inches of Hg (kPa).
5	+	Peripheral storm pressure P_∞, in inches of Hg (kPa). Default = 30.0 in Hg (101.325 kPa).

SURGE

Storm Surge Data Set

A storm surge data record immediately follows an SURGE data set identification record. The storm surge data record contains data information used to calculate storm surge elevations along ocean boundaries for time-dependent simulations. A hydrograph is developed based on the surge peak stage, characteristics of a tropical cyclone, and astronomic tides. Tropical cyclone data need to be specified if storm surge elevations are calculated.

SURGE Identification Record

Order	*Value*	*Description*
1	"SURGE"	Data set identifier.

SURGE Record

1	+	Simulation time of surge peak stage, in hours.
2	+	Storm surge peak stage or water-surface height above normal water-surface, in ft (m).
3	±	Mean astronomic tide elevation, in ft (m).
4	+	Astronomic tide range (high tide elevation - low tide elevation), in ft (m).
5	1 or 2	Number of daily astronomic tide cycles (1 = diurnal, 2 = semi-diurnal). Diurnal tides have periods of 24.84 hr, and semi-diurnal tides have periods of 12.42 hr. Default = 2 (semi-diurnal tides).
6	0 to 4	Tide phase code that defines the astronomic tide phase at storm surge peak stage as follows: 0 = No astronomic tide stage is added to storm surge. 1 = High tide occurs at storm surge peak. 2 = Mid-tide falling occurs at surge peak 3 = Low tide occurs at surge peak. 4 = Mid-tide rising occurs at surge peak.

WEIR

Weir Data Set

Weir data records immediately follow a WEIR data set identification record. Two records are needed for each weir segment. Date for each weir segment includes an identification string, numbers of the node points on the upstream and downstream sides of the segment, the weir segment type code, crest length, crest elevation, user-defined discharge and submergence function coefficients, and user-defined tailwater depth. Optionally, weir data may be read from a separate data file. The data set is terminated with one or more blank data records.

WEIR Identification Record

Order	*Value*	*Description*
1	"WEIR"	Data set identifier.
2	0 to 2	Code that defines the weir flow report(s) to be printed at the end of printed time steps and at the end of a steady-state simulation (0 = just summary reports, 1 = just comprehensive reports, 2 = both summary and comprehensive reports).
3	±	Default tailwater elevation, in ft (m), assigned to all weir segments for which tailwater elevations are not assigned.
4	+	Default minimum head difference, in ft (m), assigned to all weir segments for which minimum head differences are not specified.
5	0 or 1	Weir data record option code as follows: 0 = All weir records will follow in the data stream. 1 = All weir records will be read from a separate data file. Enter the complete name of the weir data file on the following record.

WEIR.1 Record

1	"text"	Weir segment identification string (8 characters maximum). This is a unique text string used to identify the weir segment.
2	±	Number of the node point on one side of the weir. Water will only be allowed to leave the network at this node, as if a flapgate was present, if the number is negative.
3	0	If 0, flow is allowed to leave the finite element network over the weir segment from the previously specified node point. Otherwise, the value is the number of the node point at the opposite side of the weir segment.
		Weir segment node points may be located on either the boundary or the interior of the network.

Order	*Value*	*Description*
4	"text"	Comment string used to describe the weir segment (32 characters maximum).

WEIR.2 Record

1	0 to 6	Weir segment type code that defines the weir segment as follows: 0 = Undefined (weir discharge and submergence function coefficients C_w, a_{sub}, and b_{sub} need to be specified). 1 = Paved roadway embankment. 2 = Gravel roadway embankment. 3 = Single railroad track embankment. 4 = Double railroad track embankment. 5 = Sharp-crested weir (rectangular). 6 = Sharp-crested weir (triangular). 7 = Broad-crested weir (rectangular).
2	+	Crest length of the weir segment L_w, in ft (m).
3	±	Crest elevation of the weir segment z_{wc}, in ft (m).
4	0 or +	Dimensionless discharge coefficient C_w for free-flow conditions at the weir segment. A default value based on the weir segment type is assigned if not specified (see following table).
5	0 or +	Submergence function coefficient a_{sub}. A default value based on the weir segment type is assigned if not specified (see following table).
6	0 or +	Submergence function coefficient b_{sub}. A default value based on the weir segment type is assigned if not specified (see following table).

Weir submergence factors are calculated as

$$C_s = \left(1 - Y_t^{a_{sub}}\right)^{b_{sub}}$$

where

$$Y_t = \left(\frac{z_w^d - z_{wc}}{z_w^u - z_{wc}}\right)$$

is the submergence ratio, z_w^u = upstream water-surface elevation, z_w^d = downstream water-surface elevation, and z_{wc} = weir segment

WEIR

Order *Value* *Description*

crest elevation. Unless specified, default values of weir segment coefficients C_w, a_{sub}, and b_{sub} will be used based on the assigned weir segment type as summarized in the following table:

Submergence Function Default Coefficients

Weir segment description	C_w	a_{sub}	b_{sub}
Paved roadway	0.54	16.4	0.43
Gravel roadway	0.54	15.4	0.61
Single railroad track	0.58	7.25	0.5
Double railroad track	0.52	7.25	0.5
Sharp-crested weir (rectangular)	0.54	1.5	0.39
Sharp-crested weir (triangular)	0.54	2.5	0.39
Broad-crested weir (rectangular)	0.54	7.25	0.5

7* ± Weir crest elevation increment (decrement) that is added to (subtracted from) all section point weir crest elevations, in ft (m).

Terminate the WEIR data set with one or more blank records.

Culvert Data Set

Culvert data records immediately follow a CULV data set identification record. Three data records are needed for each culvert. Culvert data consist of identification strings, numbers of the node points on the upstream and downstream ends of culverts, numbers of culvert barrels, culvert type codes, inlet and outlet control flow coefficients, barrel dimensions, and invert elevations at the culvert ends. Optionally, culvert data may be read from a separate data file. The data set is terminated with one or more blank records.

CULV Identification Record

Order	*Value*	*Description*
1	"CULV"	Data set identifier.
2	0 to 2	Code that defines the culvert flow report(s) to be printed at the end of printed time steps and at the end of a steady-state simulation (0 = just summary reports, 1 = just comprehensive reports, 2 = both summary and comprehensive reports).
3	±	Default tailwater elevation, in ft (m), assigned to all culverts for which tailwater elevations are not specified.
4	+	Default minimum head difference, in ft (m), assigned to all culverts for which minimum head differences are not specified.
5	+	Default riprap basin depth, in ft (m), assigned to all culverts for which riprap basin depths are not specified.
6	0 or 1	Culvert data record option code as follows: 0 = All culvert records will follow in the data stream. 1 = All culvert records will be read from a separate data file. Enter the complete name of the culvert data file on the following record.

CULV.1 Record

1	"text"	Culvert identification string (8 characters maximum). This is a unique text string used to identify the culvert.
2	±	Number of the node point at one end of the culvert. Water will be allowed only to leave the network at this node point, as if a flap-gate was installed on the other end of the culvert, if the node number is negative.
3	0 or +	If 0, flow is allowed to leave the finite element network through the culvert from the previously specified node point. Otherwise, the value is the number of the node point at the culvert outlet.

CULV

Order	*Value*	*Description*
	☞	Culvert node points may be located on either the boundary or the interior of the network.
4	"text"	Comment used to describe the culvert (32 characters maximum).

CULV.2 Record

1	+	Culvert type code. Type codes for various combinations of barrel materials, cross-section shapes, and inlet characteristics are defined the table at the end of this section.
2	+	Number of identical culvert barrels. Default = 1.
3	0 or +	Entrance loss coefficient K_{ce} used in outlet control flow calculations. Values of K_{ce} for various types of inlets are given in Table 2-3.
4	0 or +	Culvert barrel Manning roughness coefficient n_c used in outlet control flow calculations. Values of n_c for various culvert barrel materials and conditions are given in Table 2-4.
5	0 or +	Inlet control flow coefficient K'.
6	0 or +	Inlet control flow coefficient M.
7	0 or +	Inlet control flow coefficient c'.
8	0 or +	Inlet control flow coefficient Y.
9	0 or +	Inlet control flow coefficient α.
	☞	Culvert flow coefficients obtained from Tables 2-2, 2-3, and 2-4 and from *HDS-5* (Norman et al. 1985) based on the specified culvert type code will be used as defaults if values of K_{ce}, n_c, K', M, c', Y, and α are not specified.

CULV.3 Record

1	+	Barrel rise or height, in ft (m).
2	+	Barrel span or width, in ft (m).
3	+	Barrel length L_c, in ft (m).
4	±	Invert elevation at the first culvert end point, in ft (m).
5	±	Invert elevation at the second culvert end point, in ft (m).
6	±	Tailwater elevation, in ft (m), used in outlet flow control calculations if only one node is specified for the culvert.

Order	*Value*	*Description*
7	+	Minimum head difference in ft (m), needed for culvert flow calculations. Zero flow is assigned if the head difference is less than this value. Default = 0 ft (m).
8	0	Culvert riprap calculations will not be carried out.
	+	Riprap basin depth, in ft (m), used to size riprap at culvert outlets.
		Repeat the CULV.1-CULV.2-CULV.3 data record sequence for each culvert.

Terminate the CULV data set with one or more blank records.

CULV

Table A-1. Culvert type codes for various combinations of barrel materials, barrel cross-section shapes, and inlet characteristics.

Barrel material	Barrel cross-section shape	Inlet description	Culvert code	HDS-5 chart
Concrete	Circular	Headwall with square edge	1011	36525
		Headwall with grooved edge	1012	36526
		Projecting with grooved edge	1051	36527
		Beveled ring with 45˚ bevels	1061	3/A
		Side-tapered inlet	1071	55/1
	Rectangular	Headwall with 3/4-in chamfers	1111	36799
		Headwall with 45˚ bevels	1112	36800
		Headwall with 33.7˚ bevels	1113	36801
		Skewed headwall (45˚) with 3/4-in chamfers	1121	36830
		Skewed headwall (30˚) with 3/4 in chamfers	1122	36831
		Skewed headwall (15˚) with 3/4 in chamfers	1123	36832
		Skewed headwall (10-45˚) with 45˚ bevels	1124	36833
		Wingwalls (30˚ to 75˚) with square top edge	1131	36738
		Wingwalls (15˚ and 90˚) with square edge	1132	36739
		Wingwalls (0˚, extension of sides) with square top edge	1133	36740
		Wingwalls (45˚) with beveled top edge	1134	36769
		Wingwalls (18˚ and 33.7˚) with beveled top edge	1135	36770
		Side- or slope-tapered	1171	57/1
		Non-offset flares (45˚) with 3/4-in chamfers	1181	36860
		Non-offset flares (18.4˚) with 3/4-in chamfers	1182	36861
		Non-offset flares (18.4˚) with skewed barrel	1183	36862
		Offset flares (45˚) with beveled top edge	1191	36891
		Offset flares (33.7˚) with beveled top edge	1192	36892
		Offset flares (18.4˚) flares with beveled top edge	1193	36893
	Horizontal ellipse	Headwall with square edge	1211	29/1
		Headwall with grooved edge	1212	29/2
		Projecting with grooved edge	1251	29/3
	Vertical ellipse	Headwall with square edge	1311	30/1
		Headwall with grooved edge	1312	30/2
		Projecting with grooved edge	1351	30/3
Corrugated metal	Circular	Headwall	2011	36556
		Mitered to fill slope	2041	36557
		Projecting from fill slope	2051	36558
		Side- or slope-tapered	2071	55/2
	Rectangular	Headwall	2111	16-19/2
		Projecting from fill with thick wall	2151	16-19/3
		Projecting from fill with thin wall	2152	16-19/5
	Pipe-arch (18-in corner radius)	Headwall	2511	34/1
		Mitered to fill slope	2541	34/2
		Projecting from fill slope	2551	34/3
	Arch	Headwall	2711	41/1
		Mitered to fill slope	2741	41/2
		Projecting from fill slope	2751	41/3
Structural metal plate	Pipe-arch (18-in corner radius)	Headwall with square edge	3511	35/2
		Headwall with beveled edge	3512	35/3
		Projecting from fill slope	3551	35/1
	Pipe-arch (31-in corner radius)	Headwall	3611	36/1
		Mitered to fill slope	3641	36/2
		Projecting from fill slope	3651	36/3

GATE

Gate Structure Data Set

Gate structure data records immediately follow a GATE data set identification record. Two data records are needed to describe each gate structure. Gate structure data consist of identification strings, numbers of the node points on the upstream and downstream ends of structures, and discharge coefficients and dimensions of both underflow and overflow gates. Optionally, gate structure data records may be read from a separate data file. The data set is terminated with one or more blank records.

GATE Identification Record

Order	*Value*	*Description*
1	"GATE"	Data set identifier.
2	±	Default tailwater elevation, in ft (m), assigned to all gate structures for which tailwater elevations are not specified.
3	+	Default minimum head difference, in ft (m), assigned to all gate structures for which minimum head differences are not specified.
4	0 or 1	Gate structure data record option code as follows: 0 = All gate structure data records will follow in the data stream. 1 = All gate structure data records will be read from a separate data file. Enter the complete name of the gate structure data file on the following record.

GATE.1 Record

1	"text"	Gate structure identification string (8 characters maximum). This is a unique text string used to identify the gate.
2	+	Number of the node point at one end of the gate structure.
3	0 or +	If 0, flow is allowed to leave the finite element network through the culvert from the previously specified node point. Otherwise, the value is the number of the node point at the culvert outlet.
		Gate structure node points may be located on either the boundary or the interior of the network.
4	"text"	Comment used to describe the gate structure (32 characters maximum).

GATE.2 Record

1	+	Underflow gate opening height h_{gu}, in ft (m)..
2	+	Underflow gate opening width w_{gu}, in ft (m).

GATE

Order	*Value*	*Description*
3	±	Underflow gate bottom elevation z_{gu}, in ft (m).
4	+	Underflow gate inclination angle θ, in deg. ($0° \le \theta \le 90°$)
5	+	Overflow gate discharge coefficient C_{go} (dimensionless).
6	+	Overflow gate width w_{go}, in ft (m).
7	±	Overflow gate bottom or crest elevation z_{go}, in ft (m).
		Repeat the GATE.1-GATE.2 data record sequence for each gate structure.

Terminate the GATE data set with one or more blank records

Drop-inlet Spillway Data Set

Drop-inlet spillway data records immediately follow a DROP data set identification record. Two records are needed for each drop inlet spillway. Drop-inlet spillway data consist of an identification string, the node points on the upstream and downstream ends of the structure; a discharge coefficient, crest length, and crest elevation used to compute weir flow at the inlet; a discharge coefficient and cross-sectional area used to compute orifice flow at the inlet; and a discharge coefficient and cross sectional area used to compute conduit flow through the structure. Optionally, all drop inlet spillway records may be read from a separate data file. The data set is terminated with one or more blank records.

DROP Identification Record

Order	*Value*	*Description*
1	"DROP"	Data set identifier.
2	0 to 2	Code that defines the drop-inlet spillway flow report(s) to be printed at the end of printed time steps and at the end of a steady-state simulation (0 = just summary reports, 1 = just comprehensive reports, 2 = both summary and comprehensive reports).
3	0 or 1	Drop-inlet spillway data record code as follows: 0 = All drop-inlet spillway records will follow in the data stream. 1 = All drop-inlet spillway records will be read from a separate data file. Enter the complete name of the drop inlet spillway data file on the following record.

DROP.1 Record

1	"text"	Drop-inlet spillway identification string (8 characters maximum). This is a unique text string used to identify the spillway.
2	+	Number of the node point at the entrance of the drop inlet spillway.
3	0 or +	If 0, flow is allowed to leave the finite element network through the drop inlet spillway from the previously specified node point. Otherwise, the value is the number of the node point at the outlet of the drop inlet spillway conduit.
		The drop inlet spillway node points may be located either on the boundary or the interior of the finite element network.
4	"text"	Comment used to describe the drop inlet spillway (32 characters maximum).

DROP.2 Record

DROP

Order	*Value*	*Description*
1	+	Weir discharge coefficient C_{dw} (dimensionless).
2	+	Weir crest length L_{dw}, in ft (m).
3	+	Weir crest elevation z_{dw}, in ft (m).
4	+	Orifice discharge coefficient C_{do} (dimensionless).
5	+	Orifice cross-sectional area A_{do}, in ft^2 (m^2).
6	+	Conduit discharge coefficient C_{dc}, (dimensionless).
7	+	Conduit cross-sectional area A_{dc}, in ft^2 (m^2).
8	±	Elevation of the hydraulic energy head at the conduit outlet, in feet (meters). This value is needed only if the second drop inlet node point is not specified and flow is allowed to leave the finite element network through the drop inlet spillway.
		Repeat the DROP.1-DROP.2 data record sequence for each drop-inlet spillway.

Terminate the DROP data set with one or more blank data records.

LINK

Channel Link Data Set

Channel link data records immediately follow a LINK data set identification record. A channel link is a wide open-channel segment with a horizontal bed that can be used to link together node points of the two-dimensional network. In some cases, roadway and railroad embankments can be represented more accurately as links than as weir segments. Two records are needed for each channel link. Channel link data consist of an identification string, the numbers of the node points on the upstream and downstream sides of the link, the width and length of the channel, an entrance loss coefficient, an outlet loss coefficient, the elevation of the bed of the horizontal bed of the channel link, and a Manning roughness coefficient that describes the flow resistance of the channel bed. Optionally, all channel link records may be read from a separate data file. The data set is terminated with one or more blank data records.

LINK Identification Record

Order	*Value*	*Description*
1	"LINK"	Data set identifier.
2	0 to 2	Channel link report code that defines the report(s) to be printed at the end of printed time steps and at the end of a steady-state simulation (0 = just summary reports, 1 = just comprehensive reports, 2 = both summary and comprehensive reports).
3	±	Default tailwater elevation, in ft (m), assigned to all channel links for which tailwater elevations are not assigned.
4	+	Default minimum head difference, in ft (m), assigned to all channel links for which minimum head differences are not specified.
5	0 or 1	Channel link data record option code as follows: 0 = All channel link records will follow in the data stream. 1 = All channel link records will be read from a separate data file. Enter the complete name of the channel link data file on the following record.

LINK.1 Record

1	"text"	Channel link identification string (8 characters maximum). This is a unique text string used to identify the link.
2	+	Number of the node point on one end of the channel link.
3	0 or +	If 0, flow is allowed to leave the finite element network through the channel link from the previously specified node point. Otherwise, the value is the number of the node point at the other end of the channel link.

LINK

Order	*Value*	*Description*
	☞	The channel link node points may be located on either the boundary or the interior of the network.
4	"text"	Comment used to describe the channel link (32 characters maximum).
		LINK.2 Record
1	+	Width of the channel link w_l through which water can flow, in ft (m).
2	+	Length of the channel link L_{ll} from the upstream end to the downstream end, in ft (m).
3	+	Bed elevation of the first channel link node z_{l1}, in ft (m).
4	+	Bed elevation of the second channel link node z_{l2}, in ft (m), if the second node is specified, or the bed slope of the channel link (a positive value denotes a downward slope) if flow is allowed to exit the network at the first node point.
5	+	Entrance loss coefficient K_{le}. This coefficient depends on conditions at the upstream end of the channel link but generally $0.1 \le K_{le} \le 0.5$.
6	+	Manning's roughness coefficient that describes flow resistance of the channel link bed. This coefficient depends of the condition of the channel bed. Beds with many flow obstructions such as brush and trees, will have larger roughness coefficients than beds that are less resistance to flow.
7	±	Tailwater elevation, in ft (m), used in calculations if only one node is specified for the channel link.
8	+	Minimum head difference in ft (m), needed for channel link calculations. Zero flow is assigned if the head difference is less than this value. Default = 0 ft (m).
	☞	Repeat the LINK.1-LINK.2 data record sequence for each channel link.

Terminate the LINK data set with one or more blank data records.

RATE

Rating Curve Data Set

Rating curve data records immediately follow a RATE data set identification record. Rating curve data consist of an identification string, and a tabular relation between the water-surface elevation and the flow rate through a channel cross section. The three-record set is repeated for each rating curve that is to be defined. Optionally, all rating curve records may be read from a separate data file. The data set is terminated with one or more blank records.

RATE Identification Record

Order	*Value*	*Description*
1	"RATE"	Data set identifier.
2	0 or 1	Rating curve data record option code as follows: 0 = All rating curve records will follow in the data stream. 1 = All rating curve data records will be read from a separate data file. Enter the complete name of the rating curve data record file on the following record.

RATE.1 Record

1	"text"	Rating curve identification string (8 characters maximum). This is a unique text string used to identify the rating curve.
2	"text"	Comment used to describe the rating curve (32 characters max).

RATE.2 Record

1 to 8	+	Water-surface elevations that correspond to flow rates in the same field on the following record. Enter up to eight values.

RATE.3 Record

1 to 8	+	Flow rates that correspond to the upstream water-surface elevation in the same field on the previous record.
		Repeat the RATE.1-RATE.2-RATE.3 data record sequence for each rating curve.

Terminate the RATE data set with one or more blank records.

PIER

Pier Data Set

Pier data records immediately follow a PIER data set identification record. Two records are needed for each bridge pier. However, if piers are grouped closely together and are contained in a single element their widths may be combined to form a single "equivalent" pier to calculate drag force. Pier data consist of a code that indicates the expression used to calculate local pier scour depth, an identification string, the coordinates of the center of the pier, an optional comment describing the pier, the pier width, the pier length, a dimensionless drag coefficient, and a code that describes the shape of the pier nose (needed if scour calculations are to be carried out). Optionally, all pier records may be read from a separate data file. The data set is terminated with one or more blank data records.

PIER Identification Record

Order	*Value*	*Description*
1	"PIER"	Data set identifier.
2	0 to 2	Pier scour report code that defines the report(s) to be printed at the end of printed time steps and at the end of a steady-state simulation (0 = just summary reports, 1 = just comprehensive reports, 2 = both summary and comprehensive reports).
3	+	Local pier scour equation code read as "*i.level*", where the integer part of the number *I* = equation code, and the fractional part of the number *level* = design scour depth confidence level used in Froehlich's equation. The *HEC-18* pier scour equation (Richardson and Davis 1995) will be used if *I* = 0, 1, or 3; and Froehlich's (1988) pier scour equation will be used if *I* = 2 or 3. For example, enter 2.995 to request Froehlich's equation with a design confidence level of 0.995 or 99.5%. The confidence level is ignored if the just the *HEC-18* equation is selected (that is, if *I* = 1) and can be omitted. Default *level* = 0.5 if the fractional part of the value is zero.
4	+	Pier sediment specific gravity used in local scour calculations. Default = 2.65.
5	+	Pier rock riprap equation code (0 or 1 = *HEC-18* equation, 2 = Froehlich's equation).
6	+	Riprap safety factor. Default = 1.
7	+	Riprap specific gravity. Default = 2.65.
8	0 or 1	Rock riprap angularity code (0 = rounded, 1 = angular). Default = 0 (rounded rock).
9	+	Rock riprap angle of repose, in degrees. Default = 35^{o} for rounded rock, and 40^{o} for angular rock.
10	0	All pier records will follow in the data stream.

PIER

Order	*Value*	*Description*
	1	All pier records will be read from a separate data file. Enter the complete name of the pier data file on the following record.
		PIER.1 Record
1	"text"	Pier identification string (8 characters maximum). This is a unique text string used to identify the pier.
2	±	*X* coordinate of the center of the bridge pier, in ft (m).
3	±	*Y* coordinate of the center of the bridge pier, in ft (m).
4	"text"	Comment string used to describe the bridge pier (32 characters maximum).
		PIER.2 Record
1	+	Pier width averaged over the depth of flow at the upstream end of the pier, in ft (m).
2	+	Pier length (from nose to tail), in ft (m).
	☞	*Aligned Columns.* Groups of aligned, identical, closely-spaced columns (that is, with columns spaced less than five column diameters apart such as commonly found in pier bents) are to be treated as a *single* pier having a length equal to the combined length of all the piers in the group in accordance with *HEC-18* scour calculation guidelines (Richardson and Davis 1995).
3	±	Pier alignment angle, in degrees measured from the *X*-axis.
4	+	Drag coefficient for the pier (dimensionless). Default = 1.0. Drag coefficients for a few column shapes based on frontal area follow:

Column shape and approach flow alignment	*Drag coefficient based on frontal area*
Round cylinder 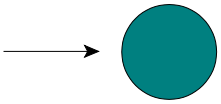	1
Square cylinder 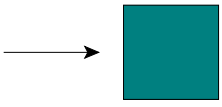	2.2
Square cylinder 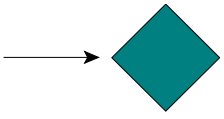	1.6

PIER

Order *Value* *Description*

Square cylinder with rounded corners

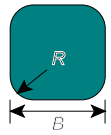

R/B	C_D
0	2.2
0.02	2
0.17	1.2
0.33	1

Hexagonal cylinder

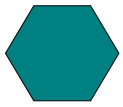

1

Hexagonal cylinder

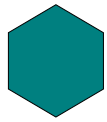

0.7

Round-nosed section

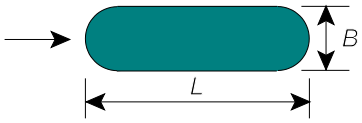

L/B	C_D
1	1
2	0.7
4	0.68
6	0.64

Square-nosed section

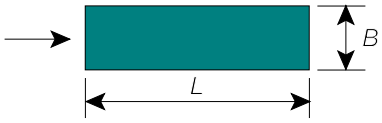

L/B	C_D
1	2.2
2	1.8
3	1.3
6	0.9

5 0 to 3 Pier nose shape code defined as follows: 1 = round-nosed, 2 = square-nosed , 3 = sharp-nosed.

Pier nose shape code controls calculation of local scour. Local scour is not calculated for the pier if the nose shape code = 0.

6 + Median diameter D_{50}, in mm, of bed material surrounding the pier.

7 + Bed material particle diameter for which 90% of the sediment by weight is finer D_{90}, in mm.

Bed material diameters are needed only if armoring is to be taken into account by the *HEC-18* equation, or if Froehlich's equation is used.

Order	*Value*	*Description*
8	-1 to 3	Bedform code defined as follows: 0 =, 2

0 = Plane bed or ripples (transverse ridges of cohesionless sediments less than about 2 in or 0.05 m high).

1 = Small dunes with height ≤ 10 ft (3 m).

2 = Medium dunes with 10 ft (3 m) < height ≤ 30 ft (9 m).

3 = Large dunes with height > 30 ft (9 m).

-1 = Bedform codes are estimated using Yalin's (1964) formula to calculate bedform heights.

The bedform code is needed when the *HEC-18* equation is used to account for the effect of transient forms on the streambed surface that cause the depth of scour below the average ambient bed elevation at a pier to vary with time.

Terminate the PIER data set with one or more blank data records.

FLUX

Flux Line Data Set

Flux line data immediately follow a FLUX data set identification record. Flux line data consist of two records. The first record contains a flux line identification string. The second record contains a list of node points that can be repeated as many times as needed for a flux line consisting of at most 260 node points. The last node point in the flux line list is given a negative value. Flow across the first flux line is used as a base flow against which other calculated flows are compared. Flux lines may be composed of either straight or curved element sides. The data set is terminated with one or more blank data records.

FLUX Identification Record

Order	*Value*	*Description*
1	"FLUX"	Data set identifier.

FLUX.1 Record

1	"text"	Flux line identification string. The first 10 characters need to be a unique identifier.
2	"text"	Comment used to describe the flux line (32 characters maximum).

FLUX.2 Record

1 to 1000	+	A list of node numbers that define a connected series of straight or curved element sides across which total flow is to be computed. Up to 1000 node points may be used to define a flux line. The node list is terminated with a negative entry.

Terminate the FLUX data set with one or more blank records.

GAGE

Gage Point Data Set

Gage point data immediately follow a GAGE data set identification record. Gage point data identify locations within a network for which solutions are reported at the end of a time step and at the end of a simulation. Gage points may be placed where a physical gage is located so measured and computed values of velocity and water-surface elevation can be easily compared. However, gage points can also be used to highlight solutions at specific locations within a network that are of interest. Gage points can be placed at specific node points, or a defined coordinates. Comment strings can be included to describe gage points locations. The data set is terminated with one or more blank records.

GAGE Identification Record

Order	*Value*	*Description*
1	"GAGE"	Data set identifier.

GAGE Record

1	"text"	Gage point identification string (8 characters maximum). This is a unique text string used to identify the gage.
2	0 or +	If 0, the location of the gage point is given by coordinates specified in the following two fields; otherwise, the value is the number of the node at which the gage point is located.
3	±	*X* coordinate of the location of the gage point, in ft (m).
4	±	*Y* coordinate of the location of the gage point, in ft (m).
5	±	Elevation of the gage, in ft (m).
6	"text"	Brief description of the gage point that will be included in printed output (32 characters maximum).
		Repeat GAGE records for each gage point to be reported.

Terminate the GAGE data set with one or more blank data records.

SEDI

General Sediment Data Set

General sediment data immediately follow an SEDI data set identification record. The data describe general bed sediment properties and sediment transport solution parameters. There are nine records in the sediment data set. The ninth record is a repeated record, and is needed only if bed-composition printout nodes are specified.

SEDI Identification Record

Order	*Value*	*Description*
1	"SEDI"	Data set identifier.

SEDI.1 Record

1	1 to 19	Sum of the codes of the following printed output options that are desired: *Code* *Option Description* 1 Sediment transport report by size classes. 2 Node point bed composition report. 16 Sediment transport degree-of-freedom equation number report.
2	0 or 1	Sediment initial condition data file option code as follows: 0 = All initial sediment data will be entered on data records. 1 = Initial sediment transport data will be read from a data file. However, additional initial sediment transport data that will supercede values read from the initial sediment transport data file may be entered on data records. The default name of the initial sediment transport data file is "FST2DH.sed".
		 Initial sediment transport data files are usually sediment transport solution output files created by previous simulations.
3	0 or ±1	Sediment transport solution output file option code as follows: 0 = Sediment transport solutions will not be written to a data file. ±1 = Sediment transport solutions will be written to a data file at the end of a steady-state run and at the end of selected time-steps during a time-dependent run. If a positive value is entered, the solution will be written in "text" form; if a negative value is entered, the solution will be written in "binary" form. The default name of the sediment transport solution data file is "FST2DH.sed".

Order	*Value*	*Description*
4	0 or 1	Bed composition report option code as follows: 0 = Bed composition will not be reported in printed output. 1 = Bed composition will be reported at nodes specified on SEDI.9 data records.
5	0 or 1	balancing diffusion option code as follows: 0 = Balancing diffusion terms will be added to the sediment transport advection diffusion equation. 1 = Balancing diffusion terms will not be added.

SEDI.2 Record

1	1 to 99	Sediment solution iteration code read as *KKJJII* where: *II* = maximum number of initial full-Newton iterations to be carried out (usually from 5 to 10). *JJ* = maximum number of quasi-Newton iterations to be carried out after all the initial full- Newton iterations, and after each additional full-Newton iteration. *KK* = maximum number of additional full-Newton iterations to be carried out. ☞ The maximum allowable number of iterations for a steady-state solution or for a time step of a time-dependent solution is 99. Therefore, $II + JJ + KK \times (1 + JJ)$ needs to be less than or equal to 99. The solution may be stopped before the maximum number of iterations are completed if convergence criteria are satisfied.
2	+	Convergence tolerance for maximum absolute changes to bed elevation, in ft (m). Default = 0 ft (m).
3	+	Convergence tolerance for maximum absolute changes to sediment concentrations, in vol/vol $\times 10^6$. Default = 0. ☞ If the convergence tolerances for bed elevation and sediment concentrations are satisfied, the time-dependent solution for the current time step will be considered to have converged.
4	+	Relaxation factor $0 < \omega_r \leq 1$ used in the sediment transport solution. Default $\omega_r = 1$.
5	+	Printed iteration control code. Results from every *i*th iteration will be printed, where *I* is the specified value. Results from the last iteration are always printed for printed time steps.

SEDI

Order	*Value*	*Description*
6	+	Number of ranked changes included in printed output. Up to the 10 largest changes at node points for each solution variable will be printed. Default = 1.
7	hhhh:mm:ss	Printed report time interval. Sediment transport solutions will be reported at this incremental time during time-dependent simulations. Default = "0000:00:00".
8	hhhh:mm:ss	Solution output time interval. Sediment transport solutions will be written to output files at this incremental time during time-dependent simulations. Default = "0000:00:00".

SEDI.3 Record

1 ± Sediment transport capacity formula code defined as follows:

Code	*Sediment Transport Capacity Formula*
0 =	Power formula (using specified coefficients)
1 =	Engelund-Hansen formula
2 =	Ackers-White formula
3 =	Laursen formula
4 =	Yang sand and gravel formulae
5 =	Meyer-Peter and Mueller formula
6 =	Ackers-White-Day formula
-1 =	A combination of sediment transport capacity formulae suggested by Garbrecht et al. (1995) will be used to calculate equilibrium sediment concentrations based on particle size class diameter as follows:

Particle Diameter D	*Formula*
$D < 0.25$ mm	Laursen
0.25 mm $\le D <$ 8.0 mm	Yang sand and gravel
8.0 mm $\le D$	Meyer-Peter and Mueller

2 + Bed sediment porosity η_s applied at all nodes. Default $\eta_s = 0.4$.

3 + Sediment specific gravity S_s applied to all particle size classes. Default $S_s = 2.65$.

Order	*Value*	*Description*
4	+	Water temperature T_{water}, in °F (°C). Default T_{water} = 68° F (20° C).
5	+	Water kinematic viscosity ν_{water}, in ft^2/sec (m^2/s). Default values are found based on water temperature. For T_{water} = 68° F (20° C), ν_{water} = 1.082×10^{-6} ft^2/sec (1.005×10^{-6} m^2/s).
6	+	Sediment power equation coefficient *a*.
7	+	Sediment power equation exponent *b*.
	☞	If the power equation $q_s = aq^b$ is used to calculate equilibrium sediment concentrations, where q_s = unit width volumetric sediment transport rate, and q = unit width flow rate, then both *a* and *b* need to be specified as non-zero values.
8	+ or 0	Sediment erosion rate coefficient K_{es}. Default K_{es} = 1.
	-	Sediment erosion rate coefficient K_{es} will be calculated as

$$K_{es} = \frac{1}{\frac{T_a}{H} + \left(1 - \frac{T_a}{H}\right)\exp\left[-1.5\frac{w_{si}}{u_*}\left(\frac{T_a}{H}\right)^{-1/6}\right]}$$

where T_a = thickness of the surface or active layer, H = water depth, w_s = terminal fall velocity or settling velocity of a sediment particle in still water, and u_* = bed friction velocity (Armanini and Di Silvio 1988).

SEDI.4 Record

1	+	Default active bed-layer thickness, in ft (m).
2	+	Default deposition bed-layer thickness, in ft (m).
3	+	Default original bed-layer thickness, in ft (m).

SEDI.5 Record

1 to 8	+	Particle size class diameters, in mm, in ascending order (that is, from smallest to largest). Up to eight particle size classes can be specified. These diameters characterize the fraction of particles in each particular size class specified in the following three data records for the active bed-layer, deposition bed-layer, and original bed-layer, respectively.

SEDI.6 Record

1 to 8	+	Default active bed-layer size class fractions corresponding to particle size classes defined on the SEDI.5 data record.

SEDI

Order	*Value*	*Description*
		SEDI.7 Record
1 to 8	+	Default deposition bed-layer size class fractions corresponding to particle size classes defined on the SEDI.5 data record.
		SEDI.8 Record
1 to 8	+	Default original bed-layer size class fractions corresponding to particle size classes defined on the SEDI.5 data record.
		SEDI.9 Record
1 to 260	+	List of nodes for which detailed bed composition reports are provided in printed output. Repeat the SEDI.9 data record to enter up to 260 node points.

Terminate the SEDI data set with one or more blank records.

Bed Elevation and Sediment Composition Initial Data

Bed elevation and sediment composition initial data records immediately follow a BEDS data set identification record. These data describe the initial bed elevation and its time-derivative, and composition of the active, deposition, and original bed layers at node points. This four-record group needs to be repeated for each node at which bed composition data are specified. The data set is terminated with one or more blank records.

BEDS Identification Data Record

Order	*Value*	*Description*
1	"BEDS"	Data set identifier.
		BEDS.1 Record
1	+	Node number.
2	±	Bed elevation at the node, in ft (m).
3	±	Time derivative of bed elevation at the node, in ft/sec (m/s).
4	+	Active bed-layer initial thickness at the node, in ft (m).
5	+	Deposition bed-layer initial thickness at the node, in ft (m).
6	+	Original bed-layer initial thickness at the node, in ft (m).
		BEDS.2 Record
1 to 8	+	Active bed-layer size class fractions corresponding to particle size classes defined on the SEDI.5 data record.
		BEDS.3 Record
1 to 8	+	Deposition bed-layer size class fractions corresponding to particle size classes defined on the SEDI.5 data record.
		BEDS.4 Record
1 to 8	+	Original bed-layer size class fractions corresponding to particle size classes defined on the SEDI.5 data record.
	☞	Repeat the BEDS.1-BEDS.2-BEDS.3-BEDS.4 data record sequence for each node at which initial bed composition data are specified.

Terminate the BEDS data set with one or more blank data records.

SEDC

Sediment Concentration Initial Conditions Data

Sediment concentration initial condition data records immediately follow a SEDC data set identification record. These data describe the initial total discharge-weighted sediment concentrations at node points. This three-record group needs to be repeated for each node at which sediment concentration data are specified. The data set is terminated with one or more blank records.

SEDC Identification Data Record

Order	*Value*	*Description*
1	"SEDC"	Data set identifier.
		SEDC.1 Record
1	+	Node number.
		SEDC.2 Record
1 to 8	+	Total discharge-weighted sediment concentrations (volume of sediment per unit volume of water-sediment mixture) corresponding to particle size classes defined on the SEDI.5 data record.
		SEDC.3 Record
1 to 8	+	Time-derivatives of total discharge-weighted sediment concentrations (volume of sediment per unit volume of water-sediment mixture) corresponding to particle size classes defined on the SEDI.5 data record.
		Repeat the SEDC.1-SEDC.2-SED.3 data record sequence for each node at which initial sediment concentration data are specified.

Terminate the SEDC data set with one or more blank data records.

RESE

Resequencing Data

Resequencing data immediately follow an RESE data set identification record. Element resequencing data consist of control instructions, and a list of elements that are used to begin the ordering of elements for a more efficient solution by the frontal method. As a general rule, try at least two starting locations, one at either end of a finite element network. The data set is terminated with one or more blank data records.

RESE Identification Record

Order	*Value*	*Description*
1	"RESE"	Data set identifier.

RESE Record 1

1	1 or 2	Element resequencing method code as follows: 1 = Resequencing will be carried out using the minimum frontgrowth method. 2 = Resequencing will be carried out using the level structure method.
2	+	Smallest maximum-length-of-stay used in minimum frontgrowth method. Default = ⅓ × number of elements in the network.
3	+	Largest maximum-length-of-stay used in minimum frontgrowth method.
2	+	Maximum-length-of-stay increment. Maximum-length-of-stay is increased from the minimum value to the maximum value by this increment. An element sequence is calculated for each maximum-length and the best sequence is retained for use in equation solution.

RESE Record 2

1 to 80	+	List of element numbers used to begin resequencing. Each list is terminated with a negative element number. Up to 80 elements may be contained in each list.
		Repeat the set RESE.1-RESE.2 data record sequence for each starting element list.

Terminate the RESE data set with one or more blank data records.

PROF

Profile Data

Profile data immediately follow a PROF data set identification record. Profile data consist of lists of node points for which solution data are written to an output file. If the nodes form a spatially sequential list, the output data can be used to plot quantity distributions either in transverse flow directions (cross-section plots), or in longitudinal flow directions (profile plots). The data consist of a profile identifier, a data code for each profile, and a list of nodes for each profile. The data set is terminated with one or more blank data records.

PROF Identification Record

Order	*Value*	*Description*
1	"PROF"	Data set identifier.

PROF Record 1

1	"text"	Profile identification string (8 characters maximum). This is a unique text string used to identify the profile.
2	1 to 15	Sum of the codes of the following items to be written to the profile data file:

Code	*Item Description*
1	Bed elevation
2	Water-surface elevation
4	Velocity magnitude
8	Unit flow rate magnitude

3	"text"	Brief description of the profile that will be included in printed output (32 characters maximum).

PROF Record 2

1 to 1000	+	List of node numbers in the profile. Up to 1000 nodes can be included in each profile. Each list is ended with a negative node number.
		Repeat the set PROF.1-PROF.2 data record sequence for each profile. Up to 10 profiles can be defined.

Terminate the PROF data set with one or more blank data records.

LOAD

Incremental-Load Data Set

Incremental load data immediately follow a LOAD data set identification record. An incremental-load data set immediately precedes boundary condition data (BOUN and BSEC data sets), that are changed in an incremental fashion in the course of achieving steady-state solution convergence. Incremental loading strategies are used when large changes are made to boundary conditions, such as during *cold starts* when trivial solutions (that is, a level water surface and zero unit flow rates everywhere) are used to begin computations. Incremental load data records contain revised iteration codes, solution convergence tolerances, and relaxation factors. An incremental load data set is needed for each set of data changes you want to make. LOAD data sets along with all accompanying BOUN and BSEC data sets form *load data packets*. All load data packets need to appear at the end of the input data stream, before any following TIME data sets.

LOAD Identification Record

Order	*Value*	*Description*
1	"LOAD"	Data set identifier.
2	"text"	Comment string (32 characters maximum).

LOAD Record

1	0	Iteration control code is not changed.
	+	Revised iteration control code read as *KKJJII*, where *II*, *JJ*, and *KK* for each time step are the same as described on the SWMS.4 data record.
2	0	Unit flow rate solution convergence tolerance is not changed.
	+	Revised solution convergence tolerance for maximum absolute changes to *X* and *Y* direction unit flow rates, in ft^2/sec (m^2/s).
3	0	Water-surface elevation solution convergence tolerance is not changed.
	+	Revised solution convergence tolerance for maximum absolute changes to water-surface elevation, in ft (m).
4	0	Bed-elevation solution convergence tolerance is not changed.
	+	Revised solution convergence tolerance for maximum absolute changes to bed-elevation, in ft (m).
5	0	Discharge-weighted sediment concentration solution convergence tolerance is not changed.
	+	Revised solution convergence tolerance for maximum absolute changes to discharge-weighted sediment concentration, in vol/vol $\times 10^6$.
6	0	Relaxation factor ω_r is not changed.
	+	Revised relaxation factor $0 < \omega_r \leq 2$ used in equation solution.

TIME

Time-dependent Data Set

Time-dependent data records immediately follow a TIME data set identification record. Time-dependent data sets immediately precedes updated boundary condition data sets used in time-dependent (unsteady) simulations. Time-dependent data records contain the simulation time in hours at which the following data become effective, solution control parameters and general system specifications that apply to all nodes in the network. TIME data sets along with all accompanying BOUN, BSEC, WIND, and STORM data sets form *time data packets*. All time data packets need to appear in chronological order at the end of the input data stream.

TIME Identification Record

Order	*Value*	*Description*
1	"TIME"	Data set identifier.
2	0	Boundary conditions will not change until the simulation time equals or exceeds the update simulation time specified on the following record.
	1	Boundary conditions will be interpolated linearly based on time between those at the previous update and those at the following update.

TIME Record

1	hhhh:mm:ss	Update simulation time at which the following boundary condition (BOUN), boundary cross section (BSEC), wind data (WIND), or tropical storm (STORM) data sets become effective.
2	0	Iteration control code will not be changed.
	+	Revised iteration control code read as *KKJJII*, where *II*, *JJ*, and *KK* for each time step are the same as described for steady-state solutions on the SWMS.4 data record. The maximum total number of iterations that can be carried out for a single time step is 99.
3	0000:00:00	Time step length will not be changed.
	hhhh:mm:ss	Revised time step length Δt.
4	0	Time integration factor θ will not be changed.
	+	Revised time integration factor θ ($0.5 \leq \theta \leq 1.0$).
5	0 or +	Default wind speed will not be changed.
	+	Default wind speed, in ft/sec (m/s). This value is assigned to each node in the network unless superceded by values read from the WIND data set.
6	0	Default wind direction angle will not be changed.

Order	*Value*	*Description*
	+	Revised default wind direction angle, in degrees measured clockwise from true north. Wind direction is the direction *from which* the wind is blowing. This value is assigned to each node in the network unless superceded by values read from the WIND data set.
7	0	Air mass density will not be changed.
	+	Revised air mass density ρ_{air}, in slugs/ft^3 (kg/m^3).
8	0	Relaxation factor ω_r will not be changed.
	+	Revised relaxation factor $0 < \omega_r \leq 2$ used in equation solution.

Mesh Data File

Finite element meshes or netowrks are described by elements and nodes. Two-dimensional elements are either three- or four-sided polygons (triangles or quadrilaterals) that are defined by a series of nodes located at their vertices, midside points, and, optionally, at the center of quadrilaterals. One-dimensional elements are polylines defined by three nodes, one at each end or vertex, and one located in between the two ends. As an option, *FST2DH* can read element and node data from a mesh data file. Mesh data files may be in either text or binary form. Data record format descriptions follow.

Record 1

Order	*Value*	*Description*
1	"text"	File header record. The first 32 characters are the *project stamp*, which is used to identify related data files.

Record 2

1	"US" or "SI"	Units identifier, U.S. customary (US) or International System (SI).

Record 3

1	+	Number of 2D node records to follow.
2	+	Number of 2D element records to follow.
3	+	Number of 1D node records to follow.
4	+	Number of 1D element records to follow.
5	+	Number of 1D cross section three-record series to follow.

2D Node Record

1	+	Node number.
2	±	X coordinate in ft (m) of the node.
3	±	Y coordinate in ft (m) of the node.
4	±	Ground (bed) elevation in ft (m) at the node.
5	±	Ceiling (bottom of bridge deck) elevation in ft (m) at the node.
6	"text"	Comment string (32 characters maximum).
		Repeat 2D node records the specified number of times. Coordinates and elevations will be converted to the appropriate system of units, if needed, when a network data file is read.

2D Element Record

1	+	Element number.
2 to 10	0 or +	Element connectivity list. The sequence of nodes connected to the element: six nodes for a triangular element, eight nodes for a

Order	*Value*	*Description*
		"serendipity" quadrilateral element, or nine nodes for a "Lagrangian" quadrilateral element. Begin connectivity lists at any vertex node and proceed in a counterclockwise direction around the element. Enter center nodes last for nine-node quadrilateral elements.
11	±	Element property set number.
12	+	Element assembly sequence.
13	"text"	Comment string (32 characters maximum).
		Repeat 2D element records the specified number of times. Velocities and water-surface elevations, along with their time derivatives, will be converted to the appropriate system of units if needed when initial conditions are read from a flow data file.

1D Node Record

1	+	Node number.
2	±	X coordinate in ft (m) of the node.
3	±	Y coordinate in ft (m) of the node.
4	"text"	Cross section identifier (8 characters maximum) associated with the node (only at vertex nodes).
5	"text"	Comment string (32 characters maximum).
		Repeat 1D node records the specified number of times. Coordinates and elevations will be converted to the appropriate system of units, if needed, when a network data file is read.

1D Element Record

1	+	Element number.
2 to 4	+	Element connectivity list. The sequence of three nodes connected to the element.
5	±	Element type code defined as follows: 0 = channel element, 1 = bridge element, 2 = culvert element, 3 = roadway element.
6	+	Element assembly sequence.
7	+	Kinematic eddy viscosity, in ft^2/sec (m^2/s).
8	"text"	Comment string (32 characters maximum).
		Repeat 1D element records the specified number of times. Flow rates and water-surface elevations, along with their time derivatives, will be converted to the appropriate system of units if needed when initial conditions are read from a flow data file.

Order	*Value*	*Description*
		1D Cross Section Record (1)
1	"text"	Cross section identifier (8 characters maximum).
2	±	Section origin *X* coordinate, in ft (m).
3	±	Section origin *Y* coordinate, in ft (m).
4	±	Section azimuth, in deg. The section is considered straight.
5	+	Manning roughness coefficient of the left overbank.
6	+	Manning roughness coefficient of the main channel.
7	+	Manning roughness coefficient of the right overbank.
8	"text"	Comment string (32 characters maximum).
		1D Cross Section Record (2)
1 to 8	+	Horizontal distances corresponding to bed elevations specified on the following record, in ft (m).
		1D Cross Section Record (3)
1 to 8	±	Bed elevations corresponding to horizontal distances specified on the preceding record, in ft (m).
		Each cross section is defined by exactly eight ground points. The third and sixth points represent the two channel banks. Repeat the three-record 1D cross section record series the specified number of times.

Flow Data File

Flow solution data are written to files at the end of steady-state simulations, and at selected intervals during time-dependent simulations. These files may be read at the start of subsequent simulations to obtain initial conditions. Flow data files may be in either text or binary form. Data record format descriptions follow.

Header Record

Order	*Value*	*Description*
1	"text"	File header record. The first 32 characters are the *project stamp*, which is used to identify related data files.

Units Record

1	"US" or "SI"	Units identifier, U.S. customary (US) or International System (SI).

Time and Count Record

1	hhhh:mm:ss	Simulation time of following flow data.
2	+	Number of flow data records to follow.

Flow Data Record

1	+	Node number to which the following flow data apply.
2	±	X-direction depth-averaged velocity in ft/sec (m/s).
3	±	Y-direction depth-averaged velocity in ft/sec (m/s).
4	±	Water-surface elevation in ft (m).
5	±	Time-derivative of X-direction depth-averaged velocity in ft/sec/sec (m/s/s).
6	±	Time-derivative of Y-direction depth-averaged velocity in ft/sec/sec (m/s/s).
7	±	Time-derivative of water-surface elevation in ft/sec (m/s).
		Repeat the Flow Data Record the specified number of times.

Sediment Data File

Sediment transport solution data are written to files at the end of steady-state simulations, and at selected intervals during time-dependent simulations. These files may be read at the start of subsequent simulations to obtain initial conditions. Sediment data files may be in either text or binary form. The header and units records apply only at the beginning of a sediment data file, all other data records and data record sequences are repeated for each simulation time at which solution data are to be read. Data record format descriptions follow.

Header Record

Order	*Value*	*Description*
1	"text"	File header record. The first 32 characters are the *project stamp*, which is used to identify related data files.

Units Record

1	"US" or "SI"	Units identifier, U.S. customary (US) or International System (SI).

Time and Count Record

1	hhhh:mm:ss	Simulation time of following sediment data.
2	+	Number of sediment data record sequences to follow.
3	+	Number of particle size classes for which data are to be read.

Bed Record

1	+	Node number to which the following sediment data apply.
2	±	Bed elevation, in ft (m).
3	±	Time-derivative of bed elevation, in ft/sec (m/s).
4	+	Active bed layer thickness, in ft (m).
5	+	Deposition bed layer thickness, in ft (m)
6	+	Original bed layer thickness, in ft (m)

Concentration Record 1

1 to 8	+	Discharge-weighted sediment concentrations, in vol/vol, for the specified number of particle size classes.

Concentration Record 2

1 to 8	±	Time-derivatives of discharge-weighted sediment concentrations, in vol/vol/sec, for the specified number of particle size classes.

Order	*Value*	*Description*
		Active Bed Layer Record
1 to 8	+	Fractions of each particle size class forming the active bed layer. The fractions will sum to unity.
		Deposition Bed Layer Record
1 to 8	+	Fractions of each particle size class forming the deposition bed layer. The fractions will sum to unity.
		Original Bed Layer Record
1 to 8	+	Fractions of each particle size class forming the original bed layer. The fractions will sum to unity.
		Repeat the sequence of sediment data records (Bed-Concentration 1-Concentration 2-Active Bed Layer-Deposition Bed Layer-Original Bed Layer) the specified number of times.

Boundary Condition Data File

Boundary condition data are read at the start of steady-state simulations and, optionally, at intervals during time-dependent simulations. Boundary condition data files may be in either text or binary form. The header and units records appear only at the beginning of a sediment data file, all other data records and data record sequences are repeated for each simulation time at which solution data are to be read. Data record format descriptions follow.

Header Record

Order	*Value*	*Description*
1	"text"	File header record. The first 32 characters are the *project stamp*, which is used to identify related data files.

Units Record

1	"US" or "SI"	Units identifier, U.S. customary (US) or International System (SI).

Time and Count Record

1	hhhh:mm:ss	Simulation time of following boundary condition data.
2	+	Number of boundary node data records to follow.

Boundary Condition Code Record

1	+	Node number to which the following boundary condition data apply.
2 to 6	+	Boundary condition codes as described on the BOUN.1 data record in the *FST2DH* Data Set descriptions.

Boundary Condition Specification Record

1 to 12	+	Boundary condition specifications as described on the BOUN.2 data record in the *FST2DH* Data Set descriptions.

Repeat the two-record sequence the specified number of times.

Wind Data File

Wind data are read at the start of steady-state simulations and, optionally, at intervals during time-dependent simulations. Wind data files may be in either text or binary form. The header and units records appear only at the beginning of wind data files, all other data records and data record sequences are repeated for each simulation time at which solution data are to be read. Data record format descriptions follow.

Header Record

Order	*Value*	*Description*
1	"text"	File header record. The first 32 characters are the *project stamp*, which is used to identify related data files.

Units Record

1	"US" or "SI"	Units identifier, U.S. customary (US) or International System (SI).

Time and Count Record

1	hhhh:mm:ss	Simulation time of following boundary condition data.
2	+	Number of wind data records to follow.

Wind Data Record

1	0	Node number at which wind data are to be applied.
2	+	Wind velocity at the node, in ft/sec (m/s).
3	+	Wind direction angle at the node, in degrees measured clockwise from true north. Wind direction is the direction *from which* the wind is blowing.
		Repeat the wind data record the specified number of times.

Wave Data File

Wave data are read at the start of steady-state simulations and, optionally, at intervals during time-dependent simulations. Wave data files may be in either text or binary format. The header and units records appear only at the beginning of wave data files, all other data records and data record sequences are repeated for each simulation time at which solution data are to be read. Data record format descriptions follow.

Header Record

Order	*Value*	*Description*
1	"text"	File header record. The first 32 characters are the *project stamp*, which is used to identify related data files.

Units Record

1	"US" or "SI"	Units identifier, U.S. customary (US) or International System (SI).

Time and Count Record

1	hhhh:mm:ss	Simulation time of following boundary condition data.
2	+	Number of wave data records to follow.

Wave Data Record

1	0	Node number at which wave data are to be applied.
2	+	Wave height, in ft (m).
3	0	Wave period, in seconds.
4	+	Wave direction angle, in degrees measured counter-clockwise from the positive x-axis.
		Repeat the wave data record the specified number of times.

Time Data File

Boundary, wind, and wave data may be updated periodically during time-dependent simulations. When reading from *FST2DH* Data Files, all TIME and time-dependent BOUN, BSEC, WIND, and WAVE data sets need to appear in chronological order at the end of the data streams. Optionally, these data sets can be placed in other files called *Time Data Files*. Time Data Files can be in only text format.

References

Armanini, A., and Di Silvio, G. (1988). "A one-dimensional model for transport of a sediment mixture in non-equilibrium conditions." *Journal of Hydraulic Research*, 26(3), 275-292.

"Coastal flooding hurricane surge model - volume 1, methodology." (1988). *FEMA Report*, Federal Emergency Management Agency, Office of Risk Assessment, Federal Insurance Administration, Washington, D.C.

Froehlich, D. C. (1988). "Analysis of on-site measurements of scour at piers." *Proceedings of the 1988 National Conference on Hydraulic Engineering*, Colorado Springs, Colorado, August 15-19, 1988, American Society of Civil Engineers, New York, NY, 826-831.

Garbrecht, J., Kuhnle, R. A., and Alonso, C. V. (1995). "A sediment transport capacity formulation for application to large channel networks." *Journal of Soil and Water Conservation*, 50(5), 527-529.

Kaplan, J., and DeMaria, M. (1995). "A simple empirical model for predicting the decay of tropical cyclone winds after landfall." Journal of Applied Meteorology, 34(11), 2499-2512.

Normann, J. M., Houghtalen, R. J., and Johnston, W. J. (1985). "Hydraulic design of highway culverts." *Hydraulic Design Series No. 5*, *Report No. FHWA-IP-85-15*, Federal Highway Administration, Washington, D.C.

Richardson, E. V. and Davis, S. R. (1995). "Evaluating scour at bridges." *Publication No. FHWA-IP-90-017, Hydraulic Engineering Circular No. 18, 3rd ed.*, Federal Highway Administration, U.S. Department of Transportation, McLean, Virginia.

Appendix B - Tropical Cyclone Model

The empirical model used in *FST2DH* to calculate windfields and atmospheric pressure distribution caused by cyclonic tropical storms is described in this Appendix. The tropical cyclone model follows closely the hurricane storm model used in the Federal Emergency Management Agency's (FEMA's) Coastal Flooding Hurricane Storm Surge Model ("Coastal Flooding" 1988), which is an extension of the National Weather Service (NWS) tropical cyclone model described in *NOAA Technical Report NWS-23* ("Meteorological criteria" 1979) and in *NOAA Technical Report NWS-38* (Ho et al. 1987).

Introduction

Tropical cyclones originate over tropical or subtropical waters, possess organized deep convection, and have a closed surface wind circulation about a well-defined center. Once formed, tropical cyclones maintain themselves by extracting heat energy from the ocean at high temperatures, and exporting heat at the low temperatures of the upper troposphere. Tropical cyclones differ in this way from extratropical cyclones, which derive their energy from horizontal temperature contrasts in the atmosphere.

Tropical cyclones in which the maximum sustained surface wind speed (using the U.S. 1-minute average) ranges from 34 kt (39 mph or 63 km/hr) to 63 kt (73 mph or 118 km/hr) are called tropical storms. When the maximum sustained surface winds are 64 kt (74 mph or 119 km/hr) or more tropical cyclones are called hurricanes or typhoons. The term hurricane is used for Northern Hemisphere tropical cyclones east of the International Dateline to the Greenwich Meridian, and the term typhoon is used for Pacific tropical cyclones north of the Equator west of the International Dateline.

Mature tropical cyclones are characterized by circular patterns of storm clouds and by torrential rains, which are accompanied by winds that may reach speeds of 100 to 180 mi/h (160 to 300 km/h) within a radius of six to 60 mi (10 to 100 km) from the storm center or core. Winds diminish rapidly with increasing distance from a tropical storm's core, and are usually less than 18 mi/h (30 km/h) at a radius of 300 mi (500 km). Tropical cyclones move with the large-scale wind currents in which they are embedded at average forward speeds of 16 mi/h (25 km/h). Although some storms may travel at twice the typical speed, others can remain stalled in the same location for several days.

For all tropical cyclones, barometric pressures decrease exponentially toward their centers and level off to relatively flat regions of the lowest pressure inside the cores. Wind speeds increase exponentially toward the centers, then drop rapidly toward calm, leaving belts of strong winds around the cores. Pressure and wind centers do not normally coincide, and they are also not necessarily at the geographical center of a storm. However, for our purposes, we can assume that they coincide without loss of generality.

A semi-empirical model of the horizontal barometric pressure field and wind structure in a tropical cyclone is presented in the next section, with subsections covering the basic features of axisymmetric winds and their approximation, the effects of asymmetries, and the types of changes that can occur after a storm moves inland.

Barometric Pressure Distribution

Barometric pressure isobars for fully-developed tropical cyclones are assumed to be circular about the storm centers following the approaches of Schloemer (1954) and Holland (1980). Barometric pressures at sea level p are given by

$$p = P_c + (P_\infty - P_c)\, e^{(-R_{max}/r)} \qquad \text{(B-1)}$$

where P_c = central pressure (that is, pressure at the storm center), P_∞ = barometric pressure surrounding the cyclone or the peripheral pressure (usually set to a climatological constant or to the value of the outer closed isobar), R_{max} = radius of maximum winds, and r = radius from the storm center. Peripheral pressure P_∞ usually ranges from 29.76 to 30.35 in Hg (100.5 to 102.5 kPa), with 30.0 in Hg (101.325 kPa) being close to ambient pressure. The radial barometric pressure gradient is obtained from the pressure profile expression as follows:

$$\frac{\partial p}{\partial r} = (P_\infty - P_c)\frac{R_{\max}}{r^2} e^{\left(-R_{\max}/r\right)} \tag{B-2}$$

Windfield Structure

The basic horizontal balance in a tropical cyclone above the boundary layer is between the sum of the Coriolis acceleration and the centripetal acceleration, and the horizontal pressure gradient force as follows:

$$\frac{V_g^2}{r} + \Omega V_g = \frac{1}{\rho_a}\frac{\partial p}{\partial r} \tag{B-3}$$

where V_g = gradient wind speed (that is, the wind speed at the top of the atmospheric frictional boundary layer under conditions of curving motion in which centripetal and Coriolis accelerations balance the horizontal pressure gradient force), ρ_a = air mass density, e = base of Napierian logarithms (approximately 2.71828), $\Omega = 2\omega \sin \phi$, ω = angular velocity of the rotating Earth (7.27×10^{-5} radians per second), and ϕ = angle of latitude. Note that air mass density ρ_a varies with pressure and temperature. Substituting the expression for the pressure gradient gives

$$\frac{V_g^2}{r} + \Omega V_g = \frac{1}{\rho_a}(P_\infty - P_c)\frac{R_{\max}}{r^2} e^{\left(-R_{\max}/r\right)} \tag{B-4}$$

Centripetal acceleration alters the original two-force geostrophic balance and creates a nongeostrophic gradient wind. Because the radius of maximum winds varies, different peak wind speeds can result in different central pressures. A storm with 40 m/s peak winds and R_{max} = 100 km will have a much lower pressure drop than one with R_{max} = 25 km.

The maximum gradient windspeed $V_{g,\,max}$ occurs where the pressure gradient is largest, that is where $r = R_{max}$. Setting $r = R_{max}$ in (2-4) and solving for V_g gives

$$V_{g,\max} = \left[\frac{1}{4}\left(\Omega R_{\max}\right)^2 + \frac{P_\infty - P_c}{\rho_a e}\right]^{1/2} - 0.5\Omega R_{\max} \tag{B-5}$$

The first term in the bracketed quantity that contains the Coriolis parameter will be much smaller than the pressure difference term and can safely be ignored (Myers 1954, p. 89-90). Consequently, the maximum gradient wind speed is approximated in "Coastal Flooding" (1988, p. 3-6) as follows:

$$V_{g,\max} = \left(\frac{P_\infty - P_c}{\rho_a e}\right)^{1/2} - 0.5\Omega R_{\max} \tag{B-6}$$

The maximum 10-m elevation, 10-min average wind speed for a stationary storm, V_{max}, occurs at a distance from the storm center equal to the radius of maximum winds R_{max}, and is given in "Coastal Flooding" (1988, p. 3-9) as

$$V_{\max} = 0.91\, V_{g,\max} \tag{B-7}$$

The 10-m, 10-min wind speed for a stationary storm varies with radial distance from the storm center as

$$V_s(r) = V_{\max} F(r) \tag{B-8}$$

where $F(r)$ = relative wind speed function given by

$$F(r) = \begin{cases} \sin^{5.73}\left(\dfrac{\pi}{2}\dfrac{r}{R_{\max}}\right); \; for \; r \le R_{\max} \\ 1 - 1.3\, e^{-\left[a\left(\frac{r}{R_{\max}} - 1\right)^b\right]^{-1}} \; ; \; for \; r > R_{\max} \end{cases} \tag{B-9}$$

in which the coefficients a and b are found from the following expressions:

$$a = \begin{cases} 0.36 + 0.0075\, r; \; for \; r \le 100\, nm \\ 1.11; \; for \; r > 100\, nm \end{cases} \tag{B-10}$$

$$b = \begin{cases} \min\{0.54, 0.4953 + 0.00483\, r - 0.00739 \min\{0, r - 14.52\}\}; for \; r \le 100\, nm \\ 0.3466; for \; r > 100\, nm \end{cases} \tag{B-11}$$

where r is given in nautical miles.

Cyclonic winds blow counterclockwise about the center of a storm in the northern hemisphere, and counterclockwise in the southern hemisphere. However, the winds are not entirely circumferential, they also have inward radial components. Inflow angles from a circumferential tangent are known as incurvature angles or inflow angles. Their values depend on distance from a storm's center and are calculated as follows:

$$\alpha(r) = \begin{cases} \alpha_{\max} \sin^{1.6}\left(\dfrac{\pi}{2}\dfrac{r}{\lambda R_{\max}}\right) + \alpha_{\min}; \; for \; r \le \lambda R_{\max} \\ \alpha_{\max} - (\alpha_{\max} - \alpha_a)\, e^{-\left[0.00622 (r - \lambda R_{\max})^{1.39}\right]^{-1}} \; ; \; for \; r > \lambda R_{\max} \end{cases} \tag{B-12}$$

where

$$\alpha_{\max} = \begin{cases} 12.59 (R_{\max} - 4)^{0.2478}; \; for \; R_{\max} > 4.05\, nm \\ 6.0; \; for \; R_{\max} \le 4.05\, nm \end{cases} \tag{B-13}$$

is the maximum incurvature angle in degrees and R_{max} is in nautical miles, α_{min} = minimum incurvature angle = 6°, λ = constant factor = 1.0, and

$$\alpha_a = \begin{cases} 0; \; for \; r/R_{max} \le \lambda \\ R_{max}; \; for \; r/R_{max} > \lambda \; and \; R_{max} \le 20\,nm \\ 20 + 0.5(R_{max} - 20); \; for \; r/R_{max} > \lambda \; and \; R_{max} \le 30\,nm \\ 25; \; for \; r/R_{max} > \lambda \; and \; R_{max} > 30\,nm \end{cases} \tag{B-14}$$

is the value in degrees of the incurvature angle as the radius approaches infinity.

Taking into account a storm's forward motion, which adds an asymmetric contribution to the velocity distribution, wind speed is found as

$$V = V_{max} F(r) + 1.5 V_f^{0.63} \cos\beta \tag{B-15}$$

where V_f = storm forward speed, and β = angle between the local 10-m, 10-min wind vector and the storm's forward motion vector.

Transformation to Cartesian Coordinates

Wind velocities and pressure gradients need to be transformed to Cartesian coordinates for use in *FST2DH*. An example of these calculations at a point *P* are shown in Figure B-1. The position of the storm center *C* moves at velocity V_f. Therefore, the wind velocity at a general point *P* varies constantly and is calculated at every hydrodynamic time-step. Letting the Cartesian coordinates x_C, y_C denote the location of the storm center, and the coordinates x_P, y_P denote the location of point *P*, the radial distance from the storm center to *P* is

$$r = \sqrt{(x_P - x_C)^2 + (y_P - y_C)^2} \tag{B-16}$$

and the angle between the radian and the positive *x* axis of the coordinate system γ is found as

$$\gamma = \arctan\left(\frac{y_P - y_C}{x_P - x_C}\right) \tag{B-17}$$

The angle between the local wind velocity and the positive *x* axis is then

$$\theta = 90^o + \gamma + \alpha \tag{B-18}$$

noting that the incurvature angle α varies with *r* according to (2-12) to (2-14). The angle β is then given by

$$\beta = \theta - \delta \tag{B-19}$$

where δ = angle between the forward velocity vector and the positive *x* axis as shown in Figure B-1. The wind speed at point *P* is found from (2-12), and the *x*- and *y*-components of the velocity are found as

$$V_x = V\cos\theta \qquad V_y = V\sin\theta \tag{B-20}$$

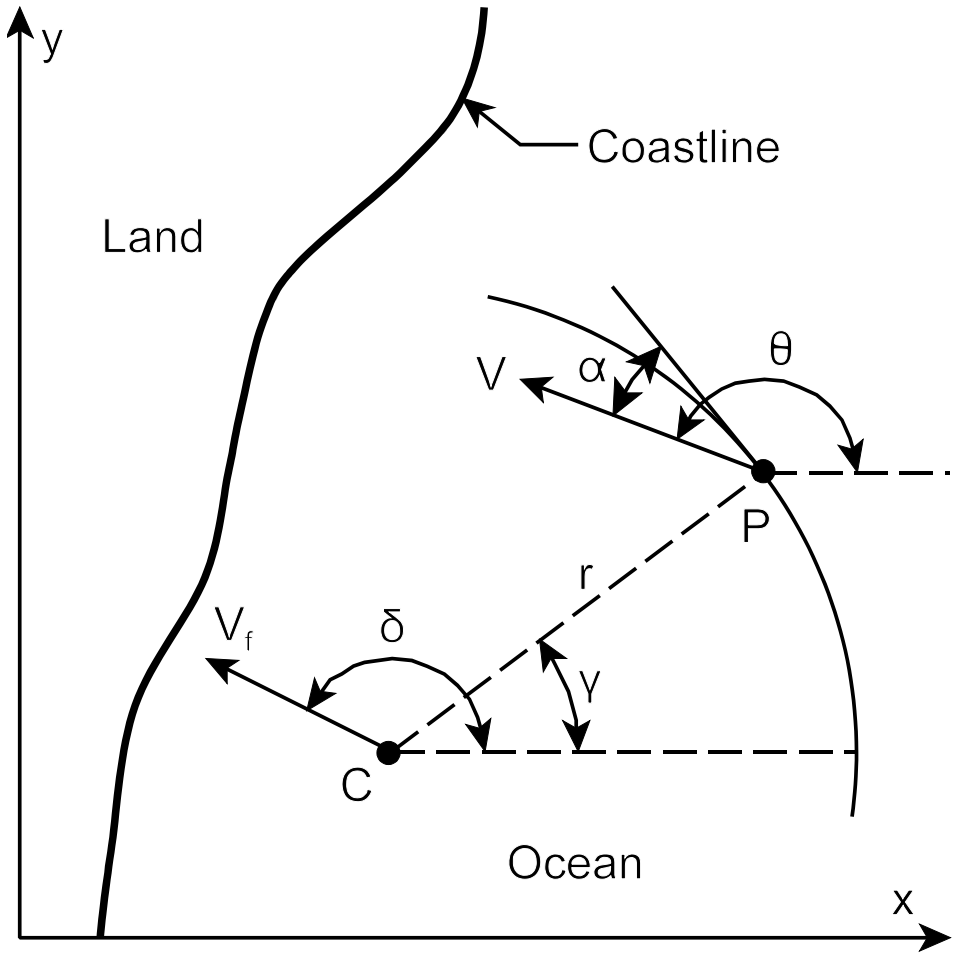

Figure B-1. Coordinate system for calculating tropical cyclone windfields where *C* = position of the tropical cyclone center or core, *P* = point at which wind velocities are calculated, V_f = forward storm velocity, *V* = wind velocity at *P*, α = incurvature angle, θ = angle between *V* and the positive *x* axis, γ = angle between *CP* and the positive *x* axis, δ = angle between V_f and the positive *x* axis, and *r* = distance between *C* and *P*.

Wind Decay After Landfall

Tropical cyclones form over oceans, relying upon the thermal energy stored there to maintain their intensity. Their winds weaken when the storm centers move across land (that is, after landfall) because land surfaces usually provide much more resistance than comparatively smooth water surfaces (even during hurricanes), and also because the surface energy flux that fuels the storm is significantly reduced.

An empirical model developed by Kaplan and Demaria (1995) is used in *FST2DH* to estimate the maximum sustained surface wind as a storm moves inland. The model applies a simple two parameter decay equation to the wind speed *V* in knots given by (B-15) as follows:

$$V_\ell = 26.7 + (0.9V - 26.7)e^{0.095\tilde{t}} - \tilde{t}(50 - \tilde{t})(0.0109 \log_e D - 0.0503) \qquad \text{(B-21)}$$

where V_ℓ = wind speed after landfall in knots, $\tilde{t} = t - t_\ell$ = time in hours since landfall, t = time in hours, t_ℓ = time in hours of landfall, and D = distance in kilometers the storm has advanced inland. No automatic adjustments are made to the storm forward speed V_f.

Summary

Tropical storms are fully described by their barometric pressure fields at sea level, and the corresponding 10-meter elevation, 10-minute average windfield over the sea surface. The model requires the following parameters: (1) initial location of the storm center, (2) radius of maximum winds, (3) forward storm speed, (4) storm track angle, (5) atmospheric pressure at the storm's center, (6) ambient atmospheric pressure outside the storm, and (7) time or location of landfall. A good source for most of these data items is *NOAA Technical Report NWS-38* (Ho et al. 1987).

References

"Coastal flooding hurricane surge model - volume 1, methodology." (1988). *FEMA Report*, Federal Emergency Management Agency, Office of Risk Assessment, Federal Insurance Administration, Washington, D.C.

Ho, F. P., Su, J. C., Hanevich, K. L., Smith, R. J., and Richards, F. (1987). "Hurricane climatology for the Atlantic and Gulf coasts of the United States." *NOAA Technical Report NWS-38*, National Weather Service, National Oceanic and Atmospheric Administration, Washington, D.C.

Holland, G. J. (1980). "An analytic model of the wind and pressure profiles in hurricanes." *Monthly Weather Review*, 108, 1212-1218.

Kaplan, J., and DeMaria, M. (1995). "A simple empirical model for predicting the decay of tropical cyclone winds after landfall." Journal of Applied Meteorology, 34(11), 2499-2512.

"Meteorological criteria for standard project hurricane and probable maximum hurricane windfields, Gulf and East coasts of the United States." (1979). *NOAA Technical Report NWS-23*, National Weather Service, National Oceanic and Atmospheric Administration, Washington, D.C.

Myers, V. A. (1954). "Characteristics of United States hurricanes pertinent to levee design for Lake Okeechobee, Florida." *Hydrometeorological Report 32*, U.S. Department of Commerce, Washington, D.C.

Schloemer, R. W. (1954). "Analysis and synthesis of hurricane wind patterns over Lake Okeechobee, Florida." *Hydrometeorological Report 31*, U.S. Department. of Commerce, Washington, D.C.